Spring 2010

Choroidal endothelial cell activation in age-related macular degeneration

Jessica Marie Skeie
University of Iowa

CHOROIDAL ENDOTHELIAL CELL ACTIVATION IN AGE-RELATED MACULAR DEGENERATION

by

Jessica Marie Skeie

An Abstract

Of a thesis submitted in partial fulfillment
of the requirements for the Doctor of
Philosophy degree in Biomedical Engineering
in the Graduate College of
The University of Iowa

May 2010

Thesis Supervisor: Associate Professor Robert F. Mullins

ABSTRACT

Age-related macular degeneration (AMD) is a devastating ocular disease affecting one third of the elderly population in the western world. Some cases of AMD develop neovascular membranes, which are characterized by the pathologic growth of new blood vessels into the retina. This pathology may be initiated by proteins capable of activating endothelial cells to become angiogenic or inflammatory, later causing them to grow abnormally. This investigation aimed to determine the causes of pathologic blood vessel growth in AMD.

Human eyes with AMD have been shown by us and others to have abnormal activities of angiogenin, complement component C5 anaphylatoxin (C5a), and/or elastin fragments. We therefore employed methods including PCR, immunoblotting, immunohistochemistry, morphometrics, tissue culture, ultrastructural observations, and functional assays to determine the effects angiogenin, C5a, and elastin fragments on the angiogenic and inflammatory changes of choroidal endothelial cells *in vitro* and *in vivo.*

It was shown that choroidal endothelial cells express the surface receptor for C5a. Also, these cells increase their expression of ICAM-1, a surface protein that mediates leukocyte trafficking, in response to elevated levels of C5a in organ culture. This indicates that increased levels of C5a associated with AMD increase the inflammatory behavior of choroidal endothelial cells. It was demonstrated that choroidal endothelial cells are able to internalize angiogenin, a potent inducer of angiogenesis. Although cells from the choroid did not increase their angiogenic responses to this protein, their ability to internalize it indicates that they may respond to it by a different mechanism. Elevated levels of elastin fragments, however, did increase the migratory response of choroidal endothelial cells in culture, which is a key event in angiogenesis. Elevated levels of elastin fragents also increased the amount of collagen IV deposition within Bruch's

membrane in a mouse model. This is relevant to AMD pathology as deposits within Bruch's membrane are common manifestations associated with AMD.

This body of work has provided new insights into the roles of angiogenin, C5a, and elastin fragments in activating choroidal endothelial cells to becoming inflammatory or angiogenic. These endothelial cell behaviors are common characteristics found in neovascular AMD. These new findings will help aid in the further understanding of the pathobiology of this disease in hopes to provide improved treatments in the future.

Abstract Approved: _____
Thesis Supervisor

_____
Title and Department

_____
Date

CHOROIDAL ENDOTHELIAL CELL ACTIVATION IN AGE-RELATED MACULAR DEGENERATION

by

Jessica Marie Skeie

A thesis submitted in partial fulfillment
of the requirements for the Doctor of
Philosophy degree in Biomedical Engineering
in the Graduate College of
The University of Iowa

May 2010

Thesis Supervisor: Associate Professor Robert F. Mullins

Graduate College
The University of Iowa
Iowa City, Iowa

CERTIFICATE OF APPROVAL

PH.D. THESIS

This is to certify that the Ph.D. thesis of

Jessica Marie Skeie

has been approved by the Examining Committee
for the thesis requirement for the Doctor of Philosophy
degree in Biomedical Engineering at the May 2010 graduation.

Thesis Committee: _____
Robert F. Mullins, Thesis Supervisor

_____
Terry A. Braun

_____
Krishnan B. Chandran

_____
Khalid N. Kader

_____
Edwin M. Stone

_____
Sarah C. Vigmostad

To my family.

ACKNOWLEDGMENTS

There is one member of our lab that deserves the first shout. Elizabeth took me under her wing when I began this journey and taught me everything she knew to jumpstart my success. Without her knowledge and patience, this project would have been off to a rough beginning.

I will next mention the wonderful personnel of Central Microscopy. My first projects began in this facility where Jean, Kathy, Tom, Jonas, and Randy opened my eyes to the wonderful world of microscopy. Many of the projects within this thesis would not have been possible without the expertise and dedication this facility has to offer.

Tyson and Stu, you both are wonderful mentors. I appreciate all of the encouraging chats, and tedious paper reviews you have endured during my career so far. I admire you both as great scientists, but even more, as great friends.

I would like to thank the members of my graduate committee, Edwin Stone, Khalid Kader, Krishnan Chandran, Terry Braun, and Sarah Vigmostad. I have achieved many of my goals because of your encouragement and helpful advice.

Rob, I could probably write a chapter of thanks just for you. I came into this position as an engineer having had a smidge of cell biology in my background. I will never forget the day I knocked on your office door to ask you what a glycoprotein was. Although there were several ways you could have answered my question, you patiently went through all of the macromolecule terminology with me. I could never have learned from a text book what I have learned during the time I have worked with you. You are an amazing teacher, mentor, and scientist. Thank you.

Beyond the science, I am so happy to have such a wonderful home. Ryan, you are my geocaching, sailing, cycling, tandem longboarding, motorbiking, scuba diving soulmate. Thank you for pushing me to be my best.

TABLE OF CONTENTS

LIST OF TABLES

LIST OF FIGURES

LIST OF ABBREVIATIONS

ANG = angiogenin

BP = bioactive elastin hexapeptide having amino acid sequence VGVAPG

BrM = Bruch's membrane

BSA = bovine serum albumin

C3 = complement component 3

C3a = complement component 3 anaphylatoxin

C5 = complement component 5

C5a = complement component 5 anaphylatoxin

CCL2 = monocyte chemotactic protein-1 (MCP-1)

CD31 = platelet endothelial cell adhesion molecule-1 (PECAM-1)

CD54 = intercellular adhesion molecule-1 (ICAM-1)

CFH = complement factor H

CNV = choroidal neovascularization

CNVM = choroidal neovascular membrane

COL4 = collagen 4

COL4a2 = collagen 4 isoform alpha 2

CTSA = cathepsin A

EDP = elastin-derived peptide

FBS = fetal bovine serum

GLB1 = beta galactosidase

HBSS = Hank's buffered saline solution

ICAM-1 = intercellular adhesion molecule-1 (CD54)

IL = interleukin

ITGAV = integrin alpha v

ITGA8 = integrin alpha 8

ITGB3 = integrin beta 3

MCP-1 = monocyte chemotactic protein-1 (CCL2)

MMP = matrix metalloproteinase

NEU1 = neuraminidase 1

PECAM-1 = platelet endothelial cell adhesion molecule-1 (CD31)

PXE = pseudoxanthoma elasticum

RPE = retinal pigment epithelium

TIMP = tissue inhibitor of matrix metalloproteinase

UEA-1 = *Ulex europaeus* agglutinin-1

VEGF = vascular endothelial growth factor

CHAPTER 1. BACKGROUND AND SIGNIFICANCE

Age-related macular degeneration: An overview

Age-related macular degeneration (AMD) is the leading cause of irreversible blindness in people over the age of 60 in the United States (1, 2). In AMD, visual acuity is dramatically affected because the disease disrupts the macula, the region of the posterior eye responsible for detailed vision. There are two commonly used classifications of AMD: 'dry', which is the atrophic form, and 'wet', which is the neovascular form (3-6). AMD begins with "dry" characteristics, which can worsen to over time in individual patients. Some cases eventually develop choroid neovascular membranes (CNVMs), changing from atrophic to neovascular AMD. Once an eye has neovascular characteristics, it is always considered to have neovascular AMD. Prior to describing the manifestations of this disease in detail, it is important to understand the tissues affected. These include the retina, the retinal pigmented epithelial layer, Bruch's membrane, and the choroid.

Anatomy and function of the retina-choroid complex

The posterior pole of the human eye is composed of several tissues including the neural retina, the retinal pigmented epithelium (RPE), Bruch's membrane, and the choroid. The retina has several layers. Moving from the vitreous outward (anterior to posterior) these layers are: the inner limiting membrane, nerve fiber layer, ganglion cell layer, inner plexiform layer, inner nuclear layer, outer plexiform layer, outer nuclear layer, external limiting membrane, and the rods/cones. The layers of the retina, the RPE, Bruch's membrane, and the choroid are shown in Figure 1.

The inner limiting membrane is composed of Muller cell basement membrane and hyalocytes. This layer is positioned anterior to the nerve fiber layer, composed of the axons of the retinal ganglion cells.

The ganglion cell layer is composed of the ganglion cell soma. These cells

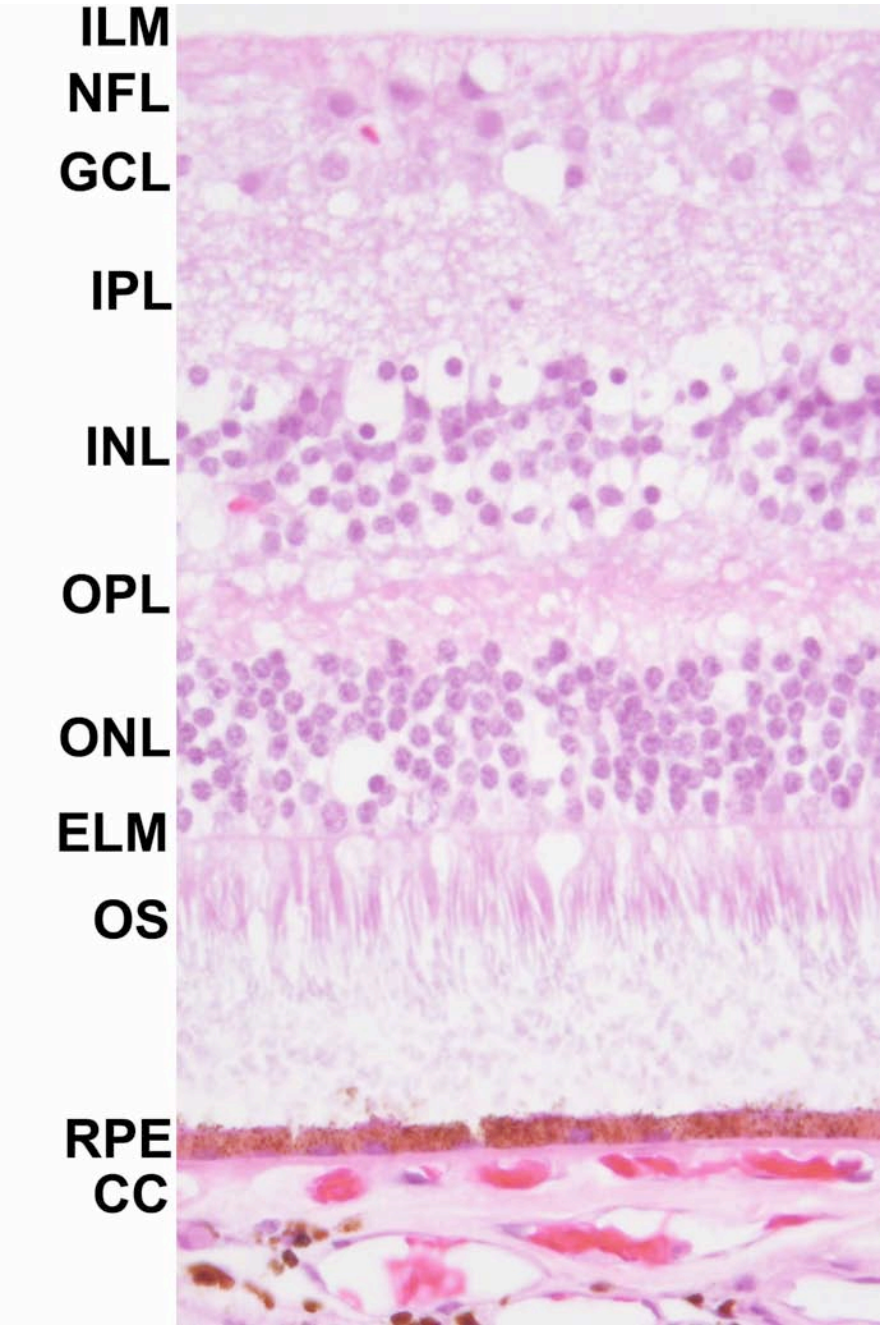

Figure 1. Histology of human retina and choroid. Hematoxylin and eosin stained section of the retina, retinal pigmented epithelial (RPE) layer, Bruch's membrane, and the choriocapillaris (CC). Bruch's membrane (not labeled) is the very thin pink layer between the RPE and the CC. ILM, internal limiting membrane, NFL, nerve fiber layer, GCL, ganglion cell layer, IPL, inner plexiform layer, INL, inner nuclear layer, OPL, outer plexiform layer, ONL, outer nuclear layer, ELM, external limiting membrane, OS, outer segments.

function to relay light sensory information to the brain. The retinal ganglion cells undergo a 25% decrease in number as a person ages (7). This demonstrates an increasing weakness, or damage, in this tissue with respect to aging. Independent of disease, the general aging of retinal and choroidal tissues is an important concept in mechanisms of AMD pathophysiology.

Adjacent to the retinal ganglion cell layer is the inner plexiform layer. This layer is composed of the axons and dendrites of bipolar cells and amacrine cells, which form synapses with the retinal ganglion cells. Bipolar cells have two axon extensions that connect the photosensory signaling cascade from the photoreceptors to the ganglion cells. Both amacrine and bipolar cells relay information from the rods and cones to the retinal ganglion cells.

The fifth layer is the inner nuclear layer, comprised of the nuclei of the amacrine, Muller, horizontal, and bipolar cells. This layer is prominent in a hematoxylin and eosin histology stain, where the nuclei stain dark blue/purple and form a tightly packed band. Posterior to the inner nuclear layer is the outer plexiform layer. The axons of the amacrine and bipolar cells synapse with the axons of the photoreceptor cells in this layer.

Following the axons of the rods and cones to the next layer, the cells' nuclei pack together to form the outer nuclear layer. On a hematoxylin and eosin stained retina, this layer appears similar to the inner nuclear layer; however, the nuclei of the rods and cones are slightly smaller and more densely packed than those of the amacrine and bipolar cells.

Between the nuclei of the rods and cones and their outer segments, there is a layer known as the external limiting membrane. This layer is not a true membrane; instead it is a complex composed of Muller cell and photoreceptor inner segment adhesion proteins.

Lastly, the retina contains the inner and outer segments of the rods and cones as its outer most layer. The inner segments of the cones are large in comparison to those of the rods, and both contain organelles and mitochondria. The rod outer segments contain a series of discs, which capture photons with rhodopsin. As a person ages, the rods that

undergo atrophy lose their rhodopsin, however, there is not an overall loss in rhodopsin because the adjacent rods appear to undergo a hypertrophy of rhodopsin (8-10). Cone outer segments are shorter than those of the rods, and express opsin in laminar folds of the cell membrane that taper towards the distal end. This attribute, along with the inner segment differences, allows a distinction from the rods in a hematoxylin and eosin stain. With age, the cone segment length does not change, but the amount of visual pigment does become reduced, especially in patients over the age of 60 years old (11).

The retinal pigmented epithelial (RPE) layer is a monolayer of pigmented epithelial cells that are responsible for trafficking nutrients to, and waste from, the photoreceptor cells. The cells are tightly packed, allowing small molecules such as ascorbic acid and glucose to reach the retina, while retaining tissue infiltrates from the blood in the choroid. The metabolites and oxygen are transferred from the underlying choroid, allowing the photoreceptor cells to be as tightly packed as physically possible without being disrupted by branching vasculature. This is very important for the high spatial resolution of the photoreceptor cells.

The proximal relationship of the epithelial cells to the outer segments of the rods and cones is very close, forming a matrix known as the interphotoreceptor matrix (IPM). This matrix fills the space between the two cell types and contains molecules that are responsible for retinoid exchange, disk phagocytosis (accomplished by the RPE cells), as well as physical stabilization (12-15). This matrix, unlike many extracellular matrices, does not contain laminin, collagen, or elastin (13). Many matrix turnover proteins are found within this space, including matrix metalloproteinases (MMPs) and their inhibitors (TIMPs) (16). These proteins are thought to be secreted by the RPE cells.

The lateral apical surfaces of RPE cells are tightly joined to one another by zonulae occludentes. The basal surface of the RPE has a very large number of infoldings in order to maximize the amount of surface area that is capable of trafficking oxygen, nutrients and waste between the retina and the choroid.

As mentioned with different cell types of the retina, the RPE cells undergo natural changes with age. Lipofuscin accumulates within the RPE cells. Lipofuscin is believed to be composed of lipids, proteins, and incompletely digested outer-segment components which autofluoresce with light excitation (17-19). Another change that the RPE cells undergo with age *in vitro* and *in vivo* is senescence, a dormant stage where the cell is unable to enter the cell cycle any more, leading to less turnover of the cell layer (20). With an increasing proportion of cells becoming dormant, the RPE layer becomes less able to phagocytose the outer-segment material, which begins to accumulate in the sub-RPE space. As the accumulation of lipofuscin and other waste materials persists, the ability of the RPE cells to function in trafficking declines, compounding the decline of RPE function. RPE cells have their own basement membrane. This extracellular matrix intimately joins the basal infoldings of the RPE cells with the innermost collagen layer of Bruch's membrane.

Bruch's membrane is a penta-laminar structure situated between the RPE and the choriocapillaris. At the center of this membrane is a network of insoluble elastin, sandwiched between two layers of collagen. The outer layer of collagen is connected to the basement membrane of the choriocapillaries of the choroid (Figure 2). Bruch's membrane is therefore very symmetrical having a central elastic layer, then two collagen layers, outlined by two cellular basement membranes. An important function of Bruch's membrane is to provide a mechanical separation between the leaky, branching vasculature of the choroid and the ordered, non-vascularized packing of the photoreceptors. Again, the structure and function relationship is important as with the layer of the photoreceptors. In patients with AMD, Bruch's membrane undergoes damage due to accumulation of deposits as well as overall thinning and fragmentation (21, 22). The thinning of Bruch's membrane is correlated with the degree of AMD, and

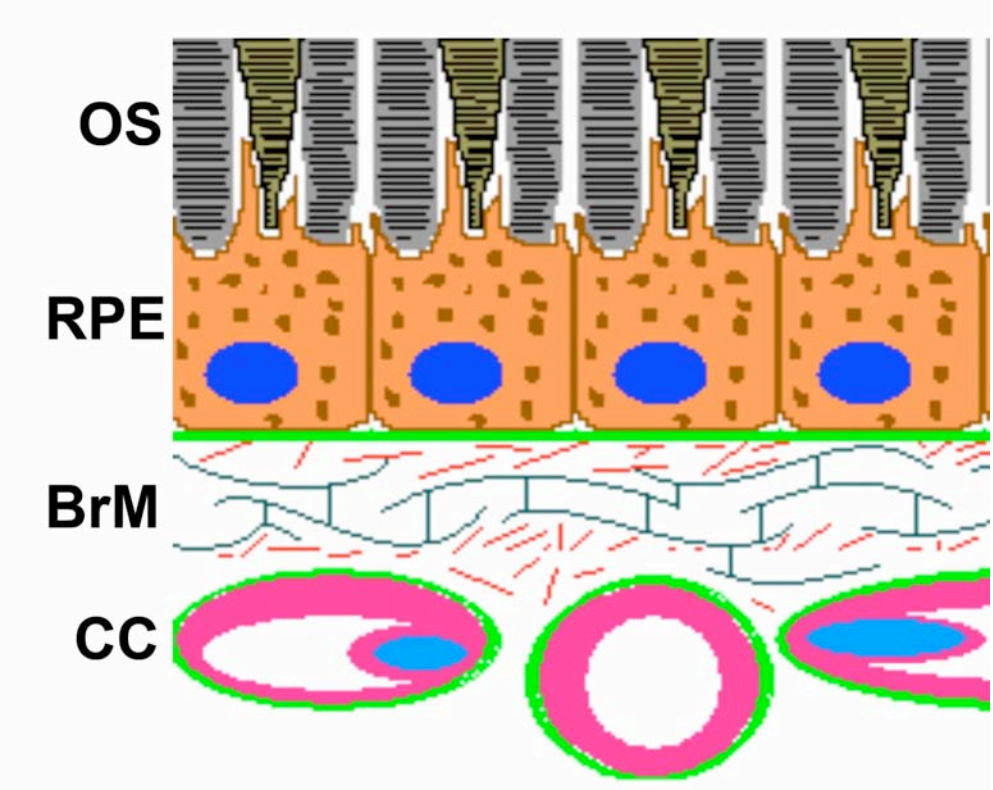

Figure 2. Bruch's membrane. Illustration depicting the five layers of Bruch's membrane. These layers include the basement membrane of the RPE cells (green), an inner collagenous layer (red), a central elastic layer (black), an outer collagenous layer (red), and the basement membrane of the CC endothelial cells (green).

is found in atrophic as well as neovascular cases (23). If the barrier properties of Bruch's membrane are compromised, the blood vessels in the choroid are capable of growing into the retina, causing damage to the photoreceptors, a phenomenon commonly seen in neovascular AMD (described below).

Atrophic AMD

The majority of patients with AMD have the atrophic form. Patients with this pathology experience a wide range of vision loss, from no detectable loss, to profound vision loss. Early signs of vision loss include blurry vision, central scotomas, and some difficulty discerning distinct lines on an Amsler grid test. This form of AMD is clinically recognized in fundus photographs by dispersed brown pigments of the RPE and/or white and yellow spots around the macula (Figure 3). Histologically, landmark characteristics of atrophic AMD include drusen, basal laminar deposits, and retinal pigment epithelial (RPE) changes, which can result in annular and/or geographic atrophy (24-27).

Drusen. The formation of drusen may be due to the deposition of metabolic waste material from the RPE and choriocapillaris (28). The rod and cone photoreceptor cells are an extremely active group of cells, and therefore undergo a high turnover of nutrients, oxygen, and outer-segment waste. The RPE cells are one of the most metabolically active cells in the human body. Situated between the non-vascularized outer segments of the retina and the highly fenestrated choriocapillaris, this layer of cells is responsible for maintaining the entire outer retina in terms of nutrients, oxygen, and waste removal. The RPE is responsible for phagocytosing and digesting cell turnover waste and if not accomplished properly, these products may end up deposited within the basement membrane. It is thought that these waste materials accumulate and form drusen.

There are three main types of drusen (Figure 4). Hard drusen, also known as nodular drusen, are spherical in shape, and the most common. Nodular drusen are found

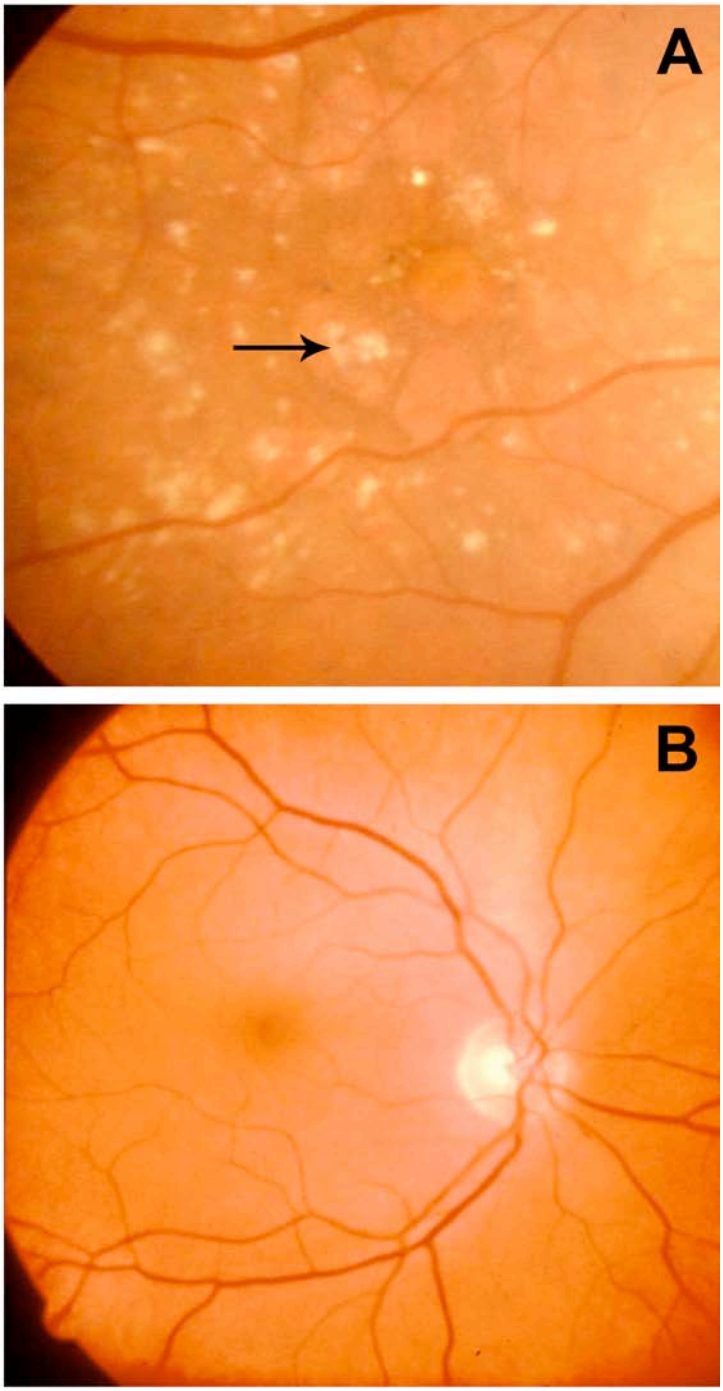

Figure 3. Atrophic AMD fundus photography. White and yellow speckling of the macular region (arrow) indicates the presence of drusen in a fundus photograph of a patient with atrophic AMD (A). A normal macula fundus photograph is shown for comparison (B). The macula is shown near the center of the photograph with the optic nerve head oriented towards the right side of the image (not present in (A)).

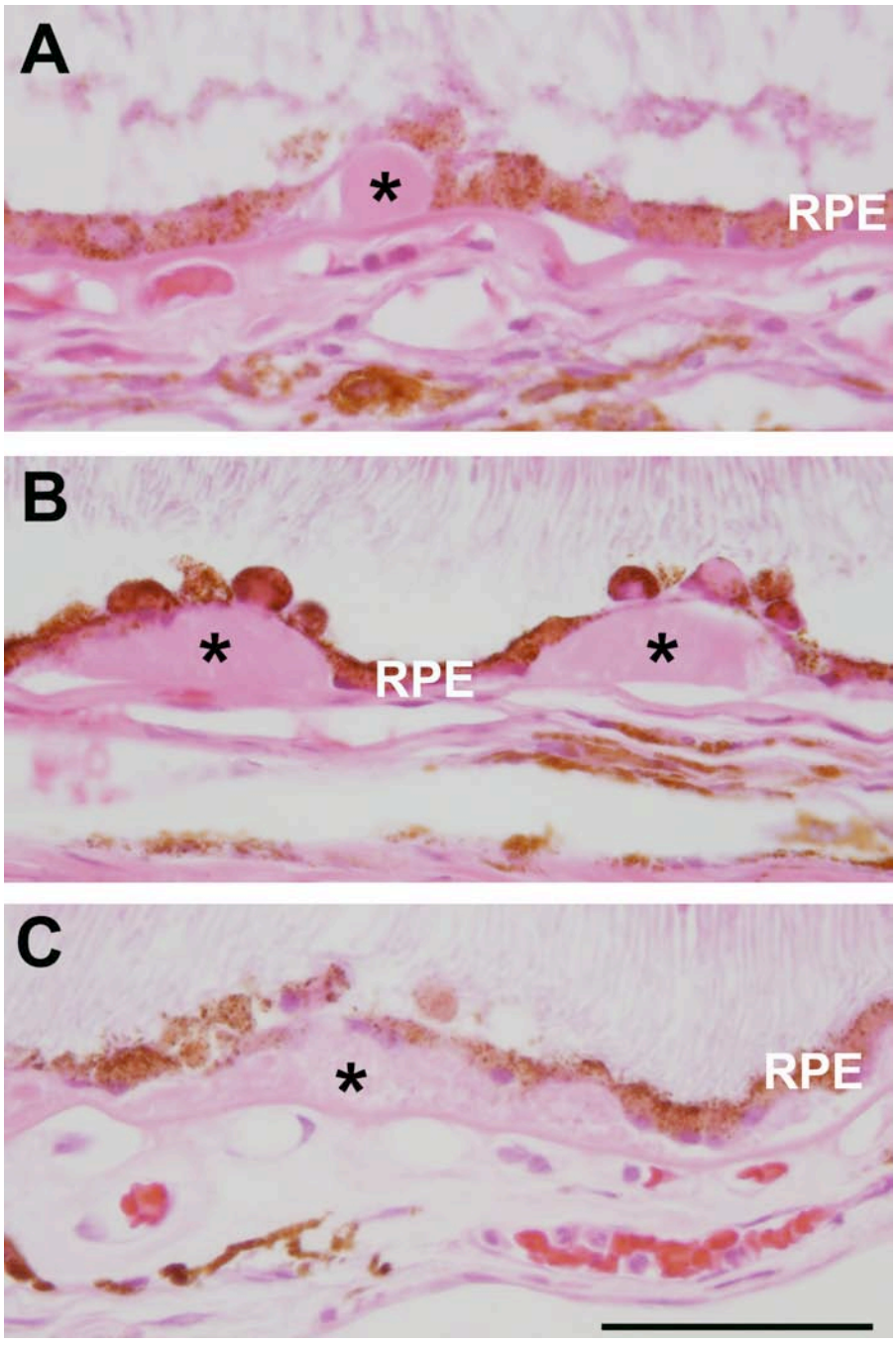

Figure 4. Examples of drusen. Hematoxylin and eosin stained micrographs of different types of drusen. The dense, round, distinct druse found in (A) is an example of hard drusen. Soft drusen are often larger in diameter than hard drusen, and have less distinct boundaries (B). Confluent drusen is even less distinct in shape than soft drusen, and often appears to be more of a layer than a round spherical deposit (C). (*) indicates the drusen for all images. Scale bar = 50 μm.

in between the basement membrane of the RPE cells and the inner collagenous layer of Bruch's membrane. Soft drusen are larger than nodular drusen and have less distinct boundaries. They are found in the same area of Bruch's membrane and appear to have similar compositions to hard drusen (29). Confluent drusen, also known as basal linear deposits, are also composed of granular material and collagen in the sub-RPE space (30). Soft drusen and confluent drusen are both associated with a higher risk for AMD, in contrast to nodular drusen. The composition and mechanical disposition of drusen can cause damage to surrounding tissues in several ways. Detachments of basal laminar deposits can lead to serous RPE cell detachment. Also, among the many deposited materials, drusen have been found to contain several proteins capable of activating endothelial cells that may then contribute to tissue damage. These proteins include immunoglobulins, complement proteins C3, C5, C5b-9, and amyloid proteins (29, 31). The importance of these local inflammatory stimuli in drusen will be discussed below as well as in chapter 3.

Theoretically, debris in drusen is from the RPE because it is first found on the basal side of the RPE cells, in contrast to apical choroidal side of Bruch's membrane. RPE cells also exhibit large amounts of their cytoplasm released to their basal side, possibly in conjunction with elimination of metabolized outer segment waste by exocytosis. There is no evidence of choroidal cell debris deposition (32), even though there is evidence of serum-derived proteins present in sub-RPE deposits.

Neovascular AMD

Roughly ten percent of patients with AMD develop the neovascular form. The onset of this pathology causes a dramatic, rapid, and mostly irreversible loss in visual acuity. This form of AMD is clinically recognized in fundus photographs by large reddish brown hemorrhage spots in the macular region (Figure 5). Histologically, neovascular AMD is characterized by the abnormal growth of choroidal blood vessels (choroidal

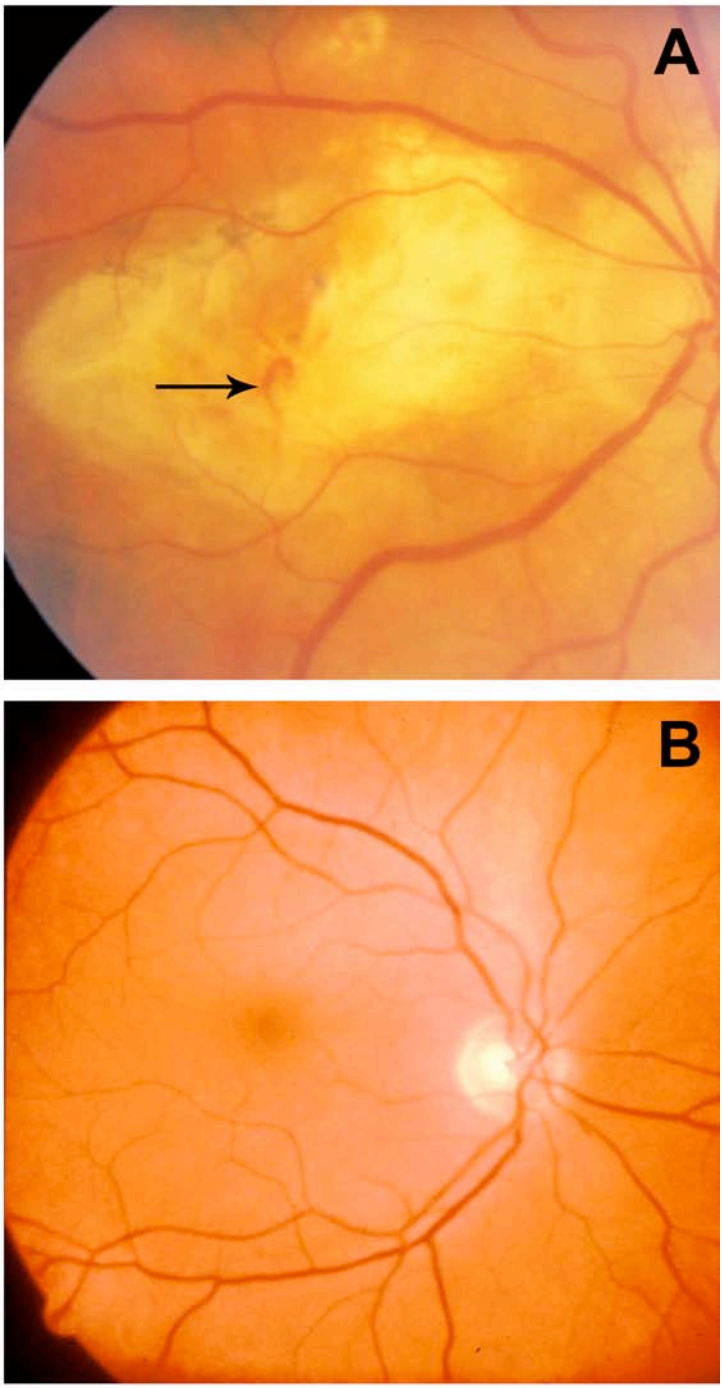

Figure 5. Neovascular AMD fundus photography. The large reddish lesion in the macula (arrow) of this patient with AMD is a neovascular membrane (A). The fundus photograph of the macula of a control patient is shown for comparison (B). The macular region is shown in the center of the photograph with the optic nerve head oriented to the right of the image.

neovascular membranes, CNVMs) in the sub-RPE/retinal space, hemorrhaging, serous detachment of the RPE and/or retinal detachment, and fibrous disciform scarring (Figure 6) (4, 27, 33-35). This multistep process is likely to be initiated by the breakdown of Bruch's membrane, which, when intact, prevents choroidal endothelial cells from entering the sub-retinal space (3, 36-38). Once the integrity of Bruch's membrane has been compromised, choroidal endothelial cells migrate from the choroid into the sub-RPE and/or sub-retinal space (39-42). These endothelial cells proliferate and form tubes (tubulogenesis), and ultimately reorganize their junctions to increase permeability across the newly formed vascular wall. The new vessels begin as capillaries and later develop into venules and arterioles (43).

The neovascular process in AMD can result in catastrophic decreases in visual acuity. Current treatments for neovascular AMD are focused primarily on vascular endothelial growth factor (VEGF)-mediated processes (44). These treatments are an effective means of minimizing neovascular membrane formation, however, understanding the role of additional angiogenic stimuli would be invaluable for the development of improved treatments (45). If alternative treatments are to be developed, a better understanding of vascular inflammation and early steps in angiogenesis would be invaluable (46).

Bruch's membrane in AMD

Bruch's membrane is a very important mechanical barrier situated between the RPE and the leaky capillary network of the choroid. Bruch's membrane is thin, only averaging 3 μm in thickness, however it is a mechanically strong complex consisting of primarily collagen and elastin (23). With age, Bruch's membrane undergoes several changes. The inner collagenous layer becomes much thicker, with almost a three-fold change in thickness in the periphery, and less dramatic changes in the macula (47, 48). Specifically, the collagen IV content of the choriocapillary basement membrane increases

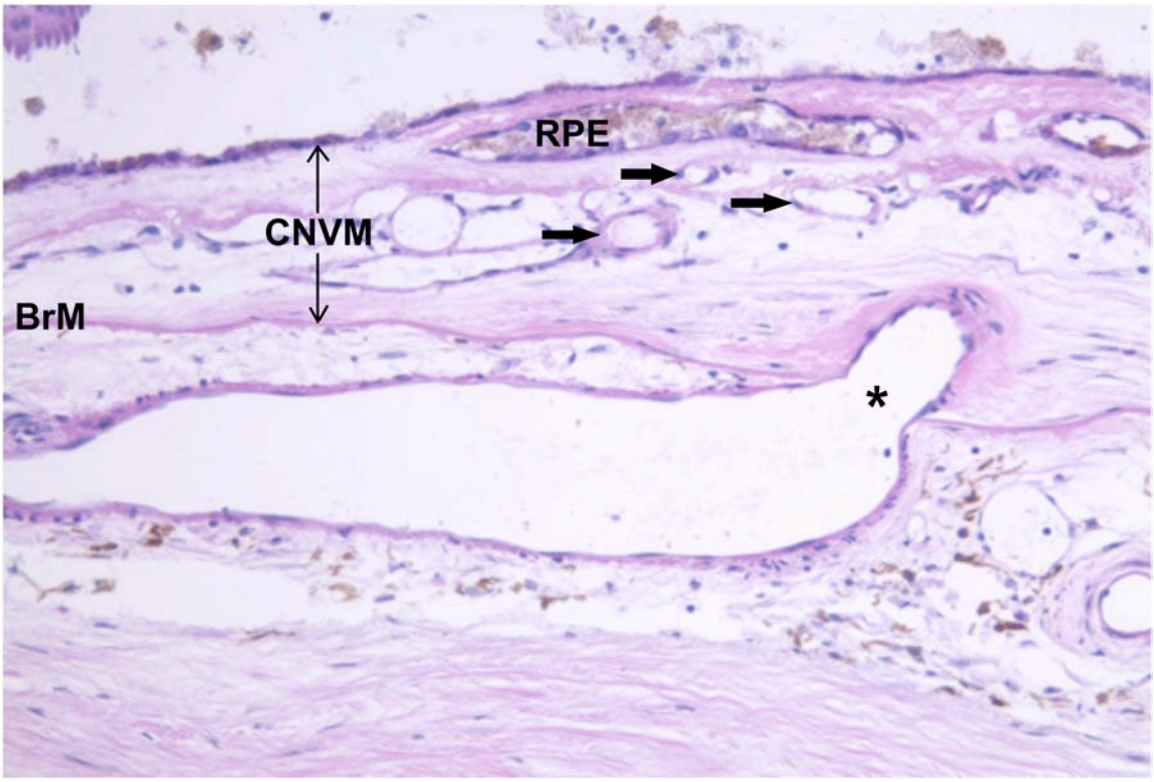

Figure 6. Histology of neovascular AMD. In this hematoxylin and eosin stain of the choroid of a patient with neovascular AMD, a vessel (*) is captured traversing from the choroid, through Bruch's membrane (BrM), and into the sub-retinal space. The region into which this vessel is captured growing is the neovascular membrane (CNVM), which is composed of other blood vessels (arrows), scar tissue, and RPE debris.

with age, causing a thickening of the membrane in the macula (49). Increased collagen layer thickness could be correlated to an increase of deposition, because the molecules have further to traverse across the membrane, and may also alter the permeability of the collagen layers (21, 23).

In addition, the inner elastic layer in the macula undergoes calcification, fragmentation, and thinning (22, 47, 50-52). The fragmentation could be attributed to aging alone, however, it could also be due to invading macrophages. Ultrastructurally, it has been shown that macrophages from the choroid are capable of invading the layers of Bruch's membrane (52). This can cause destruction of the layers of Bruch's membrane in several ways. First, the mechanical forces of macrophage movement alone are enough to displace some of the proteins composing the structure. Second, macrophages phagocytose components of the membrane, removing them entirely. Finally, macrophages release enzymes including collagenase and elastase, which are capable of digesting two of the main classes of proteins comprising Bruch's membrane (53).

Together, these changes could alter both the permeability of Bruch's membrane leading to deposition, and the capacity of Bruch's membrane to prevent CNVM formation.

The choroid in AMD

It has been shown that there is a decreased amount of foveolar blood in correlation with increasing AMD pathology (25). Reduction in choroidal flow limits nutrient and waste exchange, which provides an explanation for the nearby death of retinal and RPE cells, as well as the development of deposits in the sub-retinal space including drusen and basal laminar deposits.

The choriocapillaris is the capillary bed responsible for providing nourishment to and removing waste from the RPE and retina. During the progression of AMD, these capillaries have been shown to undergo morphologic changes, which may be either a

cause or effect of changes in surrounding tissues, including Bruch's membrane and the RPE. According to Ramrattan et al., the area of the capillaries decreases as AMD progresses (54, 55). On the other hand, other investigators, including Spraul and Grossniklaus, have found that the area of the choriocapillaries actually increases through the progression of AMD (4). Both groups measured the perfusion areas of the choriocapillaris in the macula, however, Ramrattan only measured the diameter of the choriocapillaries parallel to Bruch's membrane. Spraul et al. measured diameters both parallel and perpendicular to Bruch's membrane. The method of calculating the perfusion areas may have been the reason for the discrepancy. In either case, choriocapillary change could be an important characteristic of AMD pathogenesis.

Choroidal endothelial cell activation

The term activation is a very broad term. To activate something means to stimulate its activity. In reference to an endothelial cell, this term could mean to stimulate its expression of a particular gene, to stimulate DNA replication in preparation for cell division, to stimulate rearrangements of the actin cytoskeleton in order to move the cell to a new location, or even stimulate the cell to self-destruct. For the purpose of this investigation, endothelial cell activation refers to initiation or promotion of inflammation and angiogenesis.

Inflammation

Inflammation of vascular endothelial cells can be defined as the biological response of these cells to harmful stimuli. Harmful stimuli may include the by-products of nearby cell death, physical irritants such as shear stresses, as well as foreign pathogens. RPE cells are thought to play a major role in providing a local increase of chemotactic stimuli, such as interleukins, capable of initiating inflammatory responses of nearby cells (28, 56). Importantly, many of these peptides are released by the RPE on the basal surface towards the choriocapillaris. Activated choroidal endothelial cells are then

able to assist with the trafficking of leukocytes from the blood into the extracellular matrix. The trafficking of leukocytes into the choroid causes mechanical strain on the endothelial cells being pushed aside during the movement and increases the local concentration of leukocytes in the tissue. Both of these factors can lead to endothelial cell activation.

There are several proteins that are capable of eliciting inflammatory behaviors from endothelial cells. Monocyte chemotactic protein-1 (MCP-1; also known as MCAF) is an 8.5 kDa protein that is important for activating and/or recruiting blood monocytes and tissue macrophages (57).

The cytokines, interleukins 1 and 6 (IL-1 and IL-6), are secreted by macrophages and dendritic cells (IL-1) or by T-cells and lymphocytes (IL-6). Both molecules are associated with the up-regulation of cell surface adhesion molecules, which are in turn responsible for enabling the transmigration of leukocytes across the vascular cells.

In addition to cytokines, molecules that physically aid in the extravasation of leukocytes from the blood to surrounding tissues are upregulated in endothelial cell activation including VAP-1, ICAM-1, VCAM-1, PECAM-1, and L-sel. During this investigation, these proteins were investigated as a measure of endothelial cell activation in regards to inflammation.

Vascular adhesion protein-1 (VAP-1) is a sialylated homodimeric semicarbazide-sensitive monoamine oxidase (SSAO), which also functions as an adhesion molecule (58-60). The adhesive property of VAP-1 plays an essential role in the adhesion of lymphocytes to the endothelium during an inflammatory response, though its mechanism of activity is not clear (59). It is disputed whether the oxidative activity of the protein is required for its ability to bind lymphocytes (61-63). In culture, Salmi et al. found the enzymatic activity to be independent of binding lymphocytes, however this mechanism may differ from that occurring *in vivo*.

Intercellular adhesion molecule-1 (ICAM-1) is a type-1 trans-membrane protein, which adheres monocytes, lymphocytes and neutrophils to activated endothelium during the inflammatory response. ICAM-1 also helps leucocytes migrate from the lumen of the blood vessels into the inflammatory sites of the surrounding tissues (64, 65). There is added interest in ICAM-1 in AMD because our laboratory has shown that there is higher human choroid ICAM-1 expression in the macula than in the periphery (65). This distribution may pre-dispose the macula to higher levels of inflammation than the periphery, playing a role in the geographic discrimination of AMD to this region.

Vascular cell adhesion molecule-1 (VCAM-1) is a type-1 trans-membrane immunoglobulin that also adheres monocytes, lymphocytes and eosinophils to activated endothelium during inflammation. VCAM-1 is responsible for the tethering and rolling of lymphocytes before they migrate from the lumen of the blood vessel into the surrounding tissues (64).

Platelet endothelial cell adhesion molecule-1 (PECAM-1) is type-1 trans-membrane immunoglobulin which adheres to other PECAM-1 molecules through homophilic interactions, mediating leucocyte extravasation and vascular development (64).

L-selectin (L-sel) is a type-1 transmembrane protein on the surface of leukocytes that binds ligands on endothelial cells during the rolling and tethering process of leukocyte adhesion and translocation to tissues during inflammatory processes (64).

In recent studies, AMD has been shown to exhibit many similarities to the inflammatory response of the endothelium in disease states, such as atherosclerosis (1, 65). Inflammatory markers commonly up-regulated by activated endothelium outside of the eye include intercellular adhesion molecule-1 (ICAM-1) (64-67), vascular cell adhesion molecule (VCAM) (64), interleukin-6 (IL-6) (1), interleukin-1 (IL-1) (68), platelet endothelial cell adhesion molecule-1 (CD31 or PECAM-1) (64), monocyte

chemotactic protein-1 (MCP-1) (69), and vascular adhesion protein-1 (VAP-1) (1, 58-62, 64).

Understanding the role of endothelial cell activation in AMD, and its interface with environmental challenges such as elastin fragments, complement proteins, and angiogenin offers a spectrum of promising targets for inactivating the inflammatory response cascade, thereby halting the possibility of angiogenesis and further tissue pathogenesis.

Angiogenesis

Angiogenesis is defined as the growth of new blood vessels from pre-existing blood vessels (70). Angiogenesis is a process made up of three major steps (Figure 7). First, the vascular basement membrane has to be weakened or broken down. This step eliminates the mechanical barrier that normally keeps endothelial cells stationary within the vessel wall. Second, endothelial cells proliferate and migrate past the compromised basement membrane and into the extra-vascular space. Third, the cells form junctions with adjacent cells and form tubes, which permits the flow of blood.

The process of angiogenesis occurs in response to growth factors released by proliferating tissues in need of vascular perfusion. For example, malignant tumors induce angiogenesis in order to support their growth. Chemokines released in response to endothelial cell activation and/or the inflammatory responses are capable of initiating angiogenesis (71). Common growth factors involved in angiogenesis include interleukin 8 (IL-8), angiopoietins 1 and 2 (ANG-1, ANG-2), vascular endothelial growth factor (VEGF), fibroblast growth factor (FGF), and monocyte chemotactic protein 1 (MCP-1) (41, 69, 72, 73).

VEGF has received the most attention of these proteins in regards to neovascularization in AMD. During hypoxic conditions, cells stop destroying hypoxia-inducible factor (HIF), which is a transcription factor that increases the release of VEGF.

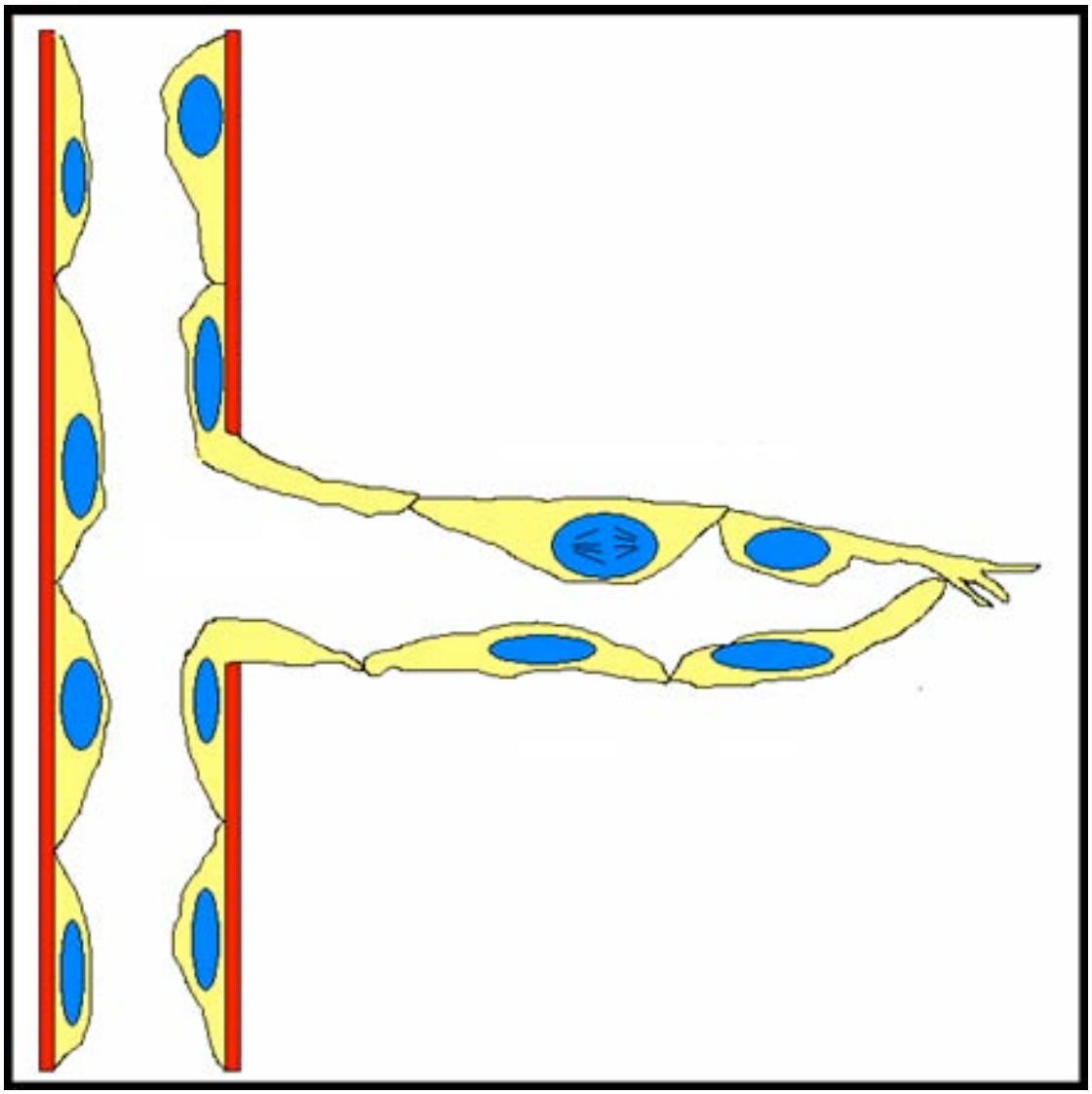

Figure 7. Angiogenesis. The process of new blood vessel growth begins by the breaking of the basement membrane, shown in red. Endothelial cells must then migrate and proliferate away from the existing vessel into a new area. Finally, the cells form junctions with adjacent cells in the formation of tubes.

Acting as an activator of endothelial cells, VEGF binds to either of its two major receptors, VEGFR-1 or VEGFR-2, and triggers a tyrosine kinase cascade, which results in angiogenic behaviors of the endothelial cell (74). In conjunction with inflammation, macrophages may stimulate the cells in the RPE to release VEGF, or release it themselves, which may stimulate the nearby choriocapillary endothelial cells to proliferate (75). Current treatments for neovascular AMD are directed at blocking either the VEGF protein from binding its receptors or altering the function of tyrosine kinases, as described in more detail below.

Choroidal neovascularization in other diseases

Neovascular AMD is not the only disorder in the eye that is complicated by the growth of new blood vessels. Other disorders include diabetic retinopathy, pseudoxanthoma elasticum (PXE), and retinopathy of prematurity (76-78).

Diabetic retinopathy (DR) is the pathology of the retina associated with diabetes mellitus. The early stages of this disease are characterized by the loss of pericytes, thickening of capillary basement membranes, and an increased level of VEGF in the vitreous (79-81). As the disease progresses, endothelial cells proliferate and neovascularization of the inner retina occurs. This is known as proliferative diabetic retinopathy (PDR) and can cause an insult to visual acuity due to retinal thickening and the breakdown of the retinal/blood barrier. The major hypothesis regarding the change from regular DR to PDR is that as the pericyte population decreases in the retina, there are fewer cells preventing endothelial cells from migrating and proliferating. Pericytes are similar to smooth muscle cells, which encompass the endothelial cells of the retina and choroid (82, 83). They provide structural stability to vessels in these tissues, while preventing them from growing abnormally (84). In endothelial-specific platelet endothelial growth factor (PEDF) knockout mice, the retinal pericyte population is decreased by more than 50% causing neovascularization of the retina that recapitulates

the pathologic proliferation found in human PDR patients (85). Therefore, as the mechanical barrier to angiogenesis decreases in its integrity (a theme common to Bruch's membrane in neovascular AMD), in DR, proliferation may occur.

Pseudoxanthoma elasticum (PXE) is a disease associated with loss of function mutations in the *ABCC6* gene (86-88). This is an autosomal recessive disorder which results in the accumulation of mineralized and fragmented elastic fibers in tissues such as the skin, arterial walls, and Bruch's membrane (89). Fragmented elastin fibers in Bruch's membrane result in breaks in the membrane known as angioid streaks. These regions are often complicated by choroidal neovascularization through Bruch's membrane into the subretinal space (40, 90). The neovascular membranes in PXE patients respond well to anti-VEGF therapies commonly used for neovascular AMD patients (91, 92), indicating similarities in the pathologies of these two diseases.

Retinopathy of prematurity (ROP) is one of the leading causes of blindness in children (79). The main characteristic of this disease is pathologic retinal neovascularization. This phenomenon occurs in premature babies who spent time in an enriched oxygen environment during the later phases of retinal development. Due to the higher level of oxygen present, normal angiogenic proteins are downregulated and the retina vasculature does not develop to the extent of which it would have under normal oxygen conditions. When the babies are removed from the oxygen rich environment, their retina undergoes hypoxic conditions due to the underdeveloped vasculature. This induces angiogenesis of the vasculature between the inner retina and the non-vascularized outer retina (93-95). The new vasculature can cause retinal scarring as well as retinal detachment, both of which can lead to early decreases in visual acuity if not blindness (94).

All of these diseases have possible neovascular manifestations, which can lead to dramatic declines in visual acuity. Although there are current treatments for the decrease or removal of these membranes, they are not complete cures because they only treat

membranes that already exist rather than prevent them from developing in the first place. Understanding more about the mechanisms by which endothelial cells become activated to undergo pathologic behaviors will provide insight for the possible treatments of all of these neovascular diseases in the future.

Treatments for neovascular AMD

Currently, treatments for neovascular AMD are targeted at existing membranes rather than preventing the membranes from forming. Common treatments include triamcinolone acetonide, anecortave acetate, and anti-VEGF therapies. The angiostatic steroids (triamcinolone acetonide and anecortave acetate) are effective in blocking neovascular membranes from forming by inhibiting angiogenesis, however these therapies have dangerous side effects including elevated intraocular pressure and cataract formation (28, 96). The effectiveness of anti-inflammatory treatments in halting pathologic angiogenesis supports the theory that the pathologic growth of blood vessels in wet AMD is associated with inflammation.

Therapies directed at preventing the action of VEGF-induced angiogenesis are currently the most common treatment for neovascular membranes in AMD patients. There are two types of therapies used to target the VEGF pathway. The first type uses anti-VEGF antibodies injected into the vitreous of the patient in order to prevent VEGF from binding to its receptors on the surface of endothelial cells. The two available products for this type of treatment are bevacazumab (Avastin), which is an anti-VEGF antibody suspension (97), and ranibizumab (Lucentis), which is an anti-VEGF antibody derivative suspension (98). These therapies have had great success in treating neovascular membranes in AMD patients for a short period of time (44, 99, 100). Over an extended period of time, there is recent evidence that this therapy may not continue to benefit patients (101). The second therapy targets the tyrosine kinase signaling cascade activated by the binding of VEGF to its receptor, preventing transcription of angiogenic

proteins by the endothelial cell. Current products include lapatinib (Tykerb), sunitinib (Sutent), and sorafenib (Nexavar), all of which are orally administered. These products offer a less invasive solution to the anti-VEGF therapies, however determining their effectiveness requires further trials (102).

Hypotheses for thesis investigations

1. *Endothelial cell activation causes development of CNVM.*
2. *Primary human choroidal endothelial cells provide an effective platform for modeling events that occur during CNVM formation.*
3. *Elastin fragments, C5a, and angiogenin promote choroidal endothelial cell activation.*

Most individuals with AMD do not develop neovascular membranes, however, roughly 10% do. The mechanisms underlying this phenomenon are poorly understood. Even the order of events in CNVM pathogenesis is poorly understood. Does capillary death cause a local decrease in metabolites and waste removal, resulting in RPE and retinal cell death and deposits to form? Or does the RPE and retinal atrophy cause a cessation of need for the choriocapillaris, and therefore these vessels dry up? These are questions that we will try to address in the following chapters of this thesis.

The choriocapillaris, Bruch's membrane, the RPE, and retinal outer segments form a highly organized and inter-dependent group of tissues. We hypothesize that neovascular membrane formation occurs with primary activation of the endothelial cell. In general, for angiogenesis to occur the endothelial cells from existing vessels would break down the restraining basement membrane, proliferate, migrate, and then start forming tubes, which will provide a new avenue for blood flow. In the eye, histological studies have shown that the choriocapillaries often serve as the pre-existing vessels from

which new pathologic vessels stem. These vessels grow through Bruch's membrane and into the sub-RPE and/or sub-retinal spaces. This form of angiogenesis follows the general pattern with a few differences.

First, Bruch's membrane is not a simple basement membrane. It is composed of two basement membranes, as well as two layers of collagen and a single layer of elastin. New vessels have to break through all five of these layers instead of only one basement membrane. It seems as though this barrier would be impermeable to migrating endothelial cells. In AMD, it has been demonstrated with TEM observations that the central layer (elastic layer) of Bruch's membrane is thinner than normal as well as more fragmented (22, 47, 50-52). It is also important to remember that the elastic layer is thinner in the macula than the periphery in normal patients (22). This pre-disposes the macula in contrast to other regions to possible weakness in the limiting properties of the membrane. Combining these characteristics, it is possible for the endothelial cells to break through weak parts of the membrane and enter the sub-RPE/retinal space.

Second, in order for endothelial cells to become inflammatory or angiogenic, they must be activated. There are several proteins capable of activating endothelial cells from different tissues. This body of research focuses on how choroidal endothelial cells are affected by proteins associated with AMD.

Overall, in AMD, we hypothesize that local increases in endothelial cell stimulatory proteins and decreases in inhibitory proteins increase their angiogenic and inflammatory behaviors. Both of these behaviors are commonly attributed to pathologic endothelial cells in neovascular AMD. Compounded with the decreasing integrity of Bruch's membrane during the progression of the disease, new vessels eventually branch off of the pre-existing choriocapillaries and grow into the sub-RPE/retinal space. Over time, these vessels form networks of vasculature while devastating the form and function of the retina and RPE (Figure 8). For this investigation, we sought to demonstrate that elastin-derived peptides, complement component C5a, and angiogenin are capable of

Figure 8. Neovascular membrane formation. Illustration of hypothesized neovascular membrane formation in AMD. With the progression of the disease in combination with normal aging, changes occur in Bruch's membrane including the deposition of foreign material and matrix turnover of the individual layers. This may render the membrane more susceptible to the pathologic growth of blood vessels from the choroid into the sub-retinal space.

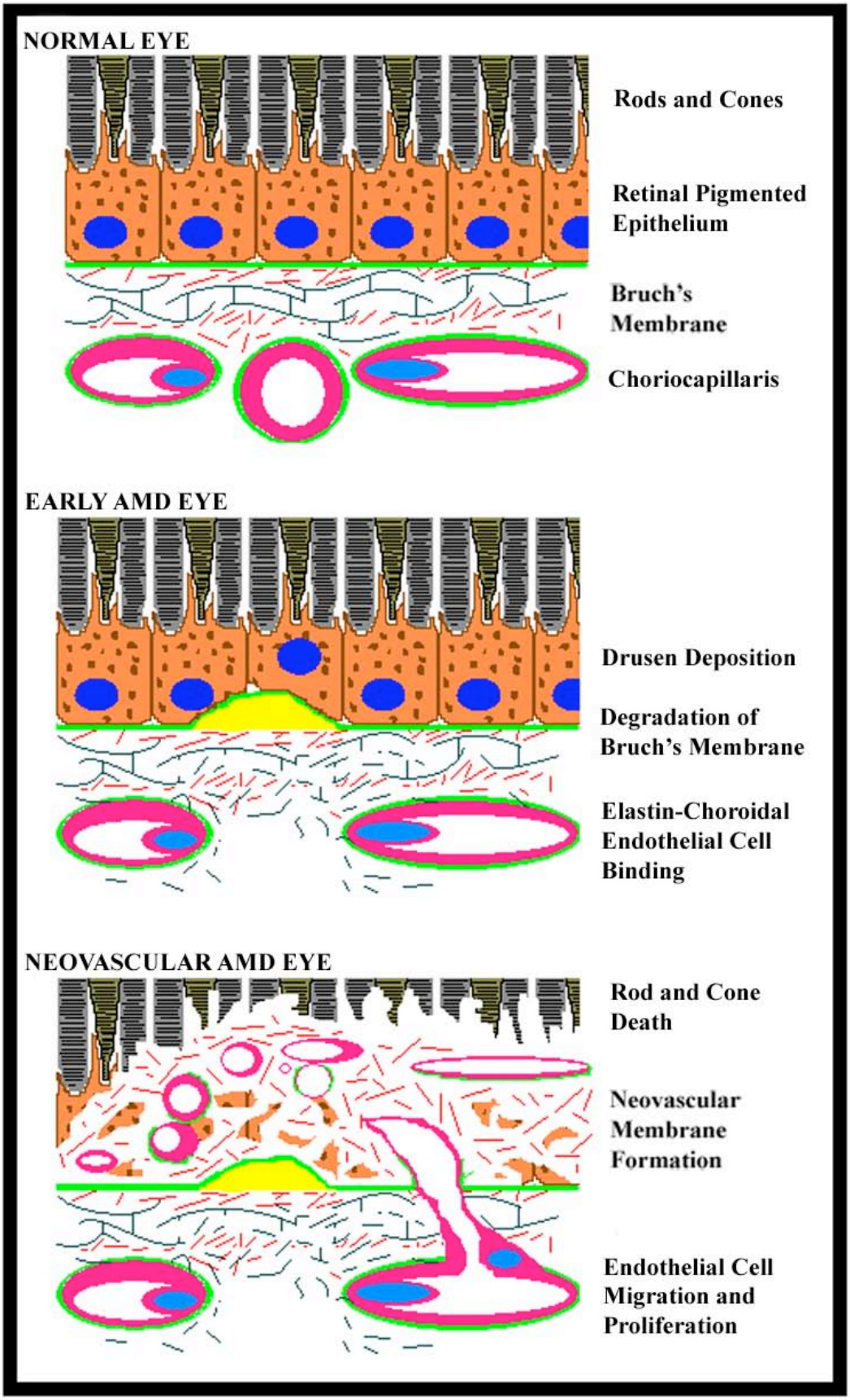

activating choroidal endothelial cells in culture by increasing their angiogenic and/or inflammatory behaviors.

Complement component C5a was chosen because recent findings have shown important correlations between complement system protein gene mutations and the risk for developing AMD. Complement proteins have also been shown to be present in

drusen, a landmark characteristic of AMD (30), demonstrating the presence of these proteins during the pathology of the disease. Since C5a is a by-product of the enzymatic cleavage of protein C5, it was not a goal to find any genetic correlation between mutations in its gene (which does not exist other than as a part of the gene for C5), but rather to determine the effects of elevated levels of this protein.

Angiogenin was chosen based on the fact that it increases angiogenesis in many other disease mechanisms, however, no one has determined its expression or impact with respect to the human eye. This was a novel protein to investigate with the base hypothesis that this protein may affect pathologic angiogenesis in AMD.

Finally, EDPs were chosen because in 2005, it was found that patients with AMD had higher serum levels of EDPs than control patients (183), and patients with CNVMs had even higher concentrations than AMD patients without CNVM. Determining if these fragments play a role in the behavior of endothelial cells during AMD progression became a large portion of this set of investigations.

The initial barrier to overcome for this research project was to obtain cell cultures. The commercially available cell line, Rf/6a, is the closest cell type to human choroidal endothelial cells. This cell line is from rhesus monkey and is composed of both retinal and choroidal endothelial cells. This poses a problem in the fact that retinal and choroidal endothelial cells are very different cell types physiologically. It was therefore important to initiate primary human cell cultures from the choroid only (Chapter 2). These cultures provided an essential platform for studying the effects of individual proteins on the human choroid in a very controlled and reproducible means. The proteins

of interest included C5a (Chapter 3), angiogenin (Chapter 4), and elastin-derived fragments (Chapter 5). Our interest in these proteins stemmed from previous findings associating them with AMD (elastin peptides and C5a) or because of novel theories (angiogenin).

To determine if angiogenic and inflammatory behaviors were changed by our endothelial cell cultures, we set up experiments that would allow for separate analysis of migration, proliferation, and expression of inflammatory markers. The assay utilized for the study of migration was a Boyden chamber assay (Chapter 3). To study proliferation, cells were counted after being exposed to activating proteins by a flow cytometer. Several techniques were used to determine the changes in inflammatory protein expression including quantitative PCR, immunohistochemistry, immunoblotting, and gene expression arrays, as described in chapters 3-7. It is our hypothesis that these proteins will individually increase at least one of these behaviors directly, indicating a role in endothelial cell activation, which could become pathogenic during the progression of AMD. Based on previous studies in microvascular cells from other systems, we thought elastin fragments would increase both proliferation and migration, C5a would increase migration, proliferation and inflammatory protein expression, and angiogenin would increase migration and proliferation.

Aside from cell cultures, we also developed an *in vivo* experiment in aged mice where the level of elastin derived peptides was held at a higher serum level than in control littermates. If elastin peptides are able to activate endothelial cells to migrate and proliferate, it is hypothesized that this activation would cause endothelial cells to invade an aged and possibly compromised Bruch's membrane. If Bruch's membrane is not compromised in the aging mouse as it is in the aging human, we hypothesized that endothelial cells would be noticeably different in treated mice, having features of an activated state. This difference may be a morphological change indicating migration or a breakdown of the capillary basement membrane indicating future angiogenesis.

The following details of our investigations outline the role of elastin fragments, complement component C5a, and angiogenin in activating choroidal endothelial cells. Our results indicate different and important roles of all three of these proteins in the pathophysiology of the endothelial cell in AMD. These findings provide several avenues for future alternative/supplemental therapies for this devastating disease.

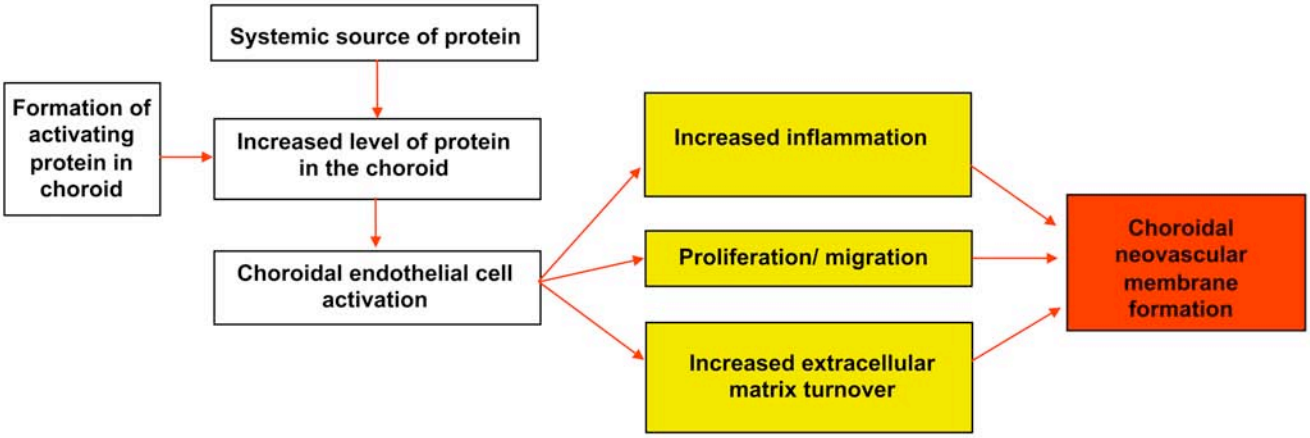

Figure 9. Flow chart of thesis hypotheses.

CHAPTER 2. CULTURE OF CHOROIDAL ENDOTHELIAL CELLS

Introduction

Human choroidal endothelial cells are likely to play a role in the inflammatory response as well as angiogenesis *in vivo* during the progression of AMD. There are several different ways to investigate whether or not this is true. The two most common are *in vitro* using purified cell cultures and *in vivo* using animal models. Both of these techniques offer their own strengths and weaknesses. Purified choroidal endothelial cell cultures provide a means to study the changes in gene expression, protein expression, and behavior of one cell type directly. Experiments are easy to control and reproduce because there are very few variables. Cells also reproduce at a reasonable rate, allowing for several experiments to be performed in a relatively short period of time. The drawback to this method is that there currently is no commercially available endothelial cell line derived from the human choroid. Using these cells *in vitro* as a model of vascular endothelium will allow for the study of their responses to microenvironmental stimuli that occur in eyes with AMD.

Endothelial cells from different tissues differ in culture requirements including types of growth supplement and types of extracellular protein composition (103-105). Endothelial cells from different tissues also differ in cellular junctions, antigenic protein expression, morphology, and function (104). It is because of all of these reasons that cells from one tissue should not be utilized to investigate properties of a disease mechanism in another tissue. However, this practice is common with regard to investigating pathologies of the choroid because microvascular endothelial cells have proven extremely difficult to culture. This is due to pericyte cell culture contamination, cell sensitivity to digestion enzymes, and mechanical damage from dissection from original tissues (103).

Despite their difficulty to culture, choroidal endothelial cells are desired for experimentation because they are expected to model the ocular endothelium *in vivo* much better than extraocular, large vessel endothelial cells such as human umbilical vein endothelial cells (HUVECs). HUVECs have been commonly used *in vitro* to study many different diseases because umbilical veins are easy to access, the cells are easy to initially isolate, and the cultures reach a high level of purity without difficulty. Primary endothelial cell cultures from the human eye are far more difficult to obtain in comparison because human donor tissue is not as freely available as umbilical veins, and the desired cells are often contaminated with many pericytes and fibroblasts. Pericytes and fibroblasts both metabolize and proliferate at greater rates in culture than endothelial cells so it is very hard for them to thrive in the presence of contaminating cells. Another problem with the primary endothelial cell cultures from the eye is that they differentiate into fibroblast-like cells within a few passages of culture. Therefore cells need to be purified and used for experimentation as soon after initial isolation as possible.

The recommended isolation and purification techniques for endothelial cells vary drastically. Initial isolation may be done mechanically with a scalpel or enzymatically with trypsin or collagenase II. Purification can also be done mechanically by scraping desired cultures from a dish and re-plating them or with immunomagnetic beads (105). Following isolation and purification, growth conditions differ as well. There are several recommendations for the type of basal medium, growth supplements, and plate surface coating to use. Since the choroidal endothelial cells from human donor eyes have not been cultured very many times, there is little evidence that any technique is better than another. It was the first objective of this thesis project to establish a reliable protocol for the isolation, purification, amplification, and continued maintenance of endothelial cell cultures from the human choroid.

Materials and methods

Endothelial cell isolation

Primary human choroidal endothelial cells were cultured to provide a research platform for neovascular AMD. Human eyes are obtained from the Iowa Lions Eye Bank following informed consent. We have developed a strong relationship with the Lions Eye Bank in which The Carver Family Center for Macular Degeneration scientists receive approximately 65 sets of eyes each year.

Choroidal endothelial cell cultures were prepared using methods similar to those described by other investigators (104, 106) except that we used PECAM-1-coated magnetic beads (107, 108) instead of lectin-coated Dynabeads. Human eyes (whole globes or posterior poles) were collected by the Iowa Lions Eye Bank and were dissected according to a standard protocol in which posterior poles were cut into 4 fragments. The neural retina was removed and frozen for other studies. The RPE was gently scraped with a scalpel while care was taken to keep the choroid attached to the sclera. The choroid was peeled from the sclera and inverted, and the outer choroid and its large vessels were removed by gentle brushing with a camel's hair brush under Hank's balanced salt solution (HBSS). The choroid was transferred to a clean Petri dish containing Hanks balanced salt solution and minced with scissors into pieces approximately $1mm^2$. These fragments were digested in 2 mg/mL collagenase (Invitrogen, Eugene, OR) in HBSS for 1 hour at 37^oC with vigorous agitation and fragments and isolated cells were pelleted at 700xg for 5 minutes; washed, and re-centrifuged. Pellets were resuspended in HBSS and passed over a 70µm nylon filter (Becton Dickinson, San Jose, CA). Cells that passed through this membrane (single cells) are primarily fibroblasts, melanocytes, remnant RPE cells, red blood cells, and endothelial cells. The cells collected in the flow through fraction were resuspended in HBSS and 1 mL of cell suspension, mixed with 25µL of freshly washed anti-PECAM-1

Dynabeads (Dynal Biotech, Oslo, Norway). Cells were incubated with Dynabeads in a cold room (~4°C) for 45 minutes on a rotary mixer. Cells adhering to the magnetic beads were collected on the side of the tube with a Dynal MPC-S magnet while the supernatant was decanted. Cells and beads were washed 3x, followed by plating in Conetics EGM-2 MV microvascular endothelial cell medium (Lonza, Walkersville, MD) and kept at 37 degrees C, 95% humidity, 5% carbon dioxide. Medium was changed 2x/week.

Determining cell culture purity using immunocytochemistry

Before cell cultures were used in research studies, their endothelial cell purity needed to be determined. Purity was assessed by immunocytochemistry on subcultures plated on 12 mm glass coverslips using either monoclonal anti-PECAM-1 (Developmental Studies Hybridoma Bank, University of Iowa, Iowa City, IA) or *Ulex europaeus* agglutinin I (UEA-1 lectin) (Vector Laboratories Inc., Burlingame, CA). Cells were fixed with 4% paraformaldehyde, pH 7.4, for 10 minutes. For anti-PECAM-1 labeling, cells were blocked with 0.1% bovine serum albumin (BSA) for 15 minutes, followed by 1 rinse in PBS. Cells were then incubated with 5.5 µg/mL of anti-PECAM-1 for 1 hour, followed by 3x5 minute rinses in PBS. Next, cells were incubated with 20 µg/mL donkey anti-mouse Alexa-Fluor 488 (Invitrogen, Eugene, OR) diluted in PBS and 100 µg/mL 4',6-diamidino-2-phenylindole (DAPI) nucleic acid stain for 30 minutes, followed by 3x5 minutes in PBS. Coverslips were mounted onto a glass slide with Aqua-Mount (Lerner Laboratories, Pittsburg, PA). UEA-1 cytochemistry was performed as described previously (46). Briefly, human choroidal endothelial cells were blocked with 0.1% BSA for 15 minutes, followed by 1 rinse in PBS. Cells were then incubated with 40 µg/mL of UEA-1 for 30 minutes, followed by 3x5 minute rinses in PBS. Next, cells were incubated with 25 µg/mL avidin-Texas red (Vector Laboratories Inc., Burlingame, CA) diluted in PBS and 100 µg/mL DAPI nucleic acid stain for 30 minutes, followed by

3x5 minutes in PBS. For UEA-1 cytochemistry, the divalent cations $CaCl_2$ and $MgCl_2$ were added to all solutions at 1 mM each. Coverslips were mounted onto a glass slide with Aquamount (Lerner Laboratories, Pittsburgh, PA). All steps were performed in a humidified chamber to prevent drying of cells. Observations were made using an Olympus BX-41 microscope with fluorescence attachments equipped with a SPOT-RT digital camera. Cell cultures used for experiments were chosen based on positive staining with CD31 and UEA-1, as shown in Figure 10.

Acetylated low density lipoprotein assay

The phagocytosis of acetylated low-density lipoprotein (ac-LDL) is a characteristic of endothelial cells and macrophages (109). In a culture of unknown cells, this attribute can be used to differentiate endothelial cells from smooth muscle cells, pericytes, and fibroblasts. Human cell cultures from the choroid were grown on round glass coverslips placed within a 12 well culture plate in F12 basal medium supplemented with 1% FBS and 1% penicillin/streptomycin. The cells were not grown to confluency in order to assure their capability to phagocytose macromolecules from the surrounding medium. The medium was removed and the cells were rinsed with fresh medium. Then the cells were incubated with 10 μg/mL ac-LDL conjugated to Alexa Fluor 488 (Invitrogen, Eugene, OR) diluted in culture medium for 4 hours at 37°C (104, 110). Control cells were incubated with fresh medium only. Following incubation, the cells were rinsed with fresh culture medium 3x and incubated with new medium for 16 hours at 37°C. After incubation, cells were rinsed 3x in fresh medium and fixed with 4% paraformaldehyde (pH 7.4) for ten minutes. Coverslips were incubated with the nuclear counterstain DAPI (4'-6-diamidino-2-phenylindole) for 30 minutes and rinsed in PBS 3x5 minutes. Coverslips were rinsed with distilled water and then mounted onto a glass slide using Aquamount (Lerner Laboratories). Observations were made using an Olympus BX-41 microscope with fluorescence attachments and SPOT-RT digital camera.

Choroid organ culture

We also desired to study choroidal endothelial cells in their native environment so organ cultures were used for some investigations. Choroid samples were collected using a 4 mm biopsy punch after the retina and vitreous were removed. If it was desired to remove the RPE cells from the choroid tissue, these cells were gently scraped away using a scalpel before the 4 mm punch was taken. The sclera was removed from the punched tissue, which was then placed into Dulbecco's Modified Eagle Medium (DMEM) supplemented with 10% FBS and 1% penicillin/streptomycin in a 96-well culture plate at 37^{o}C.

Results

Anti-PECAM-1 and UEA-1 labeling

Most of the cells isolated and purified with the above methodology had intense anti-PECAM-1 and UEA-1 labeling (Figure 10). This labeling was unique to endothelial cells and was not noticed on cells that were incubated with secondary antibody only. For experimentation, cultures were only used if more than 95% of the cells had strong anti-PECAM-1 and UEA-1 labeling.

Ac-LDL internalization assay

Cells that had been incubated with the Alexa Fluor 488 ac-LDL had obvious green punctate labeling within the cytoplasm of the cell in comparison to the control cells (Figure 11). This pattern indicates that the ac-LDL was internalized into the cell and remains within the cytoplasm in small vesicles. Experiments for this thesis were conducted with cultures of cells that demonstrated this ac-LDL internalization pattern.

Endothelial cell morphology

Observing the cell cultures, they had various morphologies when they were not confluent. They were not long and linear, typical of fibroblast cells. Instead, they had a

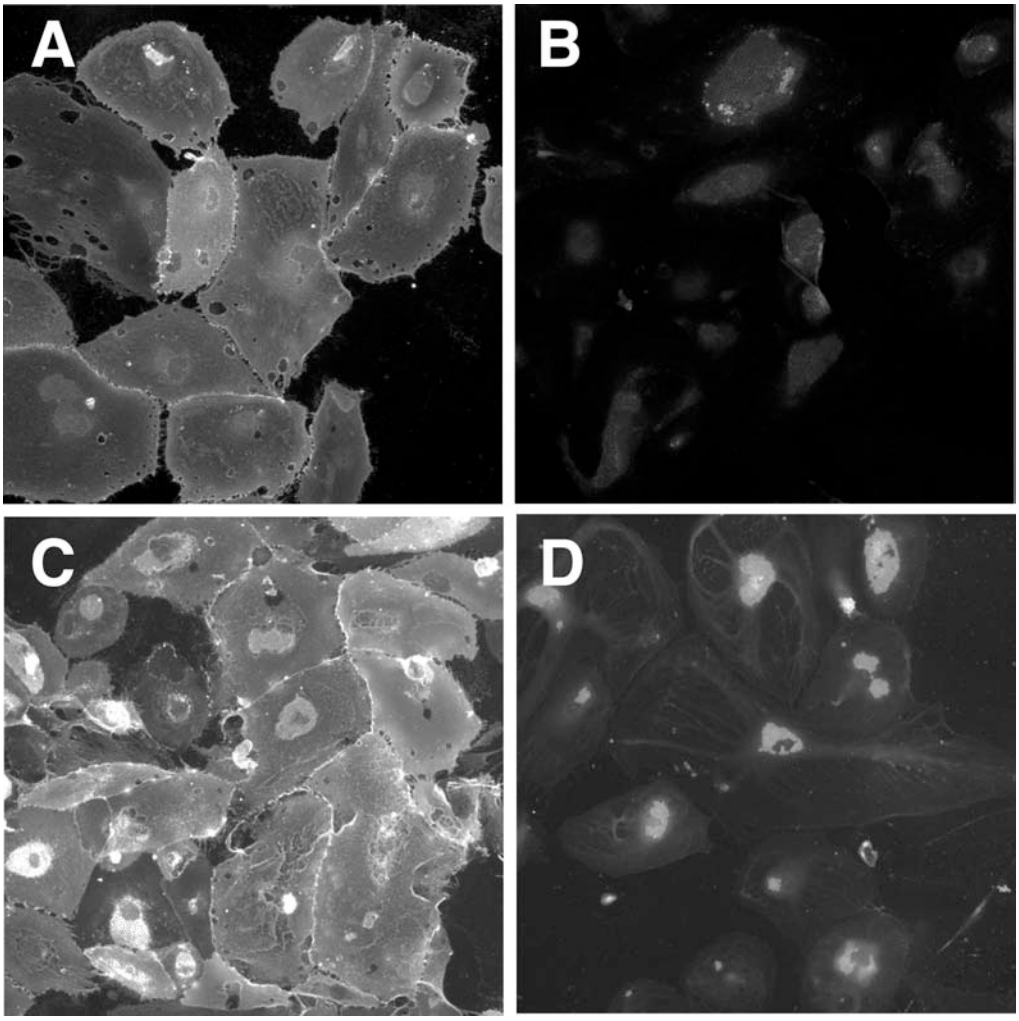

Figure 10. Endothelial cell identification. Staining of human choroidal endothelial cell primary cultures with anti-CD31 antibodies (A) or the lectin UEA-I (C). Cells that stained positively for these markers were utilized in migration assays. Controls are shown for anti-CD31 (B) and UEA-1 (D).

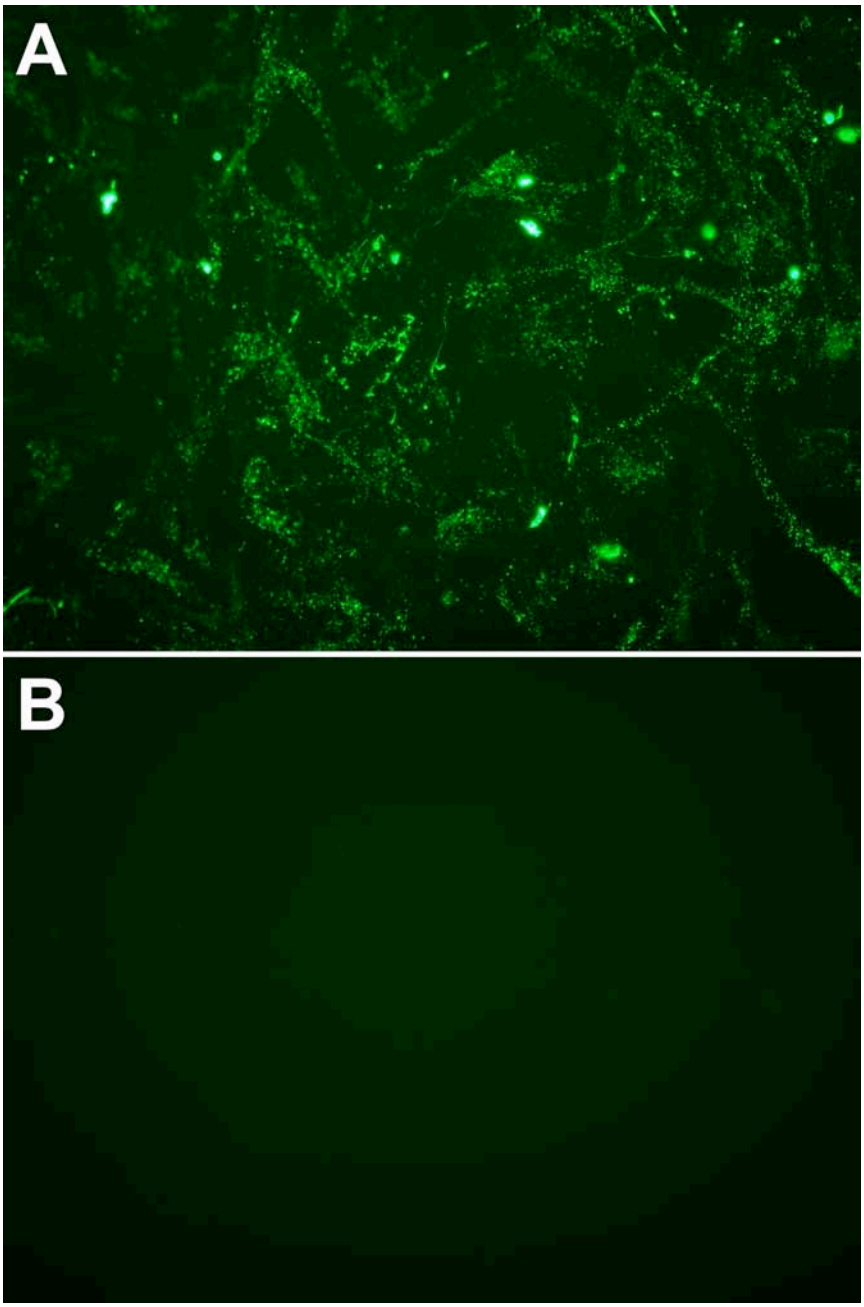

Figure 11. Endothelial cell ac-LDL internalization. The ability to internalize ac-LDL is another means of identifying endothelial cells populations when determining cell purity in a population of different cell types. Ac-LDL is shown in green. The cell cultures used for investigations in this thesis had greater than 95% of the cells able to internalize ac-LDL, as shown in (A). Control cells were not exposed to ac-LDL-488 (B).

generally round shape with some projections outward from the cell body. This morphology was indicative of the cell cytoskeleton rearranging in order for the cell to move along the culture plate. This morphology was only typical of cells found adhered to the plate alone. Once cells became confluent, they obtained a very round consistent morphology (figure 12). This morphology is referred to as the "cobblestone" morphology, which is the hallmark characteristic of endothelial cells in culture (111).

Choriocapillaris organ culture

Following 24 hours of incubation outside of the eye, the histology of the choroid was similar to tissue fixed immediately after removal. There were no signs of tissue atrophy. Sections used for morphometric analysis (Chapter 3) had antigen preservation by cells, indicating their overall survival and normal function through the culture process.

Discussion

We have initiated cultures from five donors without signs of ophthalmologic disease. Cells were stained with antibodies directed against PECAM-1 and with vascular specific lectin UEA-I. Anti-PECAM-1 and UEA-1 labeled flattened, round endothelial cells, many of which still possessed beads clumped on their cell surface (figure 10). Following re-selection with anti-PECAM-1 coated beads, pigmented cells and cells with fibroblast-like morphology were absent from the cultures, with approximately 99% of the cultured cells staining positive for anti-PECAM-1 and UEA-1.

Following the isolation, purification, and histochemistry steps, cells were tested for the ability to internalize ac-LDL. There are two types of cells that are able to internalize ac-LDL more efficiently than any other cell type, endothelial cells and macrophages (109). The cells observed had internalized a large amount of ac-LDL but did not have multi-lobed nuclei. From this result, it was concluded that the cultures were nearly pure endothelial cell cultures, without pericyte, fibroblast, RPE, or macrophage

Figure 12. Endothelial cell morphology. The human choroidal endothelial cells cultured for this thesis work had a very distinct cobblestone morphology after reaching confluency. This morphology is common to endothelial cell cultures and was used as an indicator of the culture purity.

contamination. This conclusion was finally supported by the observed cobblestone morphology of the cells when they were confluent.

In addition to the endothelial cell cultures, organ cultures were beneficial because they allowed for the study of endothelial cells within their natural extracellular matrix, surrounded by present pericytes and fibroblasts: factors likely to help the endothelial retain its natural phenotypes. The isolation of endothelial cells in culture is different than the *in vivo* environment, despite all of the attempts made to mimic *in vivo* qualities as closely as possible. Due to this difference, the endothelial cell differentiates over time, exhibiting features representative of other cell types. Organ cultures would be desired for all experiments, however, it would be difficult to run some functional assays (such as a migration assay as described in chapters 3 and 5) without being able to manipulate and visualize the endothelial cells independently from their natural environment. The other drawback is that these cultures can only be used during the duration of the cell survival. The cells are not amplified for further experimentation. Since the human donor tissue is such a rare and invaluable resource, isolation and amplification of the endothelial cells is the most efficient way to make use of the tissue. These primary human choroidal endothelial cell cultures provide an excellent model for studying the vasculature of the choroid *in vitro.*

CHAPTER 3. ACTIVATION OF CHOROIDAL ENDOTHELIAL CELLS BY COMPLEMENT COMPONENT C5A

Introduction

Age-related macular degeneration (AMD) is a potentially blinding eye disease that affects over one third of the elderly population to some degree (112). This disease affects the macula, the central region of the retina responsible for high acuity visual tasks such as reading and driving. AMD is commonly divided into two classes. The first is atrophic, or 'dry', AMD characterized by the development of sub-RPE deposits known as drusen and atrophy of the retinal pigment epithelium (RPE) that can lead to severe retinal degeneration (3, 30). The second class is called neovascular or 'wet' AMD, because of the extracellular exudation or fluid deposition, which results from choroidal neovascularization. Neovascular AMD is synonymous with the prior development of choroidal neovascularization, disciform ('disc-shaped') scarring in the sub-retinal space, and/or detachment of the RPE which leads to vision loss (4, 26, 27, 33, 35, 43). Neovascular AMD typically occurs later in the pathogenesis of the disease, and has an acute and often profound reduction in visual acuity.

The complement system is part of the innate immune system, and is comprised of a diverse array of structural proteins and enzymes, which promote or inhibit target cell chemotaxis, cellular activation, lysis, or apoptosis (113-115). Regardless of how they are initiated, complement cascades merge at the proteolytic activation of protein C3. Cleavage of C3 leads to the formation of C3a and C3b. C3b functions cooperatively as a C5 convertase, which cleaves C5 into C5a and C5b. If not inactivated or quenched, the C5b fragment combines with other complement cascade proteins to form the membrane attack complex (also known as terminal complement complex, C5b-9). This cascade is shown in figure 13. The membrane attack complex forms on the surface of target cells,

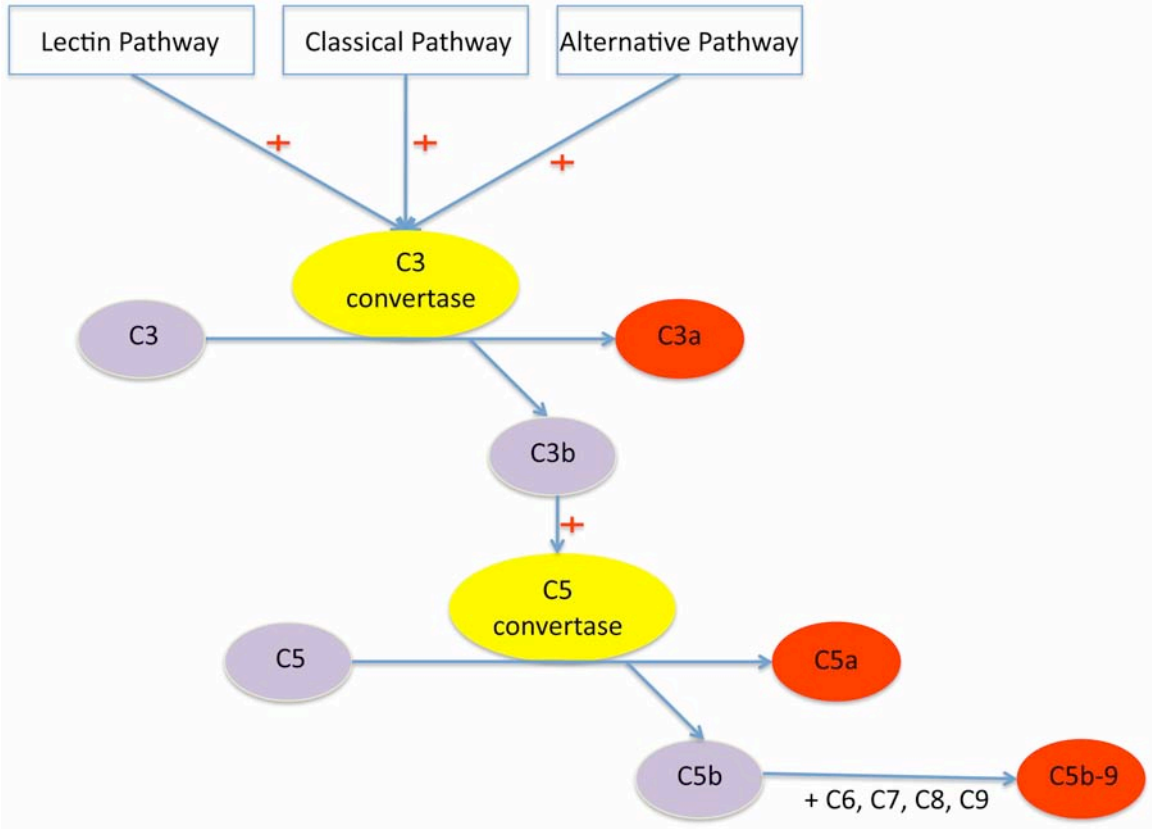

Figure 13. The complement cascade. This illustration shows the three most common initiation pathways, however, there are several others. All of the initiation processes converge at the activation of C3. From here, the cascade can continue toward the development of the membrane attack complex, C5b-9. This complex causes membrane perforation of targeted cells, a process that results in cell death. In the process, two anaphylatoxins are created, C3a and C5a. These soluble peptides are able to bind to and activate cells.

causing their destruction by forming membrane-spanning pores (116, 117). In addition to the membrane attack complex, complement activation results in the formation of anaphylatoxins, C3a and C5a. These N-terminal fragments of complement proteins are capable of promoting inflammation (68). An increase of anaphylatoxin production may cause prolonged cell activation, and an increased level of local inflammation, which may lead to tissue stress. Tissue injury may result from physical increased movement of leukocytes from the blood to the surrounding tissues, increased levels of cytokines, and/or the increased deposition of compounds such as lipids and cellular debris (26, 75, 118).

Several lines of evidence indicate that the complement system is central to the pathogenesis of AMD. These include: C5 and C5b-9 immunohistochemistry of human drusen (29, 31, 119) and CNVMs in a rodent model of neovascular AMD (120); reduced CNVM severity in C3, C3aR and C5aR deficient mice compared to wild-type littermates (120, 121); evidence that C3a and C5a trigger increased secretion of vascular endothelial growth factor (VEGF) by human RPE cells(121); and compelling evidence that genetic variants in complement genes are major risk factors for the development of AMD. One common variant in the CFH gene is associated with increased AMD risk of 2 to 4 fold in heterozygous patients and 5 to 7 fold in homozygotes (122-125). Moreover, variants in other complement genes *C2/CFB(126)*, *C3(127)*, and *SERPING1(128)* have been reported in AMD patients .

Interestingly, although the RPE is generally considered the principal cell type involved in AMD (129), complement deposits are primarily observed in and around the choriocapillaris, with little localization to the RPE (figure 14; see also (125, 130)). In light of the physical association of complement deposits and vascular cells of the choroid, we hypothesized that complement components might act directly on choroidal endothelial cells, through angiogenic and/or inflammatory mechanism(s). In the current study, we sought to determine the effects of complement fragments on the human choriocapillaris

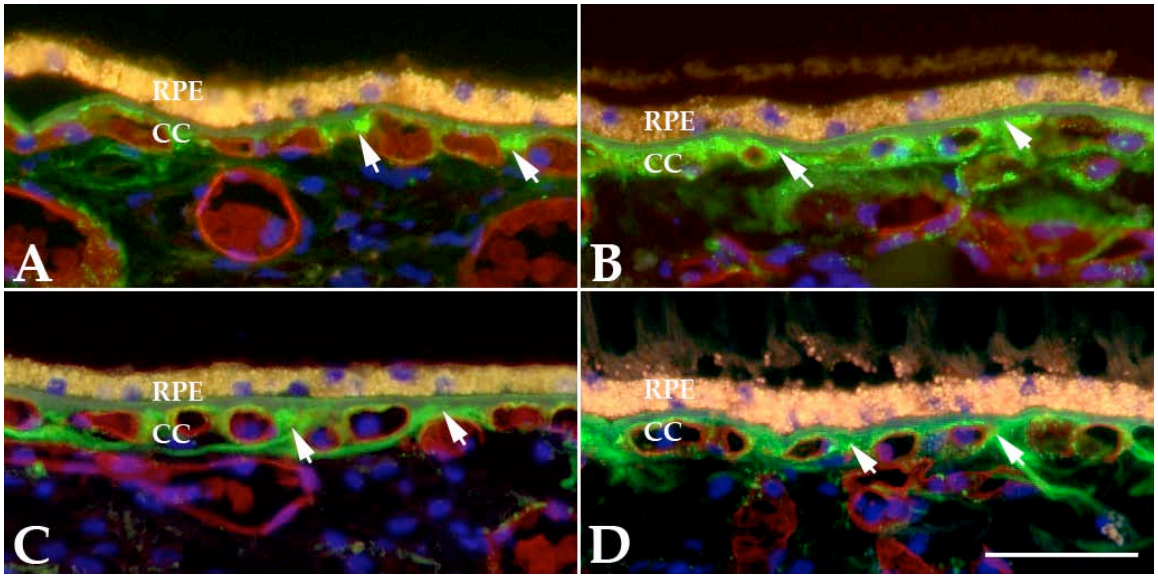

Figure 14. Localization of terminal complement complexes in human eyes. Deposits of C5b-9 complex (arrows, green) are present in Bruch's membrane and around the choriocapillaris (CC), where they may influence choroidal endothelial cell physiology. Red fluorescence represents UEA-I lectin, a vascular stain. A-D depict eyes from four different donors; B shows a 93 year old with early AMD (clinical soft drusen). Autofluorescence at the level of the RPE is due to lipofuscin. Scalebar, 50µm.

and evaluate how these molecules might promote endothelial cell activation in AMD. Our results suggest that complement complexes that form in the macula may result in elevated macrophage recruitment by increasing endothelial expression of intercellular adhesion molecule-1 (ICAM-1). This could serve as an inflammatory trigger, which contributes to the progression of AMD.

Materials and methods

Human choroid/RPE tissue isolation

Human donor eyes were received through the Iowa Lions Eye Bank (Iowa City, Iowa). The anterior portions were removed for other studies and the posterior poles were dissected into four leaflets.

For molecular studies of anaphylatoxin receptor mRNA and protein, 6 mm punches of RPE choroid were collected and frozen within 5 hours of death.

For morphologic studies, tissue sections of 15 human donor eyes, collected within 8 hours of death, were prepared that spanned from the macula to the ora serrata. Tissue wedges were fixed in 4% paraformaldehyde in PBS for 2 hours prior to washing in PBS and embedment, as described previously(131).

For organ culture experiments, the anterior segment was removed under sterile conditions and the neural retina was removed. RPE cells were either gently scraped from the Bruch's membrane/choroid (2 eyes) or left intact (2 eyes). A 4 mm biopsy punch was used to collect 16 samples, 4 from each quadrant of the choroid in paired sets.

C3a and C5a receptor RT-PCR in human choroid and retina

To determine if receptors for either anaphylatoxin, C3a or C5a, are expressed by cells in the retina and/or choroid, receptor RT-PCR was carried out using cDNA from human donor tissues. RNA was isolated from frozen punches of human RPE-choroid and human leukocytes using the RNeasy mini kit according to manufacturer's instructions

(Qiagen, Valencia, CA). Reverse transcription was performed using the High-Capacity cDNA Reverse Transcription Kit (Applied Biosystems, Foster City, CA). PCR was carried out (BIOLASE DNA polymerase kit, Bioline, Taunton, MA) using the following conditions for 35 cycles: denaturing at 94^{o}C for 45 seconds, annealing at 62^{o}C for 30 seconds, and elongation at 72^{o}C for 1 minute. Primers were designed for the amplification of C3a and C5a receptors (C3aR and C5aR): C3aR forward primer, 5'- ACC AGA CAG GAC TCG TGG AG -3', C3aR reverse primer, 5'- CAC TGG CAA ACA TGT TGA GG -3', C5aR forward primer, 5'- ACC TTC GAT CCT CGG GGA GC -3', C5aR reverse primer, 5'- GCG TAC ATG TTG AGC AGG AT -3' (Integrated DNA Technologies, Coralville, IA). Amplified PCR products were separated on a 2% agarose gel (Fisher Biotech horizontal electrophoresis system, Fisher Scientific) and visualized using ethidium bromide under UV light.

C3a and C5a receptor detection with immunoblotting

Even if the mRNAs for anaphylatoxin receptors are present in a tissue, it is necessary to determine if the proteins are created and expressed. This was analyzed using immunoblotting of human retina and choroid. Retinal and RPE/choroid punches from three different human donors were homogenized in PBS with 1% Triton X-100 and complete protease inhibitor (Roche, Indianapolis, IN). 25 µg of protein was mixed with an equal volume of 2X Laemmli buffer, boiled for 5 minutes, and then separated electrophoretically and blotted as described previously(132). Blots were probed with antibodies directed against C3aR and C5aR (Santa Cruz Biotechnology, Santa Cruz, CA) at a concentration of 0.4 µg/mL, followed by washing of the membrane, incubation with 0.4 µg/mL peroxidase-conjugated species-specific secondary antibody (Santa Cruz) and detection using the ECL plus kit (Amersham Biosciences, Little Chalfont, UK).

C3a and C5a receptor localization using immunohistochemistry

To identify the cell types that express the receptors for C3a and C5a in the human eye, immunohistochemistry was performed. Sections of posterior poles spanning from the macula to the ora serrata containing both retina and RPE/choroid were collected at a thickness of 7 micrometers using a Microm HM 505 E cryostat. Sections were blocked in 1% horse serum for 15 minutes. The primary antibodies used were 1) an antibody directed against C3aR raised in goat at a concentration of 4 µg/mL (Santa Cruz; Santa Cruz, CA); 2) an antibody directed against C5aR raised in rabbit (Santa Cruz) at 4 µg/mL; and 3) an additional antibody directed against C5aR raised in mouse (AbD Serotec, Raleigh, NC) at 5 µg/mL. Immunolabeling was performed as described previously(65).

Evaluation of choroidal endothelial cell migration and proliferation in response to C5a

Migration and proliferation assays were performed to determine angiogenic behaviors on two human, primary choroidal endothelial cell lines and a monkey chorioretinal cell line Rf/6a (ATCC, Manassas, VA), as described previously as well as in chapter 5 (133). Briefly, for the migration assays, cells were seeded into the upper chamber of an 8 µm pore culture insert (Millipore, Billerica, MA). Recombinant human protein was added to the medium on the other side of the insert in a Boyden chamber assay (Figure 15) (134). Cells were allowed to migrate for 8 hours and were then counted using scanning electron microscopy. For the proliferation assays, equal concentrations of cells were plated and allowed to grow for 48 hours in medium containing different recombinant proteins or BSA. Cells were counted using a BD LSR II flow cytometer at the University of Iowa Flow Cytometry Facility, Iowa City, IA. Recombinant human C5a protein was used at a concentration of 0.1 µg/mL for all assays.

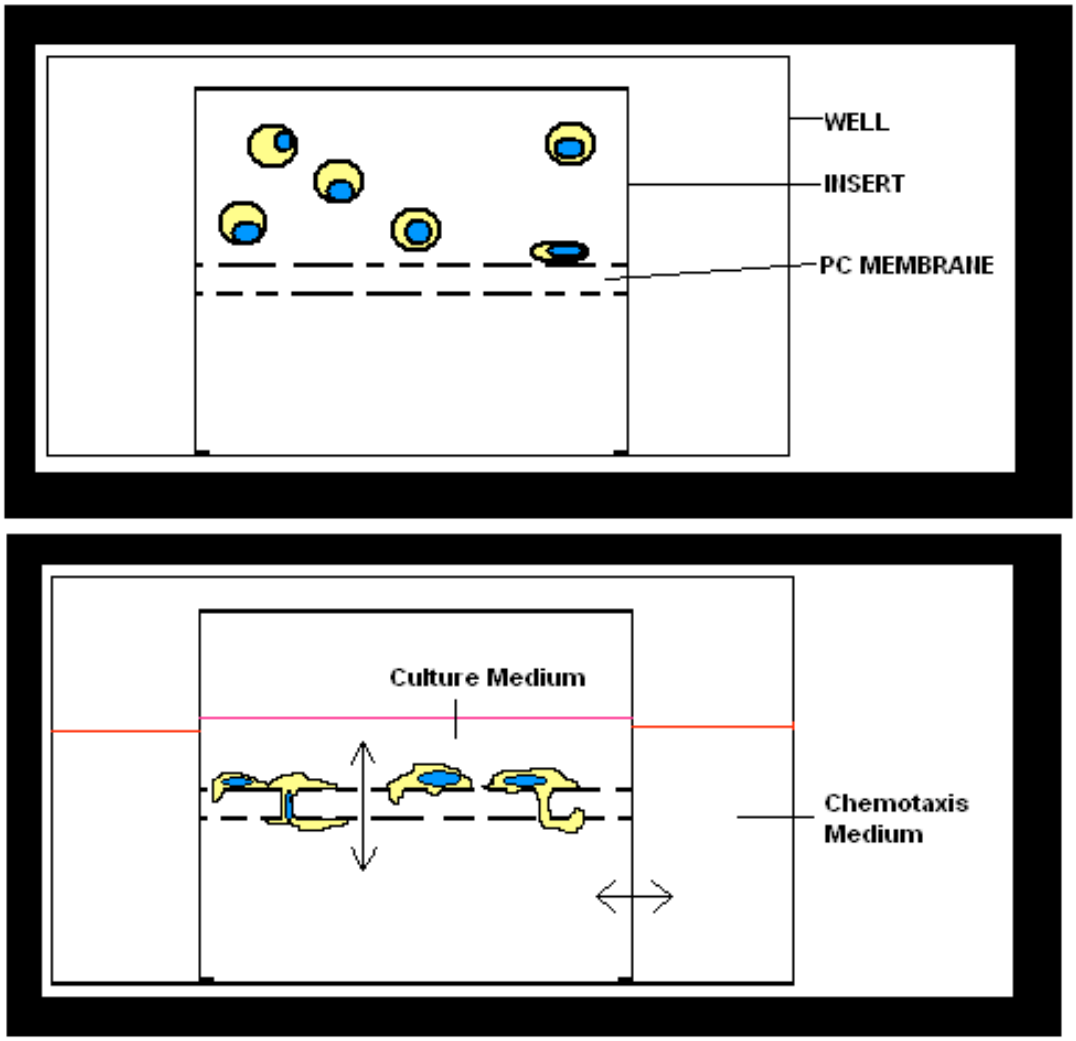

Figure 15. Boyden chamber assay. Cells are seeded into the top portion of the culture insert onto a porous membrane in culture medium. Chemoattractant proteins are added to the medium exposed to the lower surface of the porous membrane. The cells are allowed to migrate from the upper surface of the porous membrane towards the lower side of the membrane for 8 hours. Migrated cells are quantified on the lower surface of the membrane after the experiment is complete.

An equal volume of 2.5 mg/mL BSA was used as a control since this was the C5a protein diluent. All assays were performed in triplicate.

C5a treated human choroid organ cultures

To study the effects of elevated levels of C5a on endothelial cells within their native environment, organ cultures were created. Choroid punches were collected from 4 different human donors. Single punches from four different quadrants of the human eye were incubated in 1 μg/mL recombinant C5a protein diluted in Dulbecco's Modified Eagle's Medium (DMEM; Gibco) with 10% FBS and 1% penicillin/streptomycin. Adjacent punches were incubated in equal volumes of 2.5 mg/mL BSA diluted in the same medium. Incubation was for 24 hours at 37^{o}C in 5% CO_2. The choriocapillaris has been shown to survive for up to one month in organ culture, so 24 hours was well within the anticipated survival curve for the tissue (135).

Quantification of ICAM-1 expression in C5a treated human organ cultures

To quantify the ICAM-1 protein expression of tissues from the C5a and control organ cultures, quantitative PCR was used. RNA was isolated from four C5a treated and four control organ culture punches from one human donor using the RNeasy mini kit according to manufacturer's instructions (Qiagen, Valencia, CA). Reverse transcription was performed using the High-Capacity cDNA Reverse Transcription Kit according to manufacturer's instructions (Applied Biosystems, Foster City, CA). Following reverse transcription, quantitative PCR was performed using the ABI PRISM 7700 sequence detection system with the SYBR Green PCR Master Mix, according to manufacturer's instructions (Applied Biosystems). Primers used were for the amplification of ICAM-1 and ICAM-2: ICAM-1 forward primer, 5'- TGG GAA CAA CCG GAA GGT GTA T -3', ICAM-1 reverse primer, 5'- TTC AGT GCG GCA CGA GAA AT -3', ICAM-2 forward primer, 5'- CAA ACA TCT CCC ATG ACA CG -3', ICAM-2 reverse primer,

5'- GAG CAG GAC AGA TGT CAC GA -3' (Integrated DNA Technologies). For this experiment, ICAM-2 served as a housekeeping gene because it is considered to not undergo large changes in expression in endothelial cells under various culture conditions (136).

Total protein was isolated from organ cultures from 3 donors following exposure to either C5a or BSA. Western blots for ICAM-1 were performed as described previously (65) and were normalized using a beta actin antibody (Santa Cruz). Protein was quantified in each sample using a Versadoc 4000 imaging system (BioRad, Hercules, CA).

ICAM-1 intensity morphometry of C5a treated human choroid organ cultures

The quantification of ICAM-1 expression was desired for the endothelial cells of the choriocapillaris only. To obtain this measurement without measuring the expression of ICAM-1 on other cell types, it was necessary to perform a morphometric analysis instead of whole tissue PCR analysis. From each eye, four C5a treated and four control punches were embedded in sucrose as described by Barthel (131). Four sections of each punch were collected at a thickness of 7 μm. Immunohistochemistry was performed as described previously, using 2.8 μg/mL anti-ICAM-1 antibody raised in mouse (Developmental Studies Hybridoma Bank at the University of Iowa, clone P2A4) (65). All sections were developed for 2.5 minutes, a time previously established as being within the linear range of development using the same antibody(65), rinsed in distilled water, dehydrated in alcohol and Clear Rite (Richard Allan, Kalamazoo, MI). Slides were coverslipped with Permount (Fisher Scientific, Pittsburgh, PA) and images were collected using a BX-41 Olympus microscope with a SPOT-RT camera. ICAM-1 morphometry was then performed as described previously(65). Briefly, an average of 40 capillaries were traced from each punch using the polygon tool in ImageJ. The measurements were

made from four sections from each individual punch in order to account for possible variation in section thickness. Average pixel intensity values on a scale of 0 to 255 were collected for each individual capillary where a higher numerical value indicated a greater labeling intensity of anti-ICAM-1. All measurements were corrected for background by subtracting the average background intensity from the capillary intensity values per image. Comparisons were analyzed using a two-way paired Student's t-test.

C5a treated endothelial cell PCR array profiling

Primary cultures of human choroidal endothelial cells were plated into the wells of a 6-well culture plate with F12 medium supplemented with 1% FBS and 1% penicillin/streptomycin. The cells were allowed to grow to near confluency at which point the growth medium was removed and the cells were serum starved in F12 with 1% penicillin/streptomycin for 4 hours. Following the serum starvation period, the cells were exposed to 1 μg/mL recombinant C5a protein for 24 hours. RNA was extracted from the cells as described above and reverse transcribed using the RT ^{2} First Strand Kit according to manufacturer's instructions (SABiosciences Corporation, Frederick, MD). Human cDNA was added to SABiosciences RT ^{2} qPCR master mix and then added to the 96 wells of the human endothelial cell RT ^{2} Profiler PCR Array System (Product # PAHS-015A; SABiosciences). Quantitative PCR was performed using the Applied Biosystems Model 7000 sequence detection system (Applied Biosystems Inc., Foster City, CA).

C5R1 and *C3AR1* genotyping

The study was approved by the University of Iowa's Institutional Review board and informed consent was obtained from study participants. A cohort of 329 subjects with AMD and 322 control subjects from Iowa were enrolled using standard criteria(137). The cohorts were genotyped at 5 SNPs within the *C3AR1* gene and 2 SNPs within the *C5R1* gene (rs116790330 and rs4427917) using a mass spectroscopy-based system (Sequenom, San Diego, CA). Genotyping was conducted using the MassArray

platform and iPlex Gold reagents with the manufacturer's protocol by GeneSeek (Lincoln, NE). SNP Genotypes were compared between AMD patients and controls using Chi Square analysis, while allele frequencies were compared using Fisher's exact test. The Bonferroni correction was used to adjust p-values for multiple measures as needed.

Results

C3a and C5a receptor RT-PCR in human choroid and retina

To analyze the presence of C3aR and/or C5aR in the retina/choroid complex, PCR was performed on cDNA from human retina tissue and human RPE/choroid tissue (n = 3 different human donors). C3aR and C5aR were both expressed by human leukocytes, used as a positive control (Figure 16A). Transcripts for C5aR were found in both the retina and choroid (Figure 16B). In contrast, C3aR transcripts were not found in the retina or choroid (Figure 16A).

C3a and C5a receptor identification using immunoblotting

The expression of C5aR protein was detected in both the retina and RPE/choroid tissues separately (n = 3, a representative example of this result is depicted in Figure 2B). A single major band was observed at approximately 40.4 kDa (Figure 16C). A less abundant, higher molecular weight band, possibly indicative of C5aR dimers (138), was observed in both tissues. C3aR was not detected for any of the tissues evaluated (data not shown).

C3a and C5a receptor localization using immunohistochemistry

In order to determine the cell type(s) in which C3a and C5a may be capable of eliciting physiological responses in the RPE/choroid complex, immunohistochemistry was performed using anti-C3aR and anti-C5aR antibodies on sagittal sections of human donor eye tissues. We found that anti-C5aR antibodies localize to most vessels in the

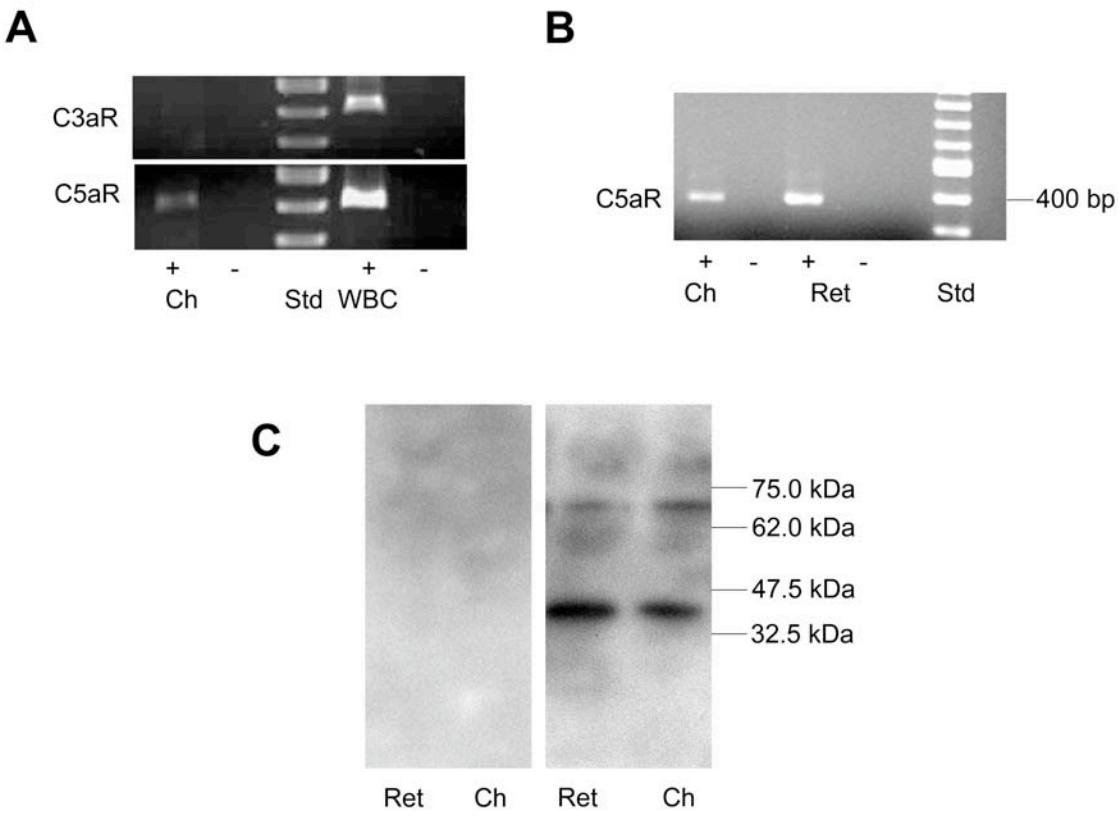

Figure 16. Expression of anaphylatoxin receptors in human eyes. (A) C3aR and C5aR RT-PCR of Human RPE/Choroid (Hu RPE Ch). Human leukocytes (Hu WBC) were used as a positive control. C3aR and C5aR transcripts were both found in leukocytes. C5aR, but not C3aR, was expressed in the RPE/choroid. (B) C5aR RT-PCR results using retina and RPE/choroid cDNA (n = 3). Retina and RPE/choroid express C5aR in all three donors. Reverse transcriptase was omitted (-) as a negative control. (C) C5aR western blot. Human retina (R) and RPE/choroid (C) from 3 human donors demonstrate positive labeling of bands corresponding to the molecular weight of C5aR protein (approximately 45 kDa). Right panels show blot following omission of primary antibody.

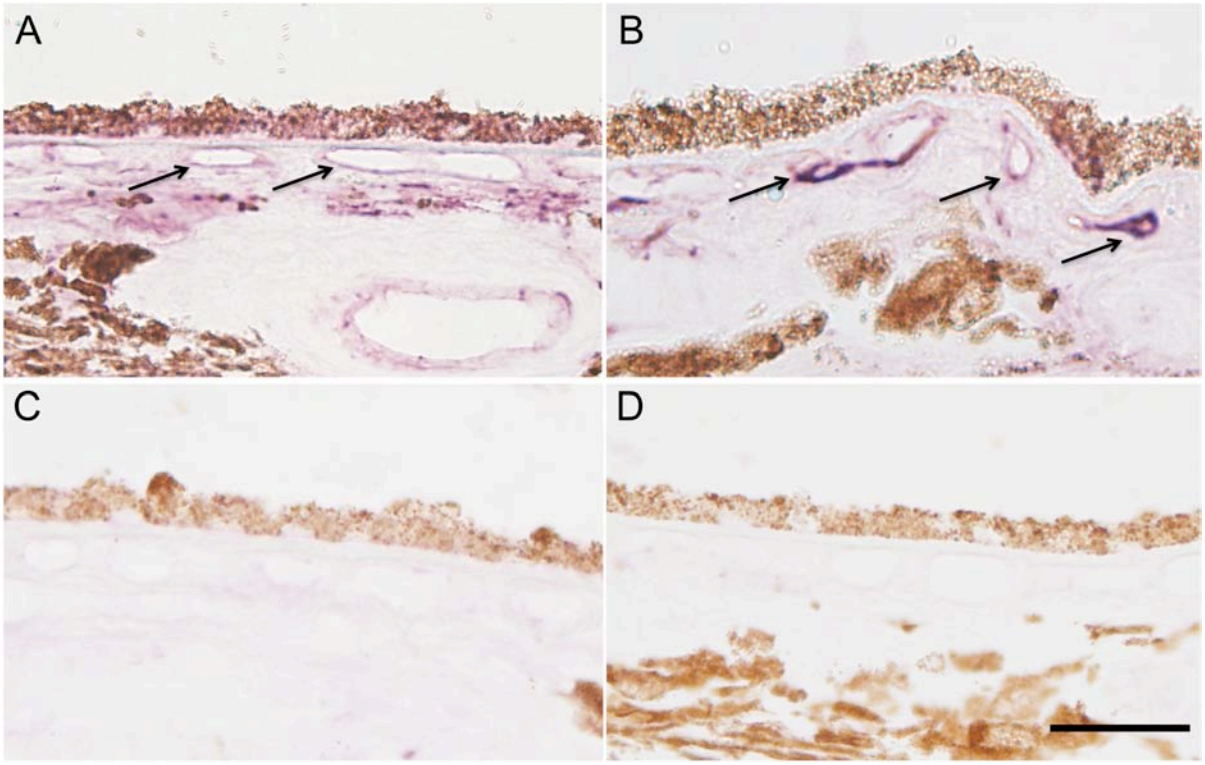

Figure 17. C3aR and C5aR immunohistochemistry. (A,B) Human tissue sections labeled with two different anti-C5aR antibodies (Santa Cruz (A), AbD Serotec (B)). C5aR labeling was localized to the RPE and the endothelial cells in the choriocapillaris (arrows). There was no labeling on tissue sections incubated with the anti-C3aR antibody (C) in contrast to tissues incubated with anti-C5aR antibodies. (D) Control tissue section in which primary antibody was omitted. CC, choriocapillaris. Scale bar represents 25 μm.

choroid, including the choriocapillaris, as well as the basal surface of the RPE (n = 15). The same vascular labeling pattern was found using two different antibodies (Figure 17A, B). Sections incubated with anti-C3aR did not exhibit any retinal or choroidal labeling (Figure 17C).

Evaluation of choroidal endothelial cell migration and proliferation in response to C5a

In order to determine whether C5a had any pro-angiogenic effects on the endothelial cells of the choroid, migration and proliferation assays were employed using human and monkey endothelial cells as described previously (133). There were no significant changes in migration or proliferation for either cell type in the presence of recombinant C5a protein compared to controls (data not shown), suggesting that C5a does not promote angiogenesis in choroidal endothelial cells.

Quantification of ICAM-1 expression in C5a treated human organ cultures

Quantitative RT-PCR of *ICAM1* cDNA showed a 13.1% increase in ICAM-1 expression in tissues treated with C5a in comparison to the BSA treated controls at 16 hrs, p-value = 0.02 (data not shown). ICAM-1 protein levels, normalized to levels of beta-actin, were on average 2.1x higher in C5a treated cultures compared to control punches (Figure 18A).

ICAM-1 morphometry of C5a treated human choroid organ cultures

Histological samples of organ cultures were evaluated to determine the site of the C5a-dependent ICAM-1 expression. Endothelial cells of the choriocapillaris showed increased labeling following C5a treatment (Figure 18B,C). Organ culture punches (C5a treated and untreated) from samples of eyes with the RPE (n = 2 donors) and without the

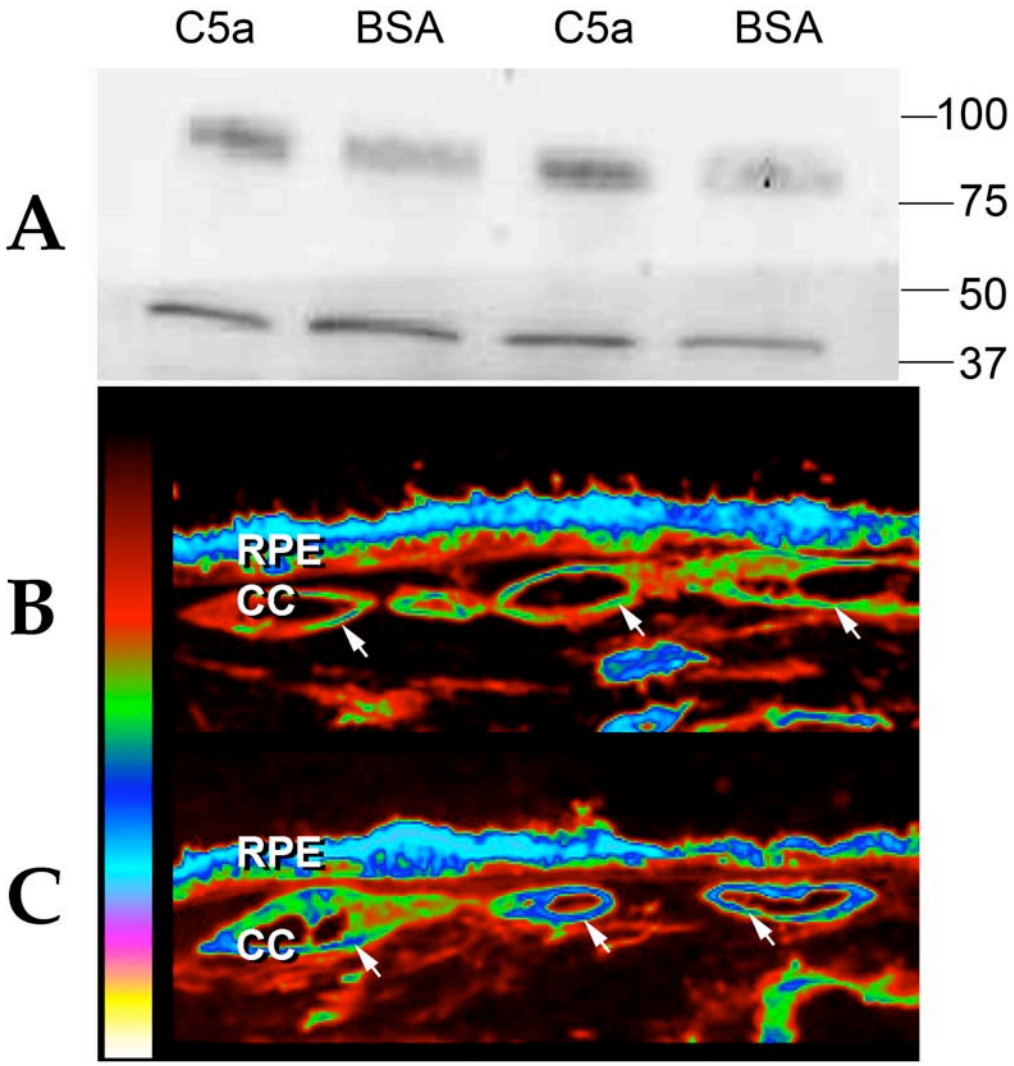

Figure 18. Increased expression of ICAM-1 in C5a treated cultures. (A) Western blot indicating ICAM-1 expression (top row) with treatment of C5a compared to BSA. Actin was used as a loading control (bottom row). Choriocapillaris labeling using anti-ICAM-1 antibody is increased following exposure to C5a (C), as compared to control samples treated with BSA (B); note that when using the "6_SHADES" lookup table in ImageJ (left side of figure) the capillaries in (B) appear red-green while the capillaries in (C) appear green-blue. RPE pigment appears bright blue. Intensities range from lowest (black) to highest (white).

RPE (n = 2 donors) were analyzed separately to determine whether having another cell type (RPE) present during the C5a incubation affects the expression of ICAM-1. Following morphometric analysis, it was found that both groups of punches exhibited an increased ICAM-1 labeling intensity on endothelial cells exposed to C5a protein compared to the controls. There was a 13.9% higher average intensity for endothelial cells in punches containing the RPE, and a 9.5% higher average intensity for endothelial cells in punches without RPE. Both groups had p-values less than 0.001 (Table 1).

C5a treated endothelial cell PCR array profiling

Human cells that were incubated with C5a protein had a 4.57 fold increased expression of integrin alpha 8 (*ITGA8*) compared to control cells. Although the fold change was significant, this difference did not reach statistical significance.

Association study of *C3AR1* and *C5R1* in AMD

A cohort of 329 AMD patients and 322 controls were genotyped at SNPs within the *C3AR1* gene (5 SNPs) and the *C5R1* (2 SNPs) gene using mass spectroscopy. No significant difference was detected between the allele frequencies and genotypes of SNPs in either the *C3AR1* or *C5R1* gene ($P>0.05$) (Table 2).

Discussion

In this study, we have shown that the gene encoding the C5a receptor is expressed in the human choroid and retina *in vivo* by PCR. We have further shown that within the choroid, C5aR is expressed in the endothelium of the choriocapillaris. We did not find convincing expression or localization of the receptor for C3a in the choroid or the retina using PCR or immunohistochemistry. These results suggest that complement cascade component C5a is more likely to be responsible for activating endothelial cells than C3a. We therefore focused on C5a for subsequent functional experiments.

No significant changes were observed in the migratory or proliferative responses

Table 1. ICAM-1 morphometry results.

Sample type	Treatment	Average pixel intensity	SEM	P-value
With RPE	C5a	129.2	1.5	<0.001
With RPE	BSA	113.4	1.1	
Without RPE	C5a	148.1	1.5	<0.001
Without RPE	BSA	135.2	1.8	

Table 2. Results of SNP screening in AMD and control samples.

Gene	SNP	Percent samples genotyped	Major/minor allele AMD	Major/minor allele control	Allele P-value (uncorrected)
C3AR1	rs7842	99.1%	.70/.30	.68/.32	0.29
C3AR1	rs2230318	99.3%	1/0	1/0	N/A
C3AR1	rs11567805	99.3%	1/0	1/0	1
C3AR1	rs7954916	98.1%	.70/.30	.69/.31	0.61
C3AR1	rs17009221	99.3%	.92/.08	.92/.08	0.5
C5R1	rs11670330	88.6%	.76/.24	.72/.28	0.087
C5R1	rs4427917	98.5%	.73/.27	.71/.29	0.26

of choroidal endothelial cells to C5a protein. These results suggest that the effect of C5a on endothelial cell activation is not through promoting angiogenesis, although it is possible that cell culture conditions do not replicate the effects of C5a *in vivo*. Following further investigation, we found that the activation of human choroidal endothelial cells was more closely linked to inflammatory mechanisms of cell activation.

Evaluation of ICAM-1 expression in the choroid following C5a exposure, using quantitative PCR, Western blot and ICAM-1 morphometry, showed that human choroid punches exposed to C5a, in contrast to those exposed to BSA alone, increased expression and localization of ICAM-1 in the choriocapillaris. This result was not dependent on the presence of the RPE, suggesting that C5a may act directly on choroidal endothelial cells. Although the overall increase in ICAM-1 expression is modest, it is comparable to the macular-peripheral differences observed previously(65). Even a small chronic increase in adhesion molecule expression might result in increased monocyte interaction (139), especially over the decades during which AMD develops.

ICAM-1 plays a role in the infiltration of leukocytes into surrounding tissues during inflammation through its interaction with CD11/CD18 integrins on circulating leukocytes, as described in chapter 1 (140, 141). An increased level of ICAM-1 on the choroidal endothelium likely enhances leukocyte trafficking from the blood as well(141, 142). Mice deficient for C5aR or ICAM-1 both demonstrate a significant reduction in neovascular membrane volume following laser induction(67, 121). Since we have now demonstrated that C5a increases endothelial expression of ICAM-1, it may be possible that a lack of ICAM-1 mediated leukocyte recruitment in these knockout mice is responsible for the reduction in neovascular membrane formation. The role of different classes of leukocytes in AMD pathogenesis is controversial (143). One possible outcome of increased leukocyte recruitment is that capillary endothelial cells may become damaged by adhesion of neutrophils or monocytes (144, 145). Moreover, following extravasation, macrophages can potentially promote CNVM formation through a variety

of processes (143). Complement mediated activation of choroidal endothelial cells could advance disease in AMD through either an ischemic/atrophic mechanism or through angiogenic events.

Although the increased expression of ITGA8 in C5a treated human endothelial cells did not reach statistical significance, this trend raises some interesting hypotheses. ITGA8 binds vitronectin (146), which is an inhibitor of the formation of the complement membrane attack complex (147). A large increase in ITGA8 expression may be a mechanism to counteract the increase in C5a detected by the cell. If C5a is elevated, it is indicative of a higher level of C5 enzymatic activation. After activation of C5, the membrane attack complex forms, which is capable of destroying cells by creating large pores in their lipid bilayer. Expressing ITGA8 may increase vitronectin binding and inhibition of membrane attack complex formation, and therefore cellular death.

Finally, we explored the role of genetic variants in the genes for C3aR and C5aR (*C5R1* and *C3R1*) in the pathogenesis of AMD by conducting a focused association study. However, we did not observe any association between SNPs in the *C3AR1* and *C5R1* genes and AMD. These data suggest that ancestral variants in these genes are not common risk factors for AMD.

In summary, we observed C5aR, but not C3aR, in the human choriocapillaris *in vivo* and found that C5a activates choroidal endothelial cells to increase ICAM-1 expression at the protein and mRNA levels. This increased expression is at the level of the choriocapillaris. The presence of monocyte derived cells in AMD eyes has been noted (recently reviewed (143)), and so has a key role for the complement system (29, 113, 120-128, 148, 149). The current study may unify these findings, as our results suggest that complement deposition and inflammation in human eyes converge at the level of the choriocapillaris. Moreover, C5aR may provide an attractive target for novel therapies for AMD.

CHAPTER 4. ACTIVATION OF CHOROIDAL ENDOTHELIAL CELLS BY ANGIOGENIN

Introduction

Age-related macular degeneration (AMD) is currently the leading cause of irreversible blindness in the western world (112). This disease is characterized by commonly described landmarks including drusen, retinal pigment epithelial atrophy, retinal detachment, as well as disciform scar formation (3, 4, 30, 43). In a subset of patients with advanced disease, blood vessels from the choroid traverse Bruch's membrane and grow into the subretinal space (4, 26, 27, 33, 35, 36). This form of the disease, referred to as choroidal neovascularization (CNV) is responsible for severe decrease in visual acuity, and is characterized by abnormal angiogenesis.

Angiogenesis is the growth of new blood vessels from existing blood vessels. This process is accomplished by endothelial cell functions including proliferation, migration, and tubulogenesis. In AMD pathophysiology, it is imperative to determine what causes endothelial cells of the choroid to take on the angiogenic behaviors characterized in CNVM patients in order to prevent vision loss.

Numerous molecular pathways affect different facets of angiogenesis, and may therefore be involved in promoting neovascularization in human patients with AMD (72). Vascular endothelial growth factor (VEGF) signaling is the best characterized of these, and the recent development of anti-VEGF therapy to treat patients with advanced AMD has been remarkably successful (44, 150, 151). Other mitogenic peptides involved in neovascular AMD may include aFGF, bFGF, TGF-β, or angiopoietins 1 and 2 (118, 152-154). An improved understanding of other molecules that may regulate angiogenesis in the human choroid is important for the development of additional and hopefully preventative therapies, especially if anti-VEGF therapies are found to have other ocular

or systemic effects in some patients that are not yet appreciated (155, 156). One possible contributor to neovascularization is angiogenin.

Angiogenin is a small polypeptide which shares one third of its amino acid sequence with the bovine enzyme, pancreatic ribonuclease A (157). Although the enzymatic activity of angiogenin is limited, it has been shown to participate in angiogenesis (158-160). There are some current hypotheses pertaining to the mechanism by which angiogenin may be capable of increasing angiogenesis in endothelial cells.

First, it has been observed that angiogenin binds to DNA in human umbilical vein endothelial cells (HUVEC) in culture within 60 minutes. It is possible that angiogenin is internalized after binding to its cell surface receptor and translocated to the nucleus of the cell. In the nucleus, angiogenin may aid in transcription of angiogenesis specific genes, thus promoting vascular growth (161). This behavior has placed angiogenin in the "third messenger" category of intracellular signaling (162). Also, evidence in rabbit corneas has shown that the presence of angiogenin protein is correlated with an increase in angiogenesis (163).

Angiogenin has been shown previously to bind to α-actin on the surface of endothelial cells and initiate pro-angiogenic responses in a chicken chorioallantoic membrane assay (164-166). The binding of angiogenin to its cell surface actin receptor causes an 11-fold increase in the enzymatic activity of plasmin and tissue plasminogen activator (tPA) (167). These proteins are involved with cellular migration and invasion in cellular mechanisms including wound healing and tumor metastasis (168). Angiogenesis of nearby vasculature is necessary for a tumor to increase in size. In mice, injections of angiogenin antibodies decrease tumor formation (169). If angiogenesis relies on angiogenin, tumor formation may be hindered by the lack of necessary vasculature formation.

In addition to its ability to activate endothelial cells in culture and animal models, angiogenin has been demonstrated to function in abnormal blood vessel growth in lung

adenocarcinoma (170) and cell proliferation in metastatic leiomyosarcoma tumor formation (171). Its potential role in neovascular disease in AMD has not yet been explored. In this report we evaluated possible effects angiogenin may have on choroidal endothelial cells in reference to pro-angiogenic behaviors, which may impact AMD pathogenesis.

Materials and methods

Angiogenin RT-PCR in human choroid and retina

It was first desired to determine if the gene for angiogenin was expressed in the human retina and/or choroid. This was accomplished using RT-PCR. RNA was isolated from frozen punches of human RPE-choroid and retina using the RNeasy mini kit according to manufacturer's instructions (Qiagen, Valencia, CA) and then reverse transcription was performed using the High-Capacity cDNA Reverse Transcription Kit (Applied Biosystems, Foster City, CA). PCR was completed (BIOLASE DNA polymerase kit, Bioline, Taunton, MA) using the following conditions for 35 cycles: denaturing at 94^{o}C for 45 seconds, annealing at 62^{o}C for 30 seconds, and elongation at 72^{o}C for 1 minute. Angiogenin primers used were: forward primer, 5'- CGT CCG TGT ACA CAC ACT CA -3', reverse primer, 5'- GCA CGA AGA CCA ACA ACA AA -3' (Integrated DNA Technologies, Coralville, IA). PCR products were separated on a 2% agarose gel (Fisher Biotech horizontal electrophoresis system, Fisher Scientific) at 135 V for approximately 45 minutes. The bands were visualized using ethidium bromide under UV light.

Angiogenin detection with immunoblotting

The expression of angiogenin protein in the human eye was determined with immunoblotting. Retinal and RPE/choroid tissue from human donors was snap frozen in liquid N_2 within 6.5 hours post mortem. Tissue was homogenized in PBS with 1% Triton

X-100 and complete protease inhibitor (Roche, Indianapolis, IN). Recombinant protein (5 ng) or 20 µg of choroid or retinal protein was mixed with an equal volume of 2X Laemmli buffer, boiled for 5 minutes, and then separated electrophoretically on a 4-20% Tris-HCl gradient SDS polyacrylamide gel as described previously (132). Next, proteins were blotted onto a polyvinylidene difluoride (PVDF) membrane (BioRad Laboratories, Inc., Hercules, CA). Following brief treatment with methanol, membranes were blocked in 1% bovine serum albumin. An antibody directed against angiogenin (R&D, Minneapolis, MN) was used in 1% bovine serum albumin at a concentration of 0.4 µg/mL, followed by washing of the membrane, incubation with 0.4 µg/mL peroxidase-conjugated species-specific secondary antibody (Santa Cruz) and detection using the ECL plus kit (Amersham Biosciences, Little Chalfont, UK).

Angiogenin localization using immunohistochemistry

The expression of the angiogenin protein has not been described in the eye. Immunohistochemistry was used to determine the localization of angiogenin in the retina and choroid. Sections of human donor eyes spanning from the macula to the ora serrata containing both retina and RPE/choroid were collected and fixed in 4% paraformaldehyde for 2 hours within 8.5 hours post mortem. The tissues were infiltrated in increasing concentrations of sucrose (up to 20%) and then embedded in 2 parts 20% sucrose to 1 part optimal cutting temperature medium (Sakura, Torrance, CA) (131). Frozen sections were collected using a Microm HM 505 E cryostat at a thickness of 7 microns.

Sections were blocked in 1% horse serum for 15 minutes. The primary antibody used was an antibody to human angiogenin raised in rabbit at a concentration of 4 µg/mL (Santa Cruz Biotechnology Inc., Santa Cruz, CA). Immunolabeling was performed as described previously (65). Antibody specificity was analyzed by incubating 40 µg/mL recombinant human angiogenin protein (R&D, Minneapolis, MN) for 1 hour on tissue

sections after the blocking step. The sections were rinsed 3 times in PBS for 10 minutes. Then 4 µg/mL anti-angiogenin antibody was applied to the sections. Following 1 hour of incubation, the antibody solution was removed from the sections and applied to sections that were not exposed to recombinant protein for 1 hour. Immunohistochemistry was completed as described previously (65).

Assessment of angiogenin-mediated choroidal endothelial cell wound closure assay

A wound healing assay was used to determine the effect of angiogenin on endothelial cell migration and proliferation. Rf/6a cells were seeded into bi-chamber inserts (Ibidi, Munich, Germany) within a 24-well plate. The cells were grown to 100% confluency and the inserts removed from the wells, leaving a consistent gap within the cell monolayer. Cells were rinsed with DPBS three times and then cultured with F12 growth medium supplemented with 1% FBS and 100 ng/mL recombinant human angiogenin or 0.1% bovine serum albumin as a control. All conditions were performed in triplicate. Images were collected at the center of the injury gap every 8 hours beginning immediately after the insert removal and continuing for 56 hours. Images were collected with an Olympus IX81 microscope and gap distances were determined using the polygon tool in ImageJ, downloadable software (http://rsbweb.nih.gov/ij/download.html). Average percent closure was calculated for each condition.

Assessment of angiogenin-mediated choroidal endothelial cell migration

To further analyze the migratory response of endothelial cells to angiogenin protein, a migration assay was used. Rf/6a cells were seeded into the upper chamber of 8 µm pore culture inserts (Millipore, Billerica, MA) within a 24-well plate. Recombinant human angiogenin protein was added to the lower chamber medium at a concentration of 0.5 µg/mL. Cells were allowed to migrate for 8 hours. Cells that migrated to the lower

surface of the insert were counted using SEM as described previously (133). Elastin derived peptides were used at a concentration of 1.0 μg/mL as a positive control and an equal volume of protein diluent (HBSS) was used as a negative control (Chapter 5).

Angiogenin uptake by retinal-choroidal endothelial cells

Previous studies have demonstrated that endothelial cells (not of eye origin) internalize angiogenin protein and translocate it to the nucleus (161). A similar assay was used with chorioretinal endothelial cells in order to determine if this behavior was exhibited by ocular endothelial cells as well. Rf/6a cells were cultured in F12 medium supplemented with 1% FBS, 20 ng/mL bFGF (161), and penicillin/streptomycin on glass coverslips for 24 hours. Cells were not allowed to reach confluency. Recombinant human angiogenin protein (concentration = 1 μg/mL) or 0.1% bovine serum albumin (BSA) control protein was added to the medium and the cultures were incubated for 24 hours. Cells were fixed for 10 minutes in 4% paraformaldehyde (pH 7.4). Immunocytochemistry was performed using an antibody to angiogenin (Santa Cruz Biotechnology, Inc., Santa Cruz, CA) as described previously(133). Phalloidin (Invitrogen, Eugene, OR) was added to the secondary antibody incubation in order to visualize actin filaments.

Results

Expression of angiogenin in human retina and choroid using PCR

In order to determine if the gene for angiogenin is expressed in the human retina and choroid, non-quantitative PCR was performed. Reverse transcribed mRNA transcripts for the angiogenin gene were amplified in both retina and choroid samples (Figure 19A).

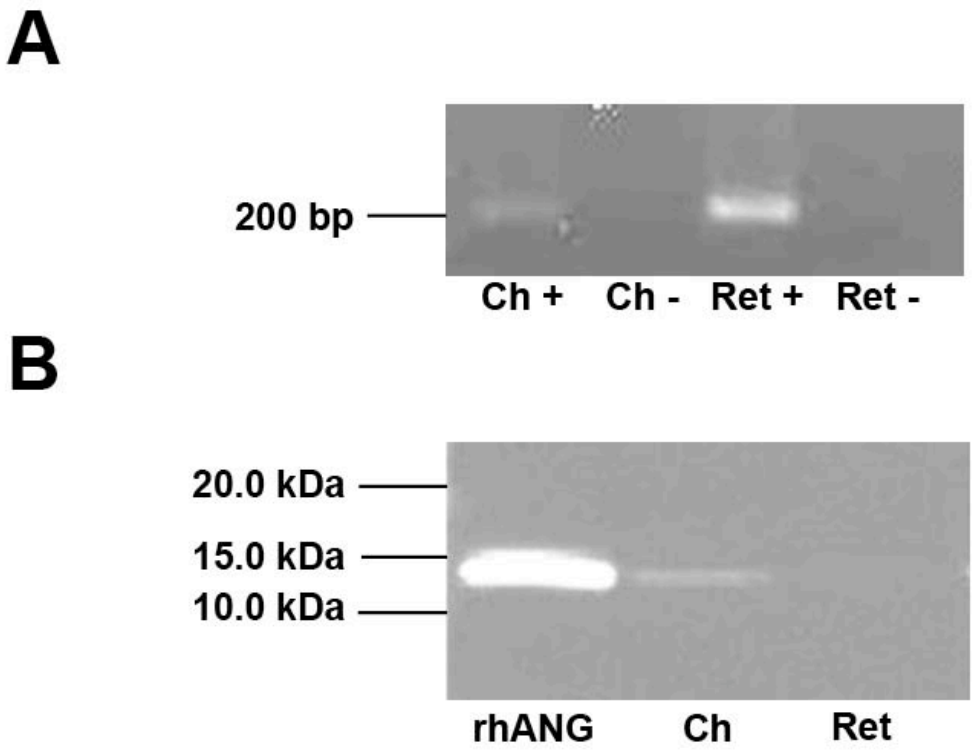

Figure 19. Angiogenin expression in the retina and choroid. (A) PCR results. Both tissues demonstrated amplification of angiogenin cDNA. Reverse transcription was performed with (+) and without (-) reverse transcriptase enzyme, the latter serving as controls. (B) Western blot results show that the angiogenin protein is present in choroid only. Recombinant protein was detected at the correct molecular weight (14 kDa) with the anti-angiogenin antibody as a positive control. The band present in the RPE-choroid sample was detected at the same molecular weight of the recombinant protein with the same antibody.

Angiogenin protein expression in human retina and choroid using immunoblotting

Western blots of human retina and RPE-choroid protein probed with anti-angiogenin antibody showed the expression of an immunoreactive band at the expected molecular weight of 14 kDa (Figure 19B). Human recombinant angiogenin protein was detected using the same antibody at the same molecular weight.

Localization of angiogenin in human retina and choroid

In order to determine the cells responsible for endogenous expression of angiogenin in the human choroid, anti-angiogenin immunohistochemistry was performed. In these sections, the choriocapillary pillars were positive, as well as some capillary endothelial cells and larger artery endothelial cells (Figure 20A). This pattern indicates that the angiogenin peptide is present in the human choroid *in vivo.* Tissues from patients with neovascular AMD had angiogenin labeling on the endothelial cells in the choroid as well as those within the neovascular membranes (Figure 20C).

The specificity of the antibody was determined by performing a blocking experiment using recombinant human angiogenin protein as well as bovine serum albumin as a control (Figure 21). Tissues sections exposed to protein but no anti-angiogenin antibody had no labeling which was similar to the secondary antibody only control. Sections incubated with BSA protein plus anti-angiogenin had similar labeling patterns to those described with anti-angiogenin above. This result was expected as there should be no specific interaction between the control protein BSA and anti-angiogenin. Sections exposed to both recombinant human angiogenin and the anti-angiogenin antibody had more intense labeling patterns than the antibody alone, as well as labeling of additional tissues. This indicates that the recombinant protein and the antibody bind one another, however, the recombinant protein may also have specific binding sites in the choroid, explaining the higher intensity of the antibody signal.

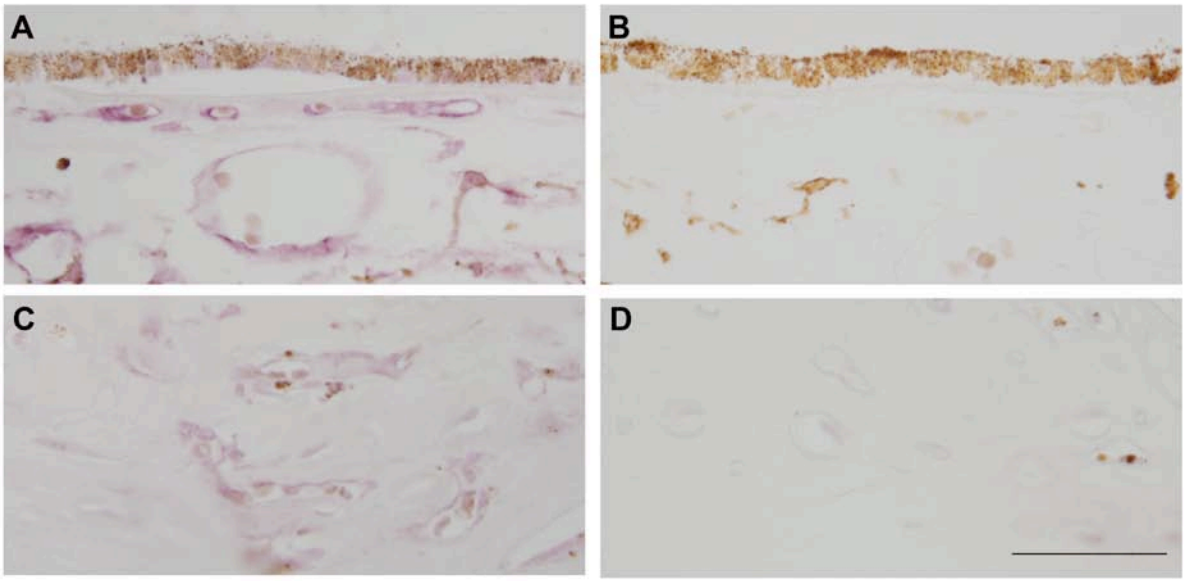

Figure 20. Angiogenin localization in the human choroid. Labeling of angiogenin is shown in a normal choroid (A) as well as in a neovascular membrane (C) from human donor tissue. In both tissues, angiogenin is expressed on the endothelial cells of choriocapillaries and large vessels. It is also found in the capillary pillars. The presence of angiogenin in the neovascular membrane vessels indicates that it may play a role in the pathophysiology of this cells in AMD. No antibody controls are shown for normal tissue (B) and neovascular tissue (D). Scale bar = 50 μm.

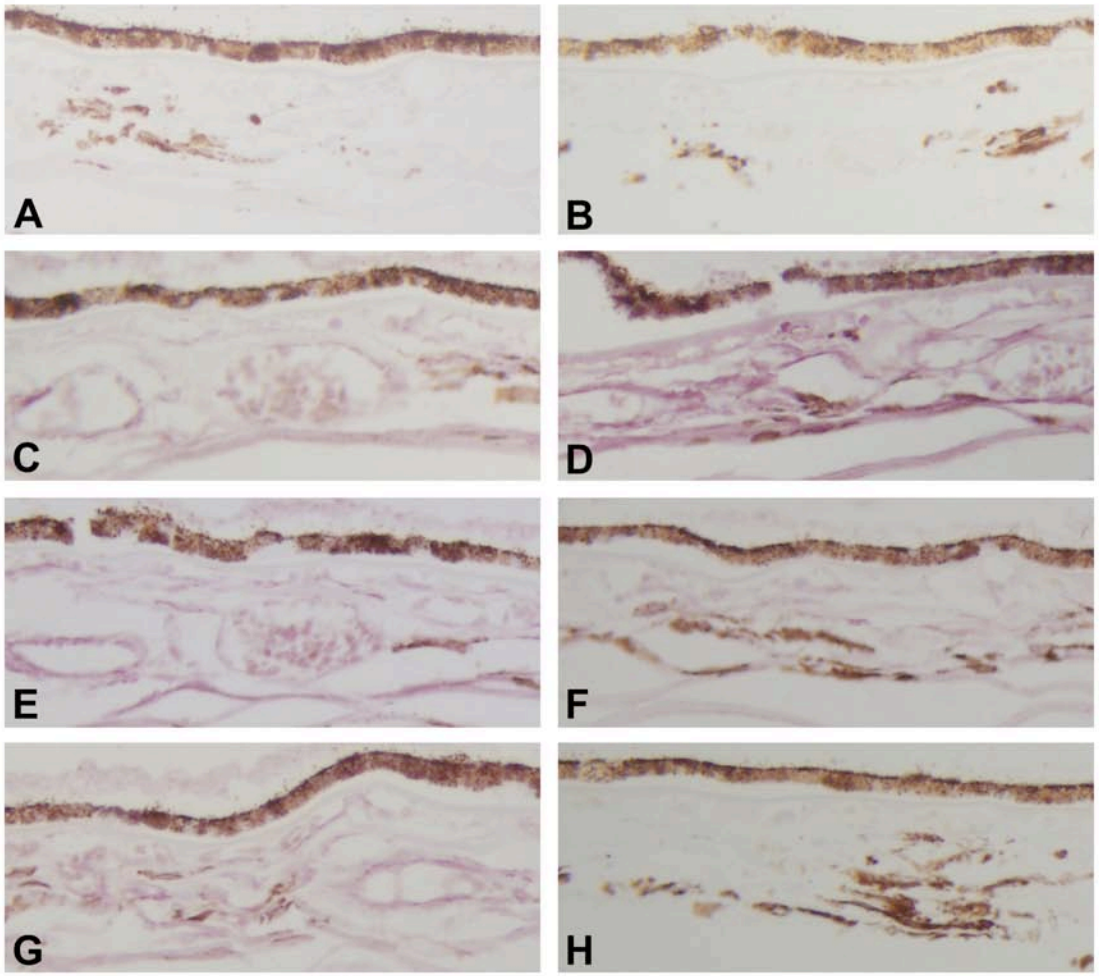

Figure 21. Angiogenin antibody specificity. Human choroid sections were incubated with (A) BSA protein only, (B) recombinant human angiogenin protein only, (C) BSA protein and anti-angiogenin, (D) recombinant human angiogenin protein and anti-angiogenin, (E) anti-angiogenin, (F) unbound anti-angiogenin from (D), (G) unbound anti-angiogenin from (C), no protein or antibody. The labeling of endogenous angiogenin is shown in (E). Tissues expressing the protein include endothelial cells of the choroid and choriocapillaris, the RPE, capillary pillars and some extra cellular matrix. The same pattern is shown in (C) and (G), as BSA protein did not inhibit the binding of the antibody to angiogenin. The interaction of recombinant angiogenin with the anti-angiogenin antibody is evident in (D) and (F). Not only endogenous angiogenin labeled, but the recombinant protein/antibody complex is also labeled, intensifying the overall signal over that found with antibody alone. The unbound antibody had a large decrease in angiogenin labeling (F), indicating that most of the antibody was bound in (D).

After anti-angiogenin was incubated with the recombinant protein (or BSA), the antibody solution was removed and placed onto sections that were not incubated with recombinant protein (or BSA). This step was performed in order to determine the amount of antibody bound to endogenous or recombinant angiogenin protein. The section incubated with the 'excess' antibody from the BSA section showed similar labeling to the anti-angiogenin antibody sections as well as the original BSA and anti-angiogenin sections. This indicates that there was enough antibody in solution to saturate available angiogenin proteins on two tissue sections. On the other hand, the section incubated with the 'excess' antibody from the recombinant angiogenin section had a decrease in labeling intensity. This decrease is due to the antibody binding both recombinant protein and endogenous protein in the previous section, resulting in less antibody available to bind to endogenous angiogenin in the new section.

It was also found that angiogenin is present on the endothelial cells of the choroid and within neovascular membranes in tissues from human donors with neovascular AMD.

Angiogenin-mediated endothelial cell wound closure assay

A wound closure assay was used to measure the migration and proliferation responses of chorioretinal endothelial cells to the presence of elevated levels of angiogenin protein. The presence of angiogenin at the tested concentrations did not affect the combined migration and proliferation response of chorioretinal endothelial cells in this assay (Figure 22).

Angiogenin-mediated endothelial cell migration

A Boyden chamber migration assay was used to measure the changes in migration of chorioretinal endothelial cells in the presence of elevated levels of angiogenin protein. The presence of angiogenin at the tested concentration did not affect the migratory response of chorioretinal endothelial cells in this assay (Figure 23). The positive control,

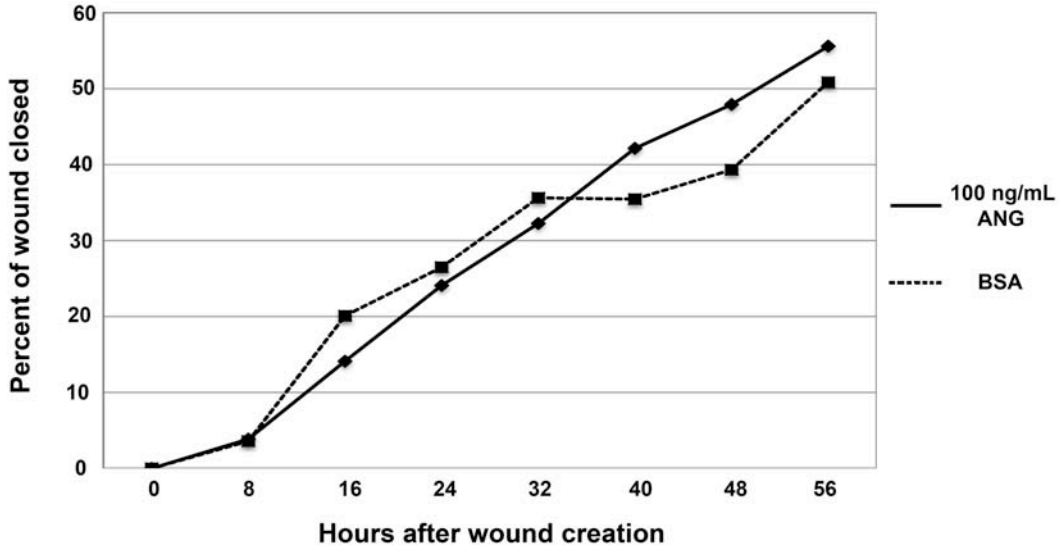

Figure 22. Angiogenin wound closure assay. Endothelial cells exposed to 100 ng/mL recombinant human angiogenin protein did not have a significant change in wound closure after 56 hours in comparison to cells exposed to BSA alone (control).

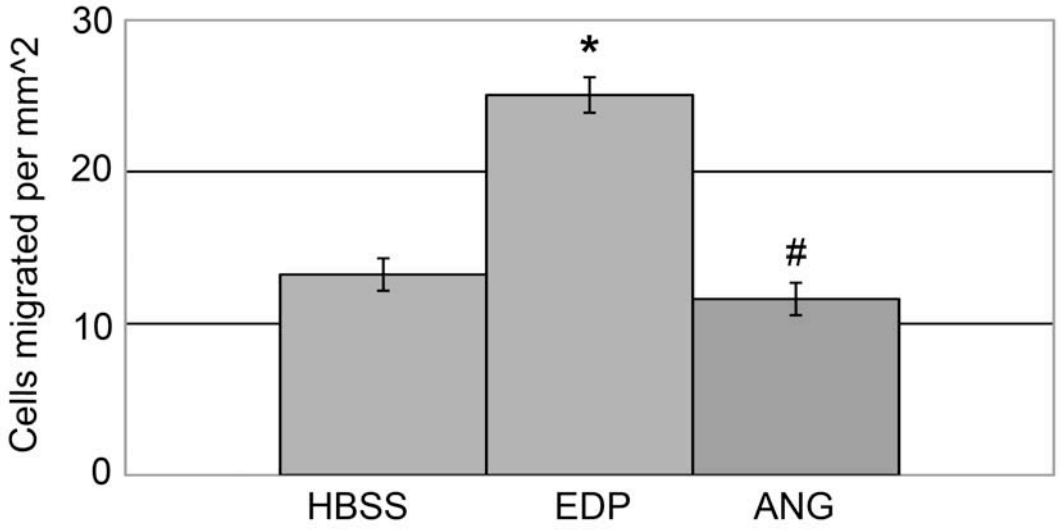

Figure 23. Endothelial cell migration assay in response to angiogenin. Chorioretinal cells did not migrate towards the angiogenin protein any differently than the negative control cells that were in the same experiment. The positive control, elastin derived peptide exposed cells, had a marked increase in migration. (*) indicates p-value < 0.01 and (#) indicates p-value > 0.25.

elastin fragments, showed a large increase in migration compared to the control, as described previously, as well as in chapter 5 (133).

Nuclear translocation of angiogenin by chorioretinal endothelial cells

Chorioretinal cells that were incubated with the recombinant human angiogenin protein showed significantly higher angiogenin labeling within the cytoplasm and the nucleus than the control cells that had been pre-incubated with BSA only (Figure 4). All cells in both experimental groups demonstrated some labeling of angiogenin, indicating the presence of endogenous protein.

Discussion

The activation of endothelial cells and the development of choroidal neovascular membranes in patients with AMD are complex events that are not well defined. Although there are very effective anti-VEGF treatments currently in use for the treatment of existing neovascular membranes, these treatments are retroactive and cannot be as effective as preventative treatment. There are many other factors that may accentuate the role of VEGF, or even play their own independent roles in accelerating the progression of the disease. Determining these other events will further our knowledge of the causal mechanisms occurring in AMD and provide more complete therapeutic options.

The effects of angiogenin on different types of cells have been shown in other diseases. The expression of angiogenin decreases in carcinoma cells during the progression of nasopharyngeal carcinoma (172). Angiogenin expression is also decreased in human hepatoma cell line H7402 from hepatocellular carcinoma as the concentration of bFGF increased as well as cellular proliferation (173). On the other hand, angiogenin positively affects cancer cell line A549 proliferation in lung adenocarcinoma (170). Smooth muscle cells also increase proliferation in response to angiogenin, as demonstrated in studies of metastatic leiomyosarcoma tumor formation

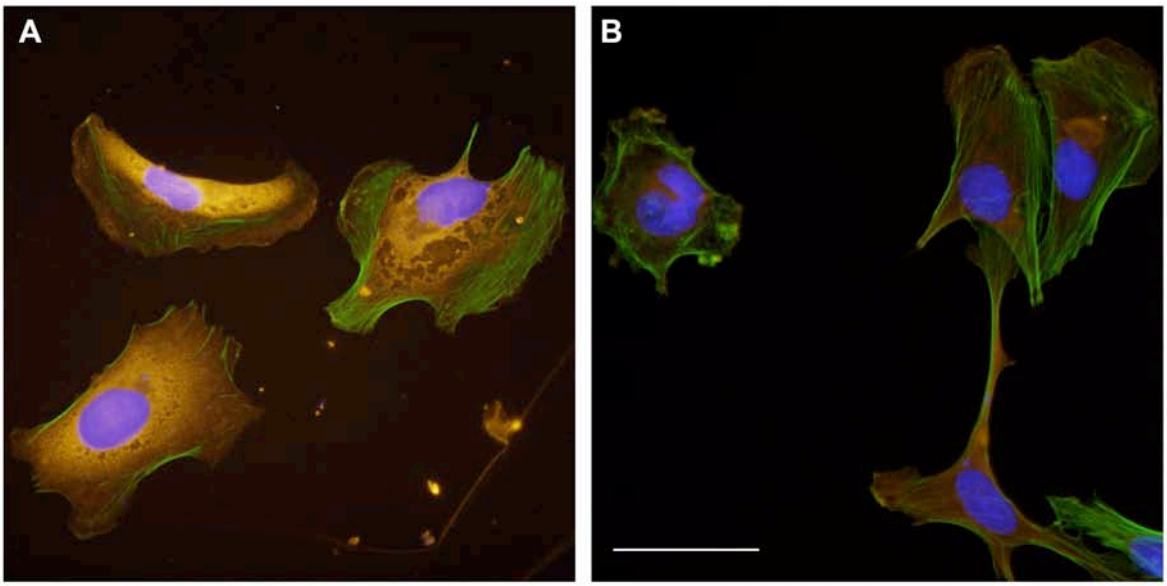

Figure 24. Endothelial cell translocation of angiogenin to nuclear envelope in cell culture. Rf/6a chorioretinal endothelial cells incubated with recombinant human angiogenin (A) and with control protein, BSA (B). Cells exposed to angiogenin have intense angiogenin labeling (red) in or near the nucleus, as well as some faint labeling in the rest of the cytosol. Control cells only demonstrated the faint labeling in the cytosol, which could be attributed to endogenous angiogenin. Actin is labeled with phallotoxin (green), and nuclei are labeled with DAPI (blue). Scale bar = 50 μm.

(171). These studies indicate a tissue specific role for angiogenin during the progression of different cancers. It is unknown what role angiogenin plays in the eye during normal or disease conditions. It was our goal to determine its location and role in unaffected eye tissues as well as tissues with neovascular AMD.

We have shown in this study that angiogenin is expressed in the normal human choroid. It is possible that this protein is responsible for the normal turnover and branching of the vascular network during development and aging. Also, we have demonstrated that chorioretinal endothelial cells are capable of internalizing angiogenin from culture medium and transporting it to the nucleus. If angiogenin is capable of acting as a 'third messenger' in affecting gene expression directly, it could be proposed that this behavior is directly correlated to endothelial cell activation, a common manifestation found in neovascular AMD.

Despite the fact that chorioretinal endothelial cells are capable of translocating angiogenin peptides, angiogenin does not appear to increase specific angiogenic behaviors of these cells. This does not indicate that angiogenin is not capable of playing a role in CNVM formation in AMD progression, it only indicates that the role may be different than hypothesized based on previous findings or dependant on another factor and requires further investigation. Since there is little known about the angiogenin receptor, one plausible explanation for the lack of angiogenic behaviors in response to angiogenin is that this cell line does not express the required receptor, or that its expression is downregulated in cell culture. If this is the case, the Rf/6a cells are only capable of responding to the protein through the nuclear translocation mechanism, which could be mediated through an alternative receptor. From these observations, it is hypothesized that angiogenin is capable of binding multiple receptors, some or all of which may be specific to endothelial cells derived from different tissues and/or species.

Interestingly, in addition to normal eyes, angiogenin is present on the pathologic vasculature within CNVMs in AMD. It is therefore plausible that angiogenin is an

important mediator of endothelial cell activation during AMD disease progression. Although angiogenin induces angiogenesis in other diseases, our findings suggest that its role in AMD is not angiogenic and therefore may be responsible for other features of endothelial cell activation. Evaluation of the role of angiogenin, and other inducers of angiogenesis, in AMD will further our understanding of this disease, and direct therapy development.

CHAPTER 5. ELASTIN-MEDIATED CHOROIDAL ENDOTHELIAL CELL ACTIVATION

Introduction

Age-related macular degeneration (AMD) is the leading cause of blindness in people over the age of 60 in the United States (1). Visual acuity is lost in this condition due to degenerative changes in the macula, the region of the posterior eye responsible for detailed vision. AMD is frequently classified as either atrophic (dry) or neovascular (wet) (3-5). In atrophic AMD, characteristics include drusen, retinal pigment epithelial (RPE) changes, and vascular dropout that may culminate in geographic atrophy. The neovascular form of AMD is characterized by the abnormal growth of choroidal blood vessels (choroidal neovascular membranes, CNVMs) into the sub-retinal space. This multistep process is likely to be initiated by breakdown of Bruch's membrane, which, when intact, prevents pathologic angiogenesis. In this process, choroidal endothelial cells migrate from the choroid into the sub-RPE and/or sub-retinal space. These endothelial cells proliferate and form tubes (tubulogenesis), and ultimately reorganize their junctions in order to increase permeability across the newly formed vascular wall.

The neovascular process in AMD can result in serous detachment of the retinal pigmented epithelium (RPE) and/or retinal detachment, as well as fibrous disciform scarring beneath the retina, causing a catastrophic decrease in visual acuity (4, 5, 27, 33, 43). Current treatments for neovascular AMD are focused primarily on vascular endothelial growth factor (VEGF)-mediated processes (44). While VEGF is a potent inducer of angiogenesis, understanding the role of additional angiogenic stimuli would be invaluable for the development of improved treatments (45).

Elastin is a glycoprotein consisting of cross-linked 72 kDa tropoelastin subunits. The function of elastin is to provide support as well as elasticity, and it is an abundant component of the extra-cellular matrix (ECM) of arteries, lung, and skin (174). Under

homeostatic conditions, elastin levels remain relatively constant because the balance between elastin degradation and formation is tightly regulated by matrix metalloproteinases (MMPs) as well as tissue inhibitors of metalloproteinases (TIMPs) (23, 174-176). MMPs, in particular MMP-2, MMP-3, MMP-9, and MMP-12, are zinc-dependent endopeptidases responsible for breaking down the cross-linked tertiary structure of elastin, a process known as elastolysis, resulting in the loss of its mechanical attributes and the liberation of biologically active elastin-derived peptides (EDPs) (176, 177). Elastin-derived peptides (EDPs) are cross-linked fragments of tropoelastin of varying sizes (178). These subunits have been shown to initiate endothelial cell migration and tubulogenesis in chicken chorioallantoic membranes, human microvascular endothelial cells (cell line HMEC-1), and human umbilical vein endothelial cells (175). Currently, it is unknown how these peptides are able to activate endothelial cells and if they are capable of activating endothelial cells from other tissues, such as the choroid. It is plausible that EDPs bind to elastin binding proteins on the cell surface, inducing pro-angiogenic behaviors such as cell migration and/or proliferation.

Since EDPs are capable of promoting angiogenic behaviors by endothelial cells, it is plausible that EDPs may play a role in progression of exudative AMD. There are several lines of evidence for abnormal elastin metabolism in Bruch's membrane in AMD. First, early onset choroidal neovascularization has been shown in patients with the condition, pseudoxanthoma elasticum. These patients may be at risk for developing choroidal neovascular membranes because of abnormalities in the elastic layer of Bruch's membrane, including breaks, clinically defined as angioid streaks (179, 180). Second, fibulin-5 missense mutations have been identified in association with AMD (181). These mutations may contribute to AMD development by affecting the elastic layer of Bruch's membrane, since fibulin-5 participates in elastogenesis (182, 183) and is localized to Bruch's membrane in human eyes (184). Third, correlations between the integrity of the elastic layer of Bruch's membrane and AMD have also been made. Light and electron

microscopic studies of human eyes have found that Bruch's membrane becomes calcified and increasingly fragmented with increasing severity of AMD (22, 30). In a mouse model, it has been shown that the lack of lysyl oxidase, the enzyme which cross links elastin into its insoluble form, causes larger CNVM formation post laser trauma to Bruch's membrane (185). It is likely that fragmentation of Bruch's membrane in the macula renders it more susceptible to the formation of neovascular membranes.

There is also evidence for abnormal systemic elastin metabolism in AMD. Blumenkranz et al. found a correlation between CNV and elastotic degeneration. In patients with neovascular AMD, there was greater than a two-fold increase in their susceptibility to elastotic degeneration of relatively sun-protected areas of the skin in dermal biopsies, suggesting that AMD is associated with systemic elastin abnormalities (179). Serum levels of EDPs in patients with neovascular AMD have also been found to be significantly higher than levels in atrophic AMD patients and control patients (186), which may possibly be due to elevated levels of MMP-9 (187). Thus, numerous lines of evidence suggest a relationship between altered elastin metabolism and AMD progression. It is feasible that EDPs, derived from serum and even locally from fragmentation of Bruch's membrane, could promote the pathogenesis observed in AMD. One interpretation of these findings is that systemic and local defects in elastin physiology lead to a compromised barrier for CNVM in Bruch's membrane. A second, non-exclusive, possibility is that fragments of elastin itself, generated by systemic or local elastolysis, lead to activation of and promote angiogenesis in choroidal endothelial cells.

It is unknown how many elastin-binding proteins exist. The best characterized binding protein was first identified as a 67 kDa cell surface moiety by Hinek et al., known as GLB1 (Figure 25) (188, 189). This high affinity receptor, with lectin-like carbohydrate-binding activity, was later identified as an alternatively spliced, enzymatically inactive form of beta-galactosidase, or S-Gal (190). This peripheral

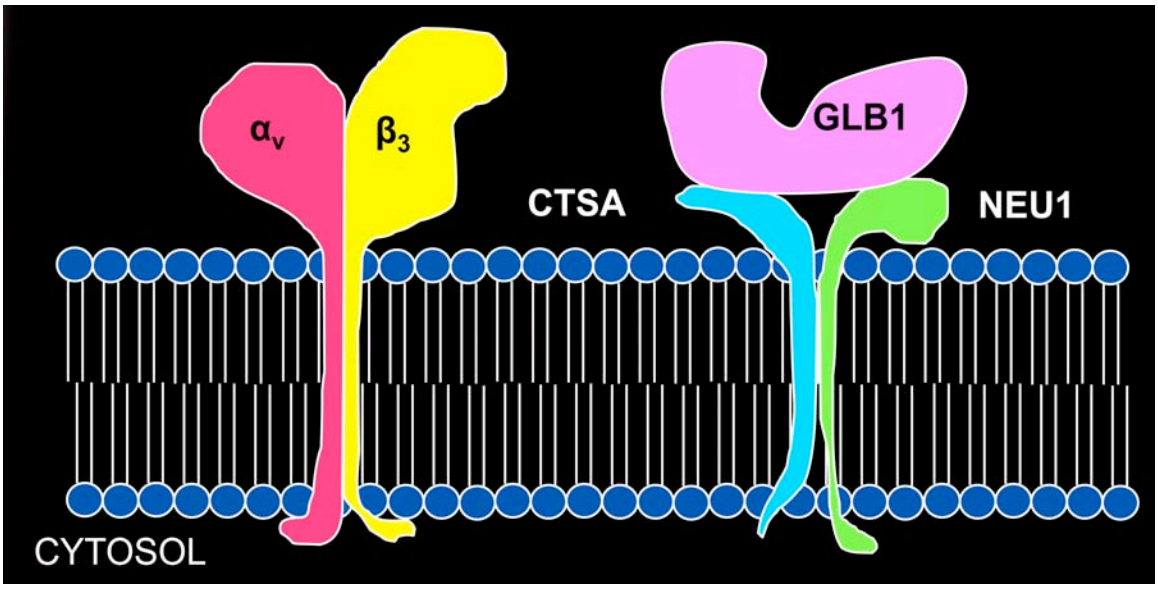

Figure 25. Possible elastin binding proteins. There are two proteins that are hypothesized to bind to soluble elastin fragments. The first is the integrin heterodimer $\alpha_v\beta_3$ (shown on the left). The second is the alternatively spliced form of beta-galactosidase, GLB1 (shown on the right). This is a peripheral protein that is associated with two transmembrane proteins, cathepsin A (CTSA) and neuraminidase (NEU1).

membrane protein is associated with the 61 kDa plasma-membrane anchored protein, neuraminidase, as well as a 55 kDa protein, which is likely to be cathepsin A (175, 191). The binding of EDPs occur at least in part through the hexapeptide sequence VGVAPG on the tropoelastin monomeric unit to a conserved sequence of GLB1 (192). This hexapeptide sequence is repeated several times within the tropoelastin monomer allowing for EDPs to be potent in triggering neoangiogenesis in capillaries by promoting cell migration and tubulogenesis, possibly by activating the ERK1/2 cell signaling pathway (175, 193-195). Two other less characterized elastin binding proteins include the 120 kDa elastonectin and integrin $\alpha_v\beta_3$ (196, 197). Integrin $\alpha_v\beta_3$ is located on endothelial cells and plays a role in angiogenesis (198). Blocking the integrin heterodimer $\alpha_v\beta_3$ has decreased induced retinal neovascularization in mouse studies (199). Blocking the integrin heterodimer may reduce neovascularization by preventing elastin peptides from binding.

In order to clarify the functional impact of elastin on the severity of exudative AMD, we sought to determine whether EDPs promote an angiogenic phenotype in choroidal endothelial cells. During our investigation, we found that EDPs are capable of promoting choroidal endothelial cell migration but not proliferation, both angiogenic phenotypes. These results support the idea that abnormal elastin metabolism in AMD patients promotes disease progression towards neovascular membrane formation.

Materials and methods

Endothelial cell cultures

Two endothelial cell types were used for these studies. The monkey chorioretinal endothelial cell line Rf/6a (ATCC, Manassas, VA) was grown and maintained in F12 medium supplemented with 10% FBS and 1% penicillin/streptomycin. Medium was changed 2x/week. Human choroidal endothelial cells were also used for some experiments. These cells were isolated and purified as described in chapter 2. Only

cultures >95% positive for anti-PECAM-1 and UEA-1 were utilized in assays for this study. Cells had a cobblestone-like morphology and were positive for acetylated low density lipoprotein (ac-LDL) internalization. Cultures were maintained after purification in F12 medium supplemented with 1% FBS and 1% penicillin/streptomycin. Medium was changed 2x/week.

Elastin-mediated endothelial cell wound response assay

To evaluate the effect of EDPs on endothelial cells in culture in terms general angiogenesis, a wound healing assay was used. Rf/6a chorioretinal endothelial cells were grown in wells of a 96-well plate until they reached confluency. A 10 μL micropipette tip (Matrix Technologies, Hudson, NH) was used to scrape a line through the cell monolayer. The cell monolayer was rinsed twice with unsupplemented F12 medium and then replaced with F12 medium (with 1% penicillin/streptomycin) containing HBSS buffer, 100 μg/mL EDPs (human aortic, Elastin Products Company), or 20% serum. HBSS was used in the medium as a negative control since HBSS is the diluent for the peptides, and 20% FBS in medium was used as a positive control as FBS contains VEGF and other factors that support angiogenesis of endothelial cells (200-203). All conditions were tested in triplicate. Cell fields were photographed immediately after creating the gap, and then every 24 hours until the injury gap of one condition had mostly closed using a PupilCAM camera (Ken-a-vision, Kansas City, MO). At this point, the pictures were analyzed using ImageJ software calibrated to a stage micrometer. The average width of the injury gap in each picture was measured and the rate of injury closure was determined.

Elastin-mediated endothelial cell migration

A wound closure assay does not allow for the study of migration and proliferation separately. To observe these behaviors separately in response to elevated EDP concentrations, two different types of assays were used. Migration assays were

performed using the Millicell sterilized culture plate insert with 8 um diameter pores (Cat. # PI8P01250, Millipore, Billerica, MA).

For Rf/6a cells, 200 μL of endothelial cell suspension were added to the upper well of each culture insert placed in a 12 well culture plate (Costar, Corning, NY). F12 medium (with 1% penicillin/streptomycin) containing one of the biochemical stimuli (0.5, 1.0, and 100 μg/mL EDPs, 1.0 μg/mL bioactive hexapeptides VGVAPG (BPs) (Elastin Products Company)) was added to the well of the 12 well culture plate (i.e., the bottom surface of the insert). An equal volume of HBSS was used in medium as a negative control, and 20% FBS in medium was used again as a positive control. The lower concentrations of the EDPs and the bioactive hexapeptides were chosen to be similar to concentrations employed previously by Robinet et al., and the concentration of EDPs found in the serum of exudative AMD patients by Sivaprasad et al. (175, 186). The 100-fold EDP concentration range was chosen to determine if the degree of cellular response was dependent on the peptide concentration.

Cells were incubated for 8 hours at 37^{o}C, 95% humidity, and 5% carbon dioxide. Following incubation, membranes containing cells were fixed in one-half strength Karnovsky's fix (½ K) for at least 1 hour (204). The membranes were rinsed 2x4 minutes in 100 mM cacodylate buffer (pH 7.4) followed by a 30 minute treatment with 1% osmium tetroxide diluted in cacodylate buffer (100 mM). The membranes were then rinsed in double distilled water and sequentially dehydrated in increasing concentrations of ethyl alcohol in double distilled water ending with 2x5 minute incubations in pure ethyl alcohol. A final dehydration step was performed with 2x10 minute incubations in hexamethyldisilizane (HMDS) (Electron Microscopy Sciences, Hatfield, PA). Polycarbonate membranes were carefully removed from their inserts and mounted on metal stubs with silver mounting medium (Ted Pella, Redding, CA), and then sputter coated with gold ions using a K550 Emitech sputter coater.

Membranes were observed using a Hitachi S-3400N scanning electron microscope (SEM) at the University of Iowa Central Microscopy Facility. Ten digital images of the membrane's lower surface were collected for each experimental sample at 150x magnification in a masked fashion. Cells were counted for each image using ImageJ software, taking care to only count cells that have established contact onto the membrane beyond the pore opening. In other words, cells that occupied pores but had not attached a portion of their surface membrane to the polymer surface were not included in the counts.

For some experiments, inclusion of an irrelevant protein (BSA, 1.25 μg/mL) was performed in order to determine the specificity of elastin's effects.

Methods were repeated using a primary culture of human choroidal endothelial cells instead of Rf/6a cells. Due to the limited material available, elastin fragments were used only at 100 μg/mL for this experiment.

Methods were also repeated with the addition of a mouse antibody to integrin heterodimer $\alpha_v\beta_3$ (R&D, Minneapolis, MN) at a concentration of 5 μg/mL or with 0.2 M lactose (Fisher Scientific, Fair Lawn, NJ) to the upper chamber with the cells. The antibody and lactose were added to competitively inhibit the binding site of the two possible elastin fragment receptors, $\alpha_v\beta_3$ and GLB1, respectively (189, 197). These blocking assays were performed with EDPs at 100 μg/mL in the lower chamber and again with 20% FBS (positive migratory control) in the lower chamber. The reason for performing assays with two different types of chemoattractants was to determine if blocking these proteins inhibited EDP-mediated migration or migration in general.

Finally, experiments were repeated with the addition of 20 mM 3-(2-aminoethyl)-5-((4-ethoxyphenyl)methylene)-2,4-thiazolidinedione hydrochloride (Sigma, St. Louis, MO) to the upper chamber of the insert with the cells at the beginning of the assay. This is an antagonist of the ERK 1/2 pathway (205). This signaling antagonist was used in

assays with EDPs as well as FBS in the lower chamber. Results were analyzed using the paired Student's t-test.

Elastin-mediated endothelial cell proliferation

Equal numbers of chorioretinal endothelial cells were seeded and grown in wells of a 6-well plate for 48 hours in F12 medium (with 1% penicillin/streptomycin) containing biochemical stimuli. The following concentrations of biochemical stimuli were used: 0.5, 1.0, and 100 μg/mL EDPs, and 1.0 μg/mL bioactive hexapeptides. Positive and negative controls included FBS and HBSS, as above. All experimental conditions were performed in triplicate. Time 0 hour seeding populations were fixed with 4% paraformaldehyde, pH 7.4, and stored suspended in PBS at 4^{o}C on a rotator until the end of the experiment. These cells were stored in order to determine initial cell populations. After 48 hours, treated cells were trypsinized with 0.25% Trypsin-EDTA (Gibco, Auckland, New Zealand) and centrifuged at 1000xg for 5 min. Cells were resuspended in 4% paraformaldehyde, pH 7.4, for 10 minutes and then centrifuged at 1000xg for 5min. Cells were resuspended in 0.5 mL PBS with 10 μg/mL propidium iodide (Invitrogen) as well as 100 μL 3.0 μm diameter Fluoresbrite YG Microspheres (Polysciences, Inc., Warrington, PA) diluted in PBS, yielding a final concentration of approximately 1.7x10^{9} beads/mL. Cell and bead counts were completed using a BD LSR flow cytometer (Becton Dickinson) at the University of Iowa Flow Cytometry Facility. Cell to bead ratios were used to standardize the samples and then percent growth was calculated for each sample in comparison to the 0 hour cell populations.

Elastin peptide overlay immunohistochemistry

The location(s) of soluble elastin peptide binding was determined using an elastin peptide overlay experiment. Human donor eye tissue was fixed in 4% paraformaldehyde for 2 hours. Wedges spanning from the macula to the ora serrata were cryoprotected in sucrose and embedded as described previously (131). The tissue was sectioned using a

Microm HM 505 E cryostat. Sections were collected at a thickness of about 7 µm onto Superfrost/Plus slides (Fisher Scientific, Fair Lawn, NJ).

Tissue sections were incubated with 100 ng/mL etna-elastin (Elastin Products Company, Owensville, MO) diluted in PBS, or in PBS alone, overnight at 4°C. Sections were then blocked with 1% horse serum in PBS for 15 minutes, followed by 1 rinse in PBS. Next, the tissue was incubated with 5 µg/mL of a monoclonal anti-elastin antibody (clone 10B8; Millipore, Billerica, MA) diluted in the blocking solution for 1 hour, followed by 3x5 minute rinses in PBS. Following incubation, the primary antibody was visualized using the Vectastain Elite kit following manufacturer's instructions (Vector Laboratories, Burlingame, CA), and then rinsed 3x5 minutes in PBS. Binding was visualized using the Vector V.I.P. horseradish peroxidase kit according to manufacturer's instructions (Vector Laboratories). Tissue was dehydrated stepwise with 80%, 95%, 100% ethanol, followed by ClearRite, and coverslipped using Permount (Fisher Scientific).

Detection of the elastin binding protein mRNA

To determine if endothelial cells from the choroid express mRNA transcripts for the alternatively spliced form of GLB1 and its associated trans-membrane proteins, RT-PCR was used. RNA was isolated from choroidal endothelial cells and frozen punches of human RPE-choroid using the RNeasy mini kit according to manufacturer's instructions (Qiagen, Valencia, CA). Reverse transcription was performed using the High-Capacity cDNA Reverse Transcription Kit according to manufacturer's instructions (Applied Biosystems, Foster City, CA). Following reverse transcription, PCR was carried out using the BIOLASE DNA polymerase kit with the following conditions for 35 cycles: denaturing at 94°C for 45 seconds, annealing at 62°C for 30 seconds, and elongation at 72°C for 1 minute (Bioline, Taunton, MA). Primers were designed for the amplification of *GLB1, CTSA*, and *NEU1* and purchased from Integrated DNA Technologies,

Coralville, IA. Since the 61 kDa elastin binding form of GLB1 is translated from an alternatively spliced transcript lacking exons 3, 4, and 6, the forward primer for *GLB1* was designed to span the boundary between exons 2 and 5 (Figure 26). This primer is not expected to anneal to the cDNA derived from the full length *GLB1* transcript. Amplified PCR products were separated on a 2% agarose gel with the Fisher Biotech horizontal electrophoresis system (Fisher Scientific) at 106 V for approximately 45 minutes. The gel was stained using ethidium bromide for visualization. Identities of amplified fragments of *GLB1* were determined by automated DNA sequencing. Primers used were: *GLB1* forward primer, 5'- GCC ATC CAG ACA TTA CCT GGC A -3', *GLB1* reverse primer, 5'- TGT CCG GTA CAG CAC AAA CCC ATA -3', *CTSA* forward primer, 5'- GTG CCC AGC CAT TTT AGG TA -3', *CTSA* reverse primer, 5'- TTC TGG TTG AGG GAA TCC AC -3', *NEU1* forward primer, 5'- GAA CCT TGG GGC AGT AGT GA -3', *NEU1* reverse primer, 5'- CTC ATA GGG CTG GCA TTC AT -3'.

EDP treated endothelial cell PCR array profiling

To determine the changes in gene expression due to elevated levels of EDPs compared to controls, quantitative PCR arrays were used. Primary cultures of human choroidal endothelial cells were plated into the wells of a 6-well culture plate and treated with 100 μg/mL EDPs in the same method as performed in chapter 3 with recombinant C5a. RNA was extracted, reverse transcribed, and quantitative PCR was performed as described in chapter 3 with the same array profiling system (product # PAHS-015A; SABiosciences).

Results

Elastin-mediated endothelial cell wound response assay

In order to determine whether EDPs elicit increased wound closure in ECs, we performed a wound response assay. We observed a greater rate of Rf/6a endothelial cell

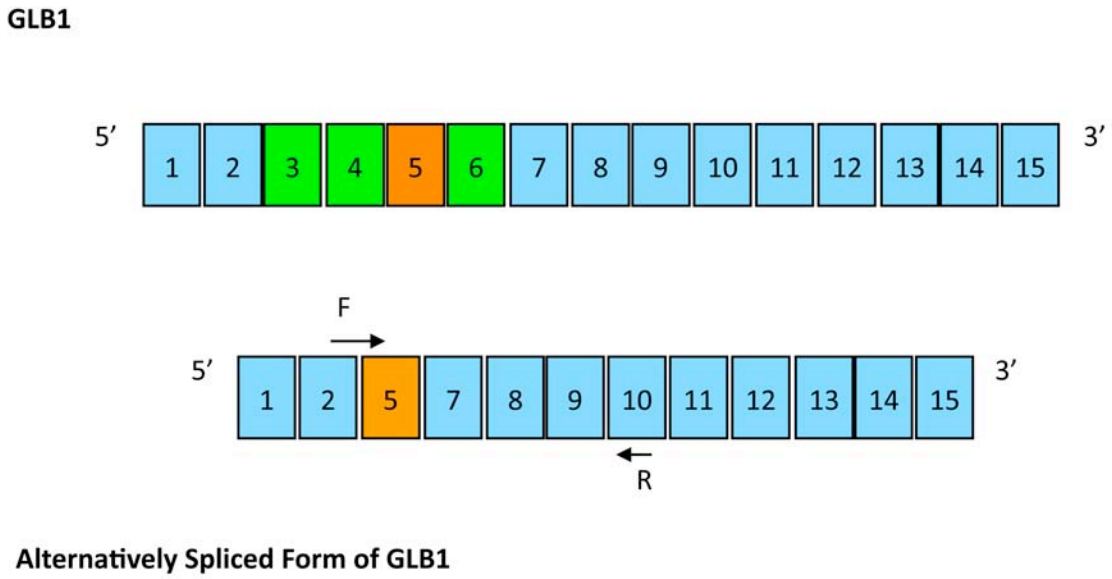

Figure 26. *GLB1* primer design. The gene for *GLB1* has 15 exons. The alternatively spliced form of *GLB1* results in the binding protein for soluble elastin fragments. In order to determine if cells expressed the mRNA for the alternatively spliced form of *GLB1*, it was important to design primers that would amplify this form only. The forward primer was designed to anneal at the boundary between exons 2 and 5 in order to accomplish the desired amplification of the spliced form.

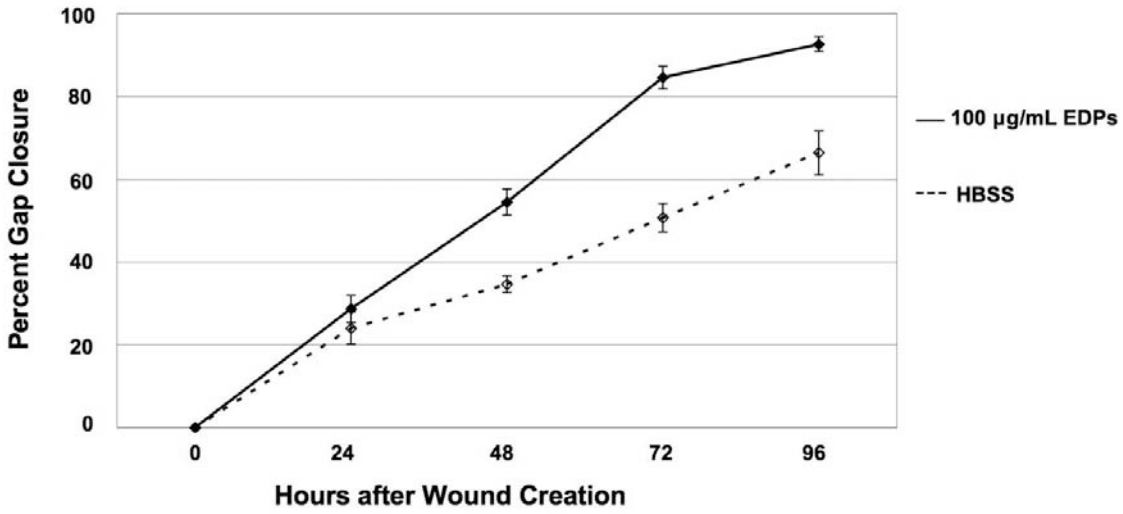

Figure 27.Elastin-mediated wound healing response. The chorioretinal endothelial cell line Rf/6a responded to 100 µg/mL EDPs more than to HBSS by closing the gap to a greater extent after 96 hours. Comparison was statistically significant with a p-value of 0.01. Cells exposed to other concentrations and types of elastin fragments demonstrated similar trends in comparison to HBSS exposed cells, however did not reach levels of statistical significance.

wound response, including migration and/or proliferation, in the presence of elastin fragments. Results are given as the fraction of gap closure over a 96 hour period. In the presence of 100 μg/mL EDPs gap closure occurred at a significantly greater rate than in the presence of buffer alone (Figure 27). Rf/6a endothelial cells exposed to 0.5 μg/mL EDPs or 100 μg/mL bioactive hexapeptides had responses similar to those exposed to 100 μg/mL EDPs, however did not reach levels of statistical significance (data not shown). The trends implicated a dependence of endothelial cell migration and/or proliferation on the presence of elastin fragments, especially at a concentration of 100 μg/mL.

Elastin-mediated endothelial cell migration

In order to determine whether elastin fragments elicit increased migration by ECs, we performed a migration study using cell culture plate inserts. In order to assess whether a chemotactic gradient is maintained across the membrane, the diffusion of FBS proteins across the culture insert membrane from lower chamber to upper chamber was analyzed at 0, 2, 4, and 8 hours in the absence of cells using SDS-PAGE. After 8 hours, the amount of protein in the lower chamber remained significantly higher than that in the upper chamber (data not shown).

Cell migration in response to EDPs was quantified in a masked fashion. Cells included in the migrated count had established a portion of their membrane onto the polymer membrane. Examples of cells counted are pictured in Figure 28. In initial experiments, we observed an increase in endothelial cell migration in the presence of elastin fragments. Following 8 hours of incubation, Rf/6a cells migrated to a greater extent in the presence of either 100 μg/mL EDPs or 1 μg/mL bioactive hexapeptides than in the presence of HBSS. Cells exposed to BSA showed a migratory response similar to those exposed to HBSS (Figure 29). Statistical analyses of the number of migrated cells

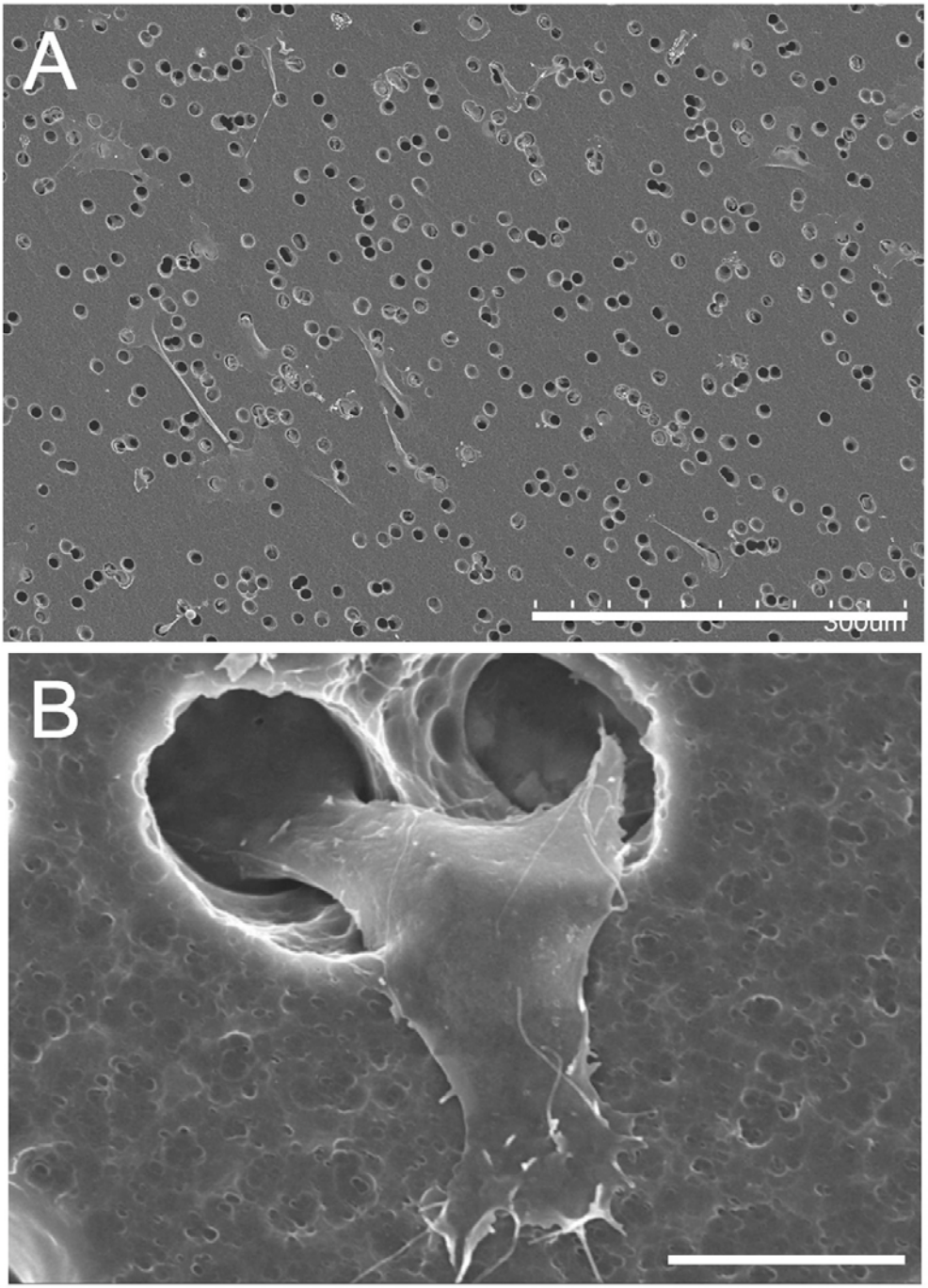

Figure 28. Migration assay SEM microscopy. Images of choroidal endothelial cells which have migrated to the bottom surface of an 8 um diameter pore polycarbonate membrane. **(A)** An example image of Rf/6a chorioretinal endothelial cells used for quantitative analysis. Scale bar = 300 µm. **(B)** Cells were counted only if a portion of the cell had begun to emerge from the pore, as shown in detail in this micrograph of a human choroidal endothelial cell. Scale bar = 10 µm.

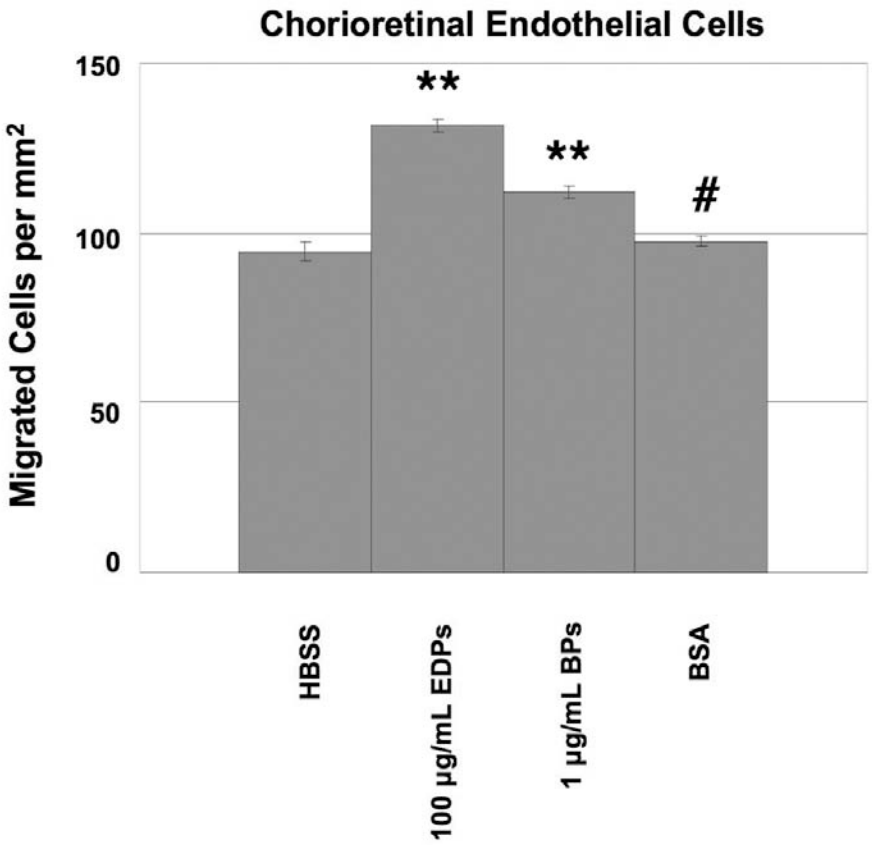

Figure 29. Elastin-mediated chorioretinal endothelial cell migration I. Chorioretinal endothelial cell migration through a polycarbonate membrane due to a chemotactic gradient. The addition of an irrelevant protein (BSA) was added to this preliminary study. Human choroidal endothelial cell migration through a polycarbonate membrane. Cells cultured in the presence of EDPs or BPs had a greater incidence of migration than those cultured in the presence of HBSS or BSA alone. (**) represents a p-value < 0.01 and (#) represents a p-value > 0.50. All p-values are representative of elastin fragment conditions compared to HBSS. All error bars are the standard error of the mean.

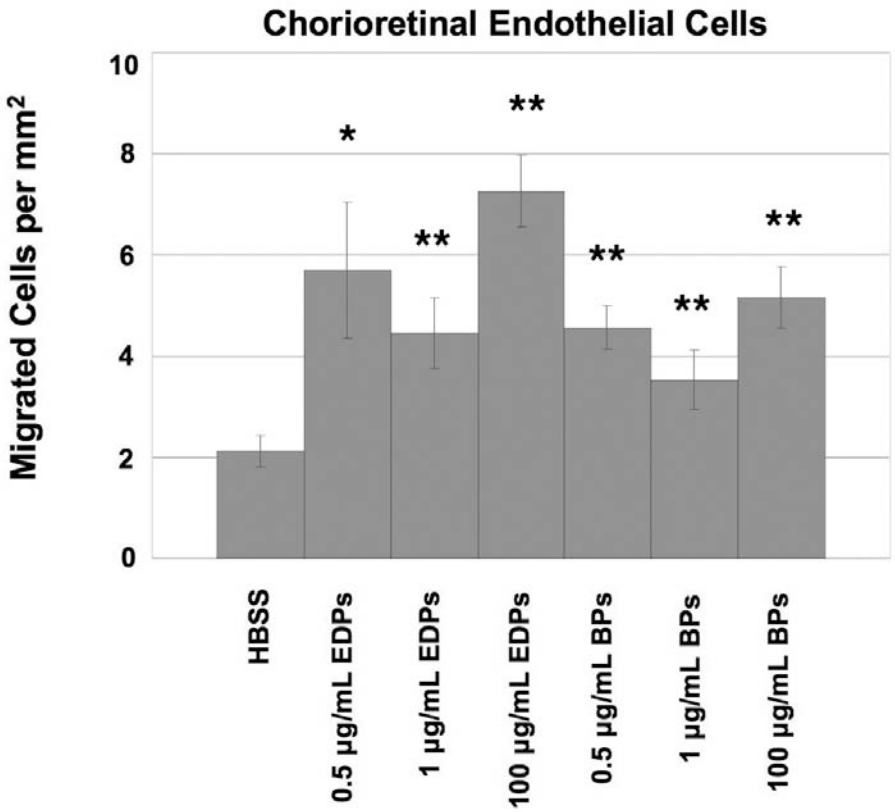

Figure 30. Elastin-mediated chorioretinal endothelial cell migration II. Different concentrations of EDPs and BPs were used to determine if the migratory response found in the preliminary study was concentration dependent. Cells cultured in the presence of EDPs or BPs, no matter the concentration, had a greater incidence of migration than those cultured in the presence of HBSS alone. (*) represents a p-value < 0.05, and (**) represents a p-value < 0.01. All p-values are representative of elastin fragment conditions compared to HBSS. All error bars are the standard error of the mean.

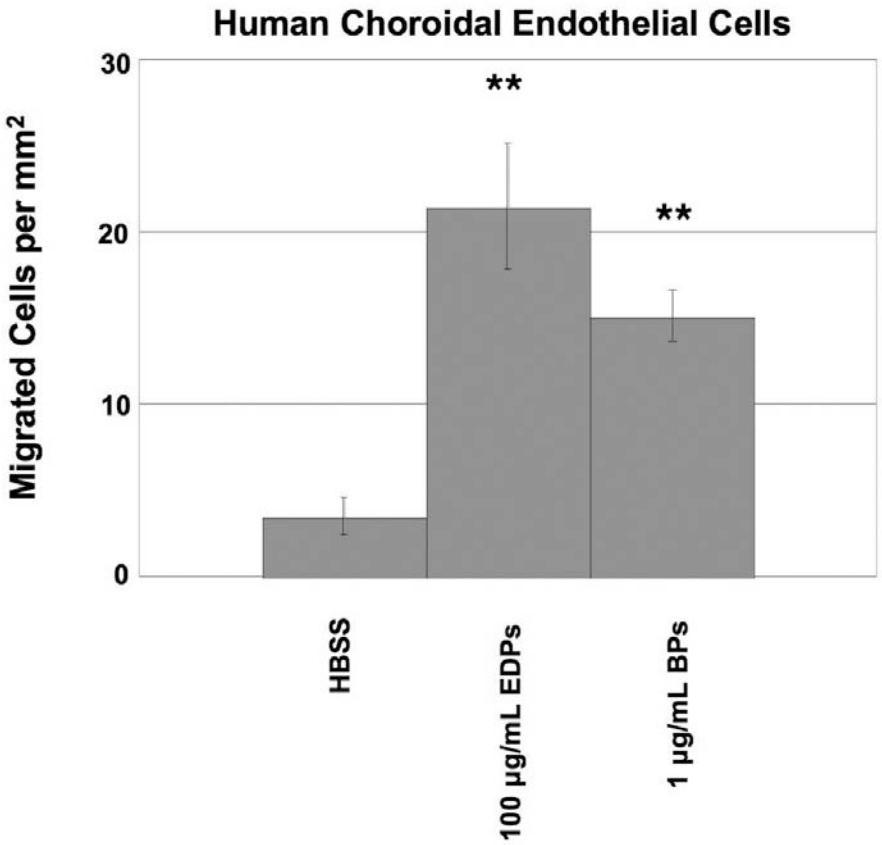

Figure 31. Elastin-mediated human choroidal endothelial cell migration. To identify if the migratory response found in chorioretinal endothelial cells was similar to that possible in humans, primary human cells were used in a separate assay. Primary endothelial cells cultured in the presence of EDPs or BPs had a greater incidence of migration than those cultured in the presence of HBSS alone. (**) represents a p-value < 0.01. P-values are representative of elastin fragment conditions compared to HBSS. All error bars are the standard error of the mean.

were determined for each experimental stimulus in comparison to HBSS. Both EDPs and FBS had p-values < 0.001 and BPs had a p-value =0.01. Further testing of Rf/6a cell migration demonstrated a migratory dependence on EDP concentration. For both EDPs and BPs, the highest concentration (100 μg/mL) did not show significantly more migration than the lowest concentration (0.5 μg/mL), p-value = 0.3, however all concentrations yielded significant increases in migration in comparison to HBSS (Figure 30). All comparisons yielded p-values < 0.05.

In order to confirm that results in the Rf/6a cell line were applicable to human endothelial cells, migration experiments were also performed on a culture of human choroidal endothelial cells. As noted for Rf/6a cells, human choroidal endothelial cells increased their migration in response to EDPs (Figure 31). Statistical analyses of cell migration rates were determined for each experimental stimulus in comparison to HBSS. Both BPs and FBS had p-values < 0.01 and EDPs had a p-value < 0.05.

Elastin-mediated endothelial cell proliferation

To determine whether EDPs and/or bioactive hexapeptides increase endothelial cell proliferation, we quantified their growth changes using flow cytometry. Cells exposed to elastin fragments did not show an altered degree of proliferation in comparison to cells exposed to HBSS after 48 hours (Figure 32).

Elastin peptide overlay immunohistochemistry

In order to examine the distribution of elastin/EDP-binding proteins in human eyes, etna-elastin overlay experiments were performed on sections of several different human eyes. Tissue sections incubated with etna-elastin or PBS both exhibited elastin labeling in Bruch's membrane, in the capillary extra-cellular matrices, as well as in vessel walls of choroidal arteries. In contrast, tissue pre-incubated with etna-elastin showed increased labeling of the RPE, choriocapillaris and choroidal endothelium, indicating the

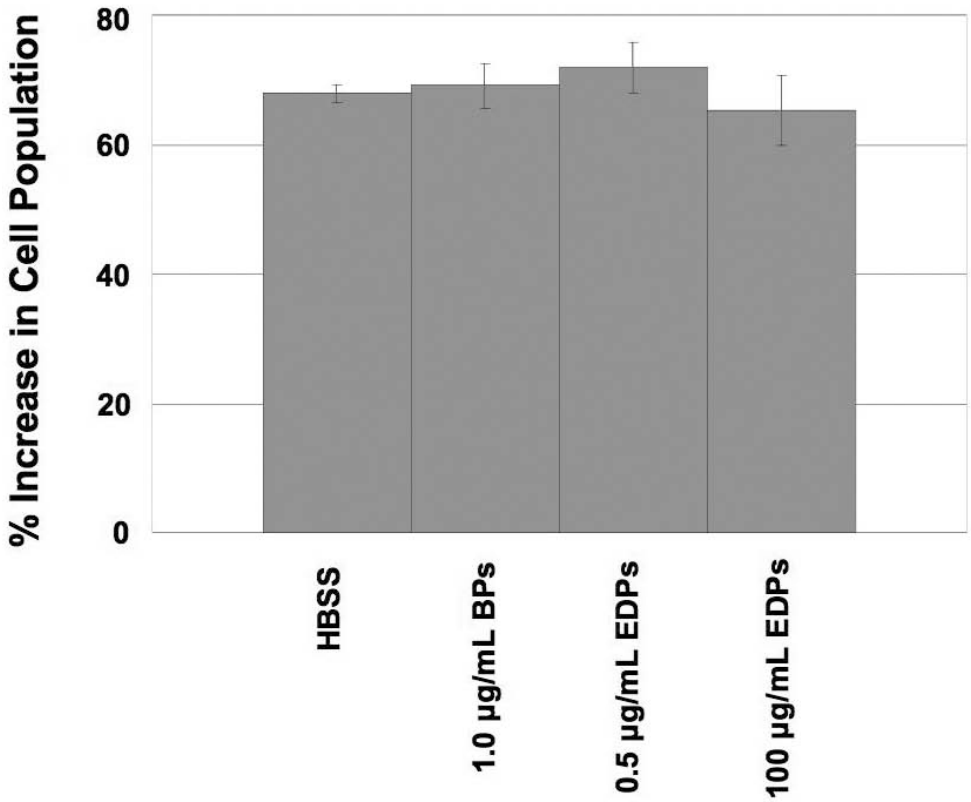

Figure 32. Chorioretinal endothelial cell proliferation in response to elastin fragments. None of the experimental conditions caused the cells to proliferate more than the HBSS control. All error bars are SEM.

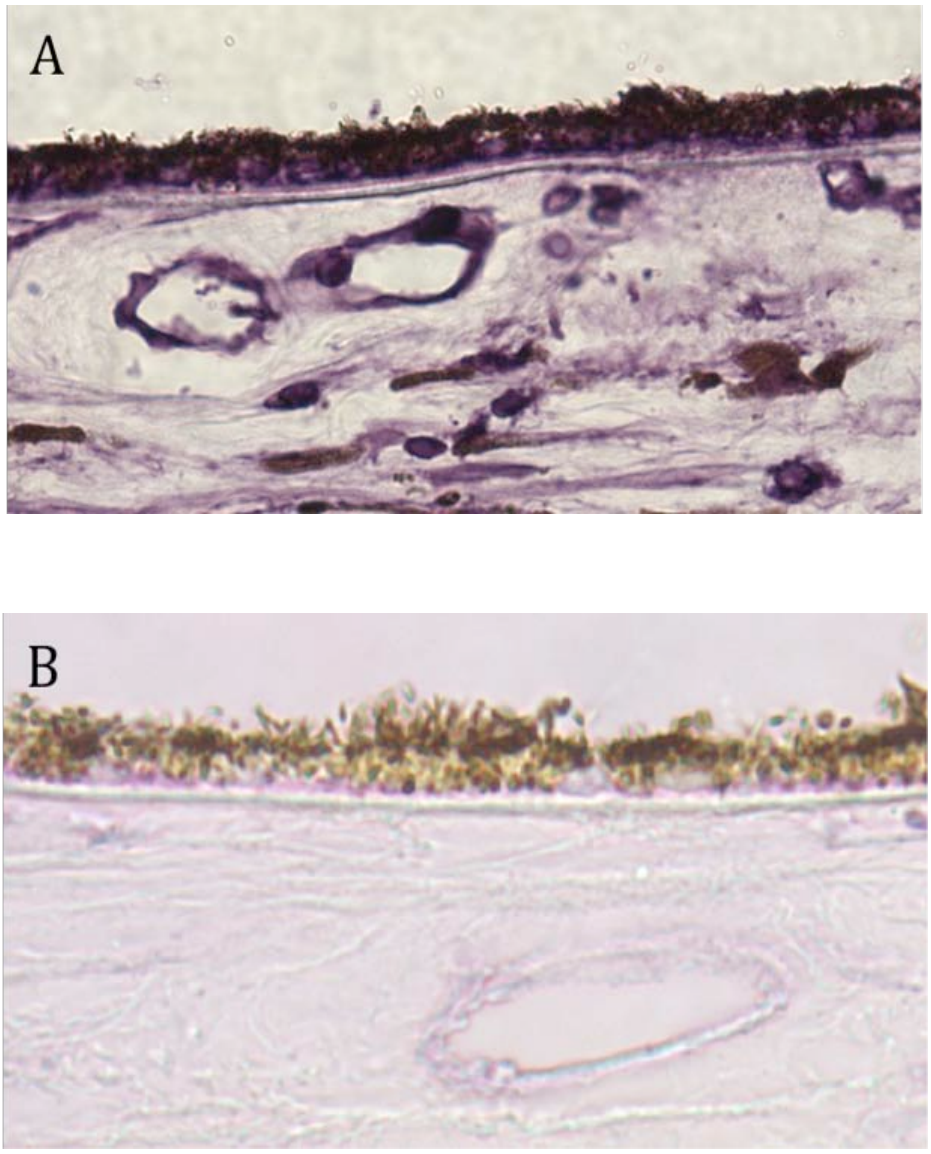

Figure 33. Elastin fragment overlay immunohistochemistry. (A) Tissue section of human RPE and choroid incubated with etna-elastin overnight and labeled with an elastin antibody. (B) Tissue section incubated with PBS overnight and labeled with an elastin antibody. Labeling of choriocapillary and choroidal vessels in the tissue exposed to etna elastin suggests the presence of elastin/EDP binding sites on the endothelium. Although intensity of labeling was variable, this pattern of elastin binding sites was similar across a panel of donor eyes.

presence of elastin/EDP binding sites on human choroidal endothelial cells *in vivo*. Some heterogeneity between donors and between capillaries within donors was observed, however the pattern was similar in almost all of the cases. An example of this labeling is shown in Figure 33.

GLB1 elastin-binding protein mRNA RT-PCR

In order to identify whether human choroidal endothelial cells synthesize transcripts for the alternatively spliced, elastin binding form of GLB1, as well as its associated membrane proteins, CTSA and NEU1, RT-PCR was utilized. Amplimers of *GLB1, CTSA,* and *NEU1* were all detected following separation on an agarose gel as shown in Figure 34. Sequencing of a *GLB1* PCR fragment showed that the alternatively spliced form of *GLB1* is expressed by these cells (data not shown).

Blocked elastin binding protein migration assay

Cells that were exposed to an antibody against $\alpha_v\beta_3$ had a significant reduction in their migratory response towards EDPs or FBS (p-values < 0.01). Cells exposed to 0.2 M lactose had a significant reduction in migration towards EDPs (p-value = 0.01), however did not have a significant change in migration towards FBS (p-value = 0.65) in comparison to cells not exposed to either inhibitor (Figure 35).

Blocked ERK 1/2 pathway migration assay

Cells that were exposed to the inhibitor of the ERK 1/2 signaling cascade had a non-significant increase in migration towards EDPs (p-value = 0.24) and a significant increase in migration towards FBS (p-value = 0.018) compared to cells not exposed to the inhibitor migrating towards the same attractant (Figure 36). This finding indicates that inhibiting the ERK 1/2 cascade does not inhibit EDP-mediated migration, but increases it. This increase occurred in FBS-mediated migration also. The inhibitor used for this assay must activate endothelial cells to migrate by an unknown mechanism.

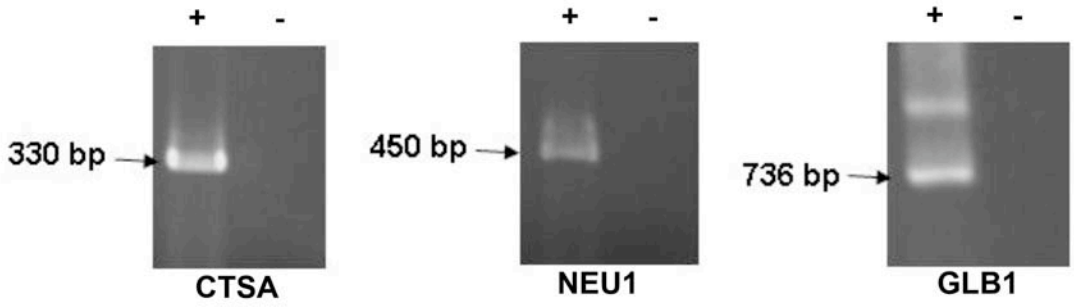

Figure 34. Expression of *GLB1* in the human choroid. Transcripts for the peripheral elastin fragment binding protein, GLB1, and its two associated trans-membrane proteins are present in human RPE/choroid *in vivo*. The smaller (expected size) band for *GLB1* was confirmed by sequencing.

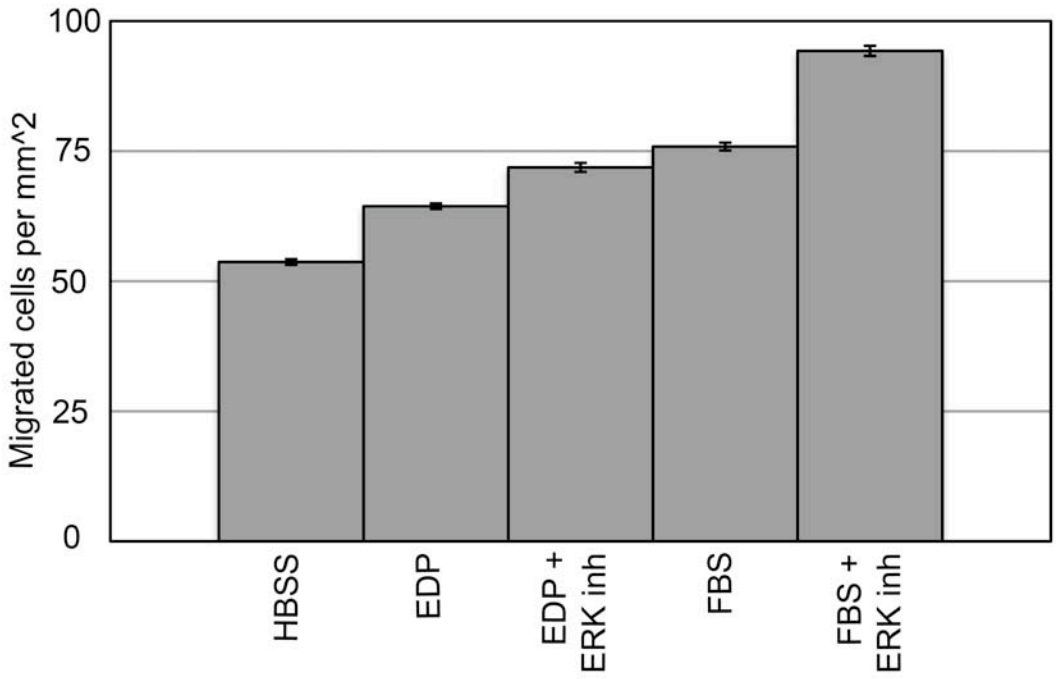

Figure 35. ERK 1/2 blockage migration assay. The ERK 1/2 pathway, which is the intracellular signaling cascade hypothesized to participate in elastin-mediated migration, was blocked with the addition of 20 mM 3-(2-aminoethyl)-5-((4-ethoxyphenyl)methylene)-2,4-thiazolidinedione hydrochloride in the upper chamber with the seeded chorioretinal endothelial cells. EDPs (100 μg/mL) or 20% FBS were applied to the bottom chamber as chemoattractant agents. Blocking the ERK 1/2 pathway did not inhibit migration, but rather increased the migratory response of cells towards EDPs and FBS. Error bars represent SEM.

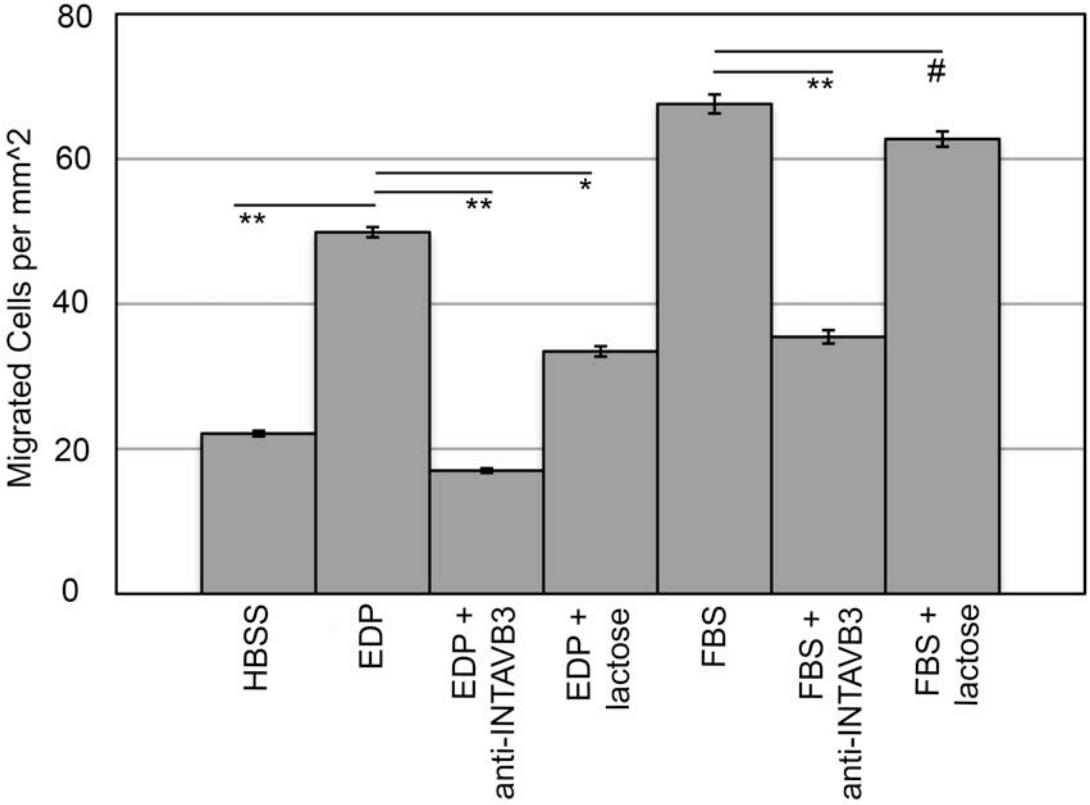

Figure 36. Elastin fragment binding protein blockage migration assay. To block the possible binding sites for the EDPs, an antibody to $\alpha_v\beta_3$ at a concentration of 5 μg/mL or 0.2 M lactose (to inactivate GLB1) was added to the upper chamber with the seeded cells. EDPs (100 μg/mL) or 20% FBS were added to the lower chamber. The addition of an antibody to $\alpha_v\beta_3$ decreased the migratory response to EDPs or FBS significantly in comparison to the cells original responses to these proteins. The addition of 0.2 M lactose only significantly reduced the migratory response induced by EDPs, not the response induced by FBS. (**) indicates a p-value < 0.01, (*) indicates a p-value = 0.01, and (#) indicates a p-value > 0.5.

Table 3. EDP exposed human choroidal endothelial cell gene expression.

Gene	Fold Change	P-value
CCL2	2.34	0.04
ICAM1	0.53	0.03
LSEL	4.80	0.04
NOS3	5.65	0.04
MMP9	4.30	0.04

EDP treated endothelial cell PCR array profiling

The statistically significant results of the EDP exposed and control human endothelial cell quantitative PCR array are summarized in Table 3. Out of the changes found, the expression of *MMP9, CCL2,* and *SELL* had a greater than 2-fold increase in the EDP treated endothelial cells compared to the control cells (p-values < 0.05). These changes were interesting to find because of their roles in inflammation (*CCL2* and *SELL*) or extracellular matrix turnover (*MMP9*).

Discussion

Elastin is a glycoprotein, which provides structural support as well as elasticity to tissues such as arteries, lung, and skin. Elastin is also the major component of the central layer of Bruch's membrane, which is located between the RPE and the choriocapillaris. Bruch's membrane likely functions as a physical barrier, allowing for the diffusion of essential nutrients and gases to the retina, and removal of waste from the retina, while preventing the choroidal blood vessels from growing into and disrupting the delicate structure of the retina. Disruption of Bruch's membrane by disease or experimental intervention is associated with CNVM formation (4, 22, 185).

As discussed above, elastin within Bruch's membrane is abnormally metabolized in AMD. In this study we sought to determine if, in addition to disruption of the physical barrier, elastolysis may affect the behavior of choroidal endothelial cells, and found that EDPs increase the migration of these cells.

Choroidal neovascularization is a multistep process including the breakdown of Bruch's membrane, choroidal endothelial cell migration from the choroid into the sub-RPE and/or sub-retinal space, as well as endothelial cell proliferation and tubulogenesis.

In this study, we observed that when sections of human choroid are incubated with elastin fragments, the fragments localize to vessel walls. This observation indicates

that there are binding sites for elastin fragments on the choroidal vascular endothelium and that choroidal ECs may be capable of responding to EDPs *in vivo*.

We have demonstrated that EDPs can play a role in choroidal angiogenesis. First, we observed that upon disrupting a monolayer of chorioretinal endothelial cells by scraping a gap into them, cells in the presence of EDPs were able to close the gap more efficiently. Increased gap closure may result from cell proliferation, cell migration, or both. Therefore it was necessary to test these events separately. When testing migration responses, EDPs played a significant role as a chemoattractant for both human and monkey choroidal endothelial cells, as these cells migrated to a greater extent in the presence of distinct forms of elastin. The magnitude of the observed migratory response was dependent on the concentration of EDPs used. The greatest response was elicited when the concentration was 100 µg/mL compared to 0.5 µg/mL, which also yielded a cell migratory response significantly greater than buffer alone. Cells that were incubated with inhibitors to the elastin binding proteins had a decrease in migration. Decreased migration with the application of anti-$\alpha_v\beta_3$ was independent of the presence of EDPs as a chemoattractant as anti-$\alpha_v\beta_3$ inhibited migration regardless of the migrating stimulus. The addition of 0.2 M lactose lead to a decrease of migration in cells migrating towards EDPs, but did not lead to a decrease in migration of the cells that were attracted towards FBS. These results show that GLB1 is the elastin binding protein on the surface of choroidal endothelial cells. We verified that its gene is expressed in the human choroid *in vivo.*

Blocking the ERK 1/2 signaling cascade lead to results that were opposite of those expected. The addition of the inhibitor increased the migration of the cells, independent of the type of attractant used. It seems that this inhibitor is actually activating the cells to migrate more. The ERK 1/2 pathway is responsible for several angiogenic behaviors of endothelial cells, including migration, proliferation, and differentiation. It does not appear that this cascade mediates migration in

choroidal endothelial cells. An explanation for the opposite effect may be that this cascade mediates one of the other angiogenic behaviors in this cell type, and when it is blocked the cells are able to increase other angiogenic behaviors (i.e. migration).

In contrast to the migration response, proliferation assays indicated that choroidal endothelial cells replicate at similar rates in the presence of EDPs as in the presence of buffer alone, suggesting that some events in angiogenesis are not driven by EDPs.

The findings of the endothelial cell PCR profiling array indicated that EDPs can cause an increase in inflammation as well as extracellular matrix turnover, as EDPs caused an increase in the expression of *CCL2, SELL,* and *MMP9*. Monocyte chemotactic protein 1 (MCP-1) is a small chemokine that attracts monocytes from the circulation to a given site (57). L-selectin (L-sel) is a surface protein on leukocytes that aids in their extravasation from blood into nearby tissues by binding ligands (ex. CD34) found on the surface of endothelial cells. L-sel is also found on the surface of endothelial cells themselves and CD34 is present on leukocytes (206). Although this method of leukocyte tethering is not the most common via L-sel, it is possible that the increased expression of L-sel on the endothelial cell surface increases binding to antigens on the leukocytes cell surface, including CD34. Both MCP-1 and L-sel could play a role in increasing local inflammation. Matrix metalloproteinase (MMP-9) is an enzyme that breaks down extracellular proteins, including elastin and collagen. An increased amount of MMP-9 in the choroid could increase the breakdown of Bruch's membrane, decreasing its ability to serve as a barrier, possibly allowing for the growth of new vessels to grow through the membrane.

With respect to the events occurring in neovascular AMD, it is plausible that the ability of choroidal endothelial cells to demonstrate pro-angiogenic behaviors and increase inflammatory and matrix altering proteins in response to elevated EDPs plays a role in the progression of the disease pathogenesis. Morphologically, it has been demonstrated that the elastic layer of Bruch's membrane is thinner and more fragmented

in patients with AMD. Loss of the barrier function of Bruch's membrane likely permits choroidal endothelial cells to migrate through into the sub-retinal space. Clinically, EDPs are at higher levels in the serum of AMD patients, especially those with neovascular AMD, in comparison to patients without AMD, indicating that there may be a systemic source of soluble elastin fragments in AMD patients. The breakdown of this membrane also possibly provides a local increase in soluble elastin fragments that could bind to and activate endothelial cells to migrate. Therefore, choroidal endothelial cells in a patient with AMD may potentially be activated by an increased level of EDPs, both from the serum and from elastolysis of Bruch's membrane, to become pro-angiogenic. Coupled with the decreased integrity of Bruch's membrane in AMD patients, these cells may migrate into the sub-retinal space where they proliferate and form new vessels, beginning the cascade of events involved in neovascular membrane formation.

In summary, elastin degradation plays a role in both the weakening of the barrier to endothelial cell migration into the sub-retinal space as well as activating endothelial cells to migrate and form tubes (175). We suggest that elastin degradation may play an important role in choroidal neovascularization during late stage AMD. Halting this breakdown of elastin or interfering with EDP signaling may provide a target for slowing the progression of AMD towards neovascularization.

Portions of this chapter were published in Investigative Ophthalmology and Visual Science in 2008:

Skeie JM, Mullins RF. Elastin-mediated choroidal endothelial cell migration: possible role in age-related macular degeneration. Invest Ophthalmol Vis Sci. 2008;49(12):5574-80. PMCID: 2609900.

CHAPTER 6. INVESTIGATING CHOROIDAL ENDOTHELIAL ACTIVATION USING AN ANIMAL MODEL

Introduction

Investigating the mechanisms of human ocular diseases can be a daunting task due to the physiological and mechanical complexity of the eye, and the species-specific features of the human eye. Utilizing *in vitro* methods provides an efficient, reproducible means of studying specific reactions of purified cell types in response to discrete variables. While this provides a single question, single answer solution, we know that in the human eye there are additional, and often unidentified variables to consider. An *in vivo* platform offers a complementary approach to cell culture methods used in the majority of this work.

In this investigation, we set out to study the effect of elevated serum elastin fragments in the mouse. In humans, there is a correlation between a higher level of elastin fragments in the serum with increasing severity of AMD (186), and highest serum levels recorded in patients with neovascular AMD. The elevated levels of fragments may be from systemic sources, or created locally in the eye as Bruch's membrane breaks down with age. Either way, elevated circulating levels of elastin fragments are associated with AMD.

Serum levels of extracellular matrix proteins, collagen and elastin, have been elevated in mice previously to study the effects on disease progression in a model of emphysema. (207). It was shown that elastin fragments are a chemoattractant for macrophages, which build up in the interstitium, septum, and alveolar spaces in emphysema patients. There have not been similar studies of the eye until this investigation.

The two most commonly used mammalian models for the research of AMD are mouse and monkey. There are advantages and disadvantages to both of these models. The advantages for using monkeys are that they are genetically closer to humans than mice, and they have a macula, which for studying AMD is very important. Utilizing monkeys, on the other hand, is very expensive, requires more time because of longer life cycle, and raises greater concern with animal welfare. Although mice are less genetically similar to humans than monkeys and do not have a macular region in their eye, they do have similar posterior tissues including the retina, RPE, Bruch's membrane, and choroid. So, studying differences in macular vs. peripheral changes is not possible, but studying tissue specific manifestations similar to those found in AMD is possible. Mice are also the most commonly used model due to genome sequence availability, genetic manipulability, short life cycle, and ease of maintenance. This means that there is a wealth of baseline data and good capacity for comparison between studies.

In the case of AMD, mouse models have provided many insights, however, there are still many disadvantages. Currently, there are three mouse models that recapitulate some of the characteristics of atrophic AMD in humans. These models include the Ccl-2 knockout mouse, developed by Ambati et al. (208), the ApoE transgenic mouse developed by Malek et al. (209), and the Sod-1 knockout mouse developed by Imamura et al. (210). These models contain several of the manifestations that are found in atrophic AMD, including drusen-like deposits in the sub-RPE space, possible retinal atrophy (or at least abnormalities), RPE abnormalities, and choroidal neovascularization. Although this provides researchers in ophthalmology a method for studying human etiology, there have been several disputes regarding the accuracy and reproducibility of this model. For instance, it was found by Luhmann et al. that the drusen-like deposits in Ccl-2 knockout mice are actually engorged macrophages in the sub-retinal space (211).

A mouse model for neovascular AMD is more commonly used. This model is created by laser photocoagulation of Bruch's membrane (121, 185, 211). Disrupting

Bruch's membrane allows vessels from the choroid to proliferate into the sub-RPE and sub-retinal spaces. This model demonstrates the role of Bruch's membrane in preventing of vessels from the choroid growing into the RPE and retinal areas. The volume of the neovascular membrane formed anterior to Bruch's membrane post-laser photocoagulation is measured to quantify the severity of the lesion. Although this model is effective for studying neovascularization with respect to angiogenesis in the eye, it is not a model of neovascularization arising from chronic or progressive pathology.

In addition to these models, it is common for researchers to change the level and/or function of a desired protein in mice to determine the effects of that particular protein in a desired tissue. In regards to AMD, these types of models do not recapitulate the entire disease pathology. Instead, they often answer questions regarding a portion of the pathology or something very similar to it. For example, increasing the level of angiotensin II in mice has been shown to increase sub-RPE matrix turnover, which may play a role in the formation of deposits in this space in AMD (212). This model demonstrates a single protein effect on a single manifestation of AMD pathology. There are different methods that can be used to create this type of mouse model.

Protein injections are typically used to increase the circulating level of a protein over a desired length of time. The drawback of this technique is that a fraction of protein gets metabolized and excreted before it reaches its target destination. Calculations have to be made accordingly. Knockin or transgenic models can also be used to increase protein expression or function but this approach is laborious and has not been widely used in studies of AMD.

Protein expression or function can be decreased by small interfering RNA (siRNA) that blocks the production of a specific protein by inactivating the mRNA that codes for it. This technique is useful for studying various levels of protein expression. Knockout and loss of function knockin mice are genetically modified to carry reduced or absent function alleles of a specific gene. For example, the AMD model mouse does not

have a functioning Ccl-2 allele, and therefore cannot create the Ccl-2 protein. A common problem with this technique is that the gene knocked out may be necessary for survival. Also, knocking out a gene completely removes a protein from the system, which is not representative of the physiology of an aging disease where protein expressions are fluctuating, but still present.

Combinations of model techniques can be used to overcome these issues and provide more effective models of disease states. For instance, gene knockout or protein injection can be used in conjunction with laser photocoagulation to determine the effects of protein expression on neovascular membrane volume.

We elevated the elastin fragment serum level using a series of injections. After the course of injections, we sought to determine any changes in Bruch's membrane, the retina, and the choroid using immunohistochemistry, TEM ultrastructural observations, and microarray analyses. Based on previous *in vitro* studies, we expected to see an increase in expression of proteins involved in angiogenesis, specifically migration (133). Based on the studies in emphysema, it could be possible to see elevated levels of recruited macrophages in the choroid/RPE complex, indicating an inflammatory response. Determining the effect of elevated elastin fragments *in vivo* on angiogenesis and inflammation in the mouse eye will further our understanding about similar AMD pathologies.

Materials and methods

Mouse injections of elastin derived peptides

To elevate the level of EDPs within the circulating serum of mice, a series of EDP injections were given. All experiments were performed within ARVO guidelines for the use of animals in research experiments. C57BL/6J mice (The Jackson Laboratory, Bar Harbor, ME) were given intraperitoneal injections of 200 ng etna-elastin in phosphate buffered saline (PBS) (concentration = 1 ng/μL) or an equal volume of Hank's buffered

saline solution (HBSS) in PBS. Each condition was performed in triplicate. Injections were performed every other day for 4 weeks beginning when the mice were 7 months old. This method of administration was used because it has been demonstrated that rats will metabolize roughly 60% of orally administered elastin within the first 22 hours, however, elastin remained in the system at elevated levels for more than 2 weeks after intraperitoneal injection (213, 214). Following four weeks of injections, the mice were evaluated by electroretinography (below), and then sacrificed. The eyes were enucleated and fixed in 4% paraformaldehyde (pH 7.4) for 4 hours, fixed in ½ strength Karnovsky's fixative for greater than 12 hours, or flash frozen in liquid nitrogen.

Electrophysiology of mouse eyes

At the end of the EDP injection series, it was desired to know if the EDP injections affected the physiological function of the retina. This was determined using electroretinography. Mice were dark adapted overnight and then were anesthetized with 1.75/0.25 mg Ketamine/Xylazine intraperitoneally. Eyes were dilated with 0.5% Tropicamide (one drop per eye) and gold ring electrodes were placed on each eye. The reference eye was covered completely to prevent stimulus from reaching the retina. A ground wire was placed in the tail (215, 216). A 525 nm light stimulus was applied to the measured eye. The mouse, lead wires and light stimulus were fully contained within the dark. Data were collected using Labview software. ERG output curves were analyzed for the heights of the a- and b-waves and compared.

Retina and choroid immunohistochemistry

To determine if there was a change in the expression of inflammatory surface protein ICAM-1 between EDP-injected and control mice, anti-ICAM-1 immunohistochemistry was performed. Mouse eyes that were fixed in 4% paraformaldehyde (three control eyes, and three EDP injected) were dissected, removing the anterior portion and the lens. The posterior poles of 4% paraformaldehyde fixed

mouse eyes were embedded in sucrose as described by Barthel et al. (131). Cryosections were collected at a thickness of 7 μm. Sections were blocked with 1% bovine serum albumin for 15 minutes. Following the blocking step, 5 μg/mL rat anti-mouse ICAM-1 (eBioscience Inc., San Diego, CA) was applied to the sections for 1 hour. This step was followed by 3x5 minute rinses in PBS and then application of 10 μg/mL goat anti-rat Alexa Fluor 488 (Invitrogen, Eugene, OR) and the nuclear counterstain DAPI (4'-6-diamidino-2-phenylindole) for 30 minutes. Slides were coverslipped with Aquamount (Lerner Laboratories, Pittsburgh, PA) and images were collected using a BX-41 Olympus microscope with a SPOT-RT camera at 40x.

Ultrastructural analyses using transmission electron microscopy

To observe morphological changes in the retina, RPE cells, Bruch's membrane, and the choroid due to EDP serum elevation, transmission electron microscopy was used to obtain greater detail. Posterior halves of eyes fixed in ½ strength Karnovsky's fixative were rinsed 3x30 minutes in 0.1 M cacodylate buffer followed by a 2 hour treatment with 1% osmium tetroxide and 1.5% potassium ferrocyanide diluted in cacodylate buffer (0.2 M). The tissue was then rinsed in double distilled water and sequentially dehydrated in increasing concentrations of ethyl alcohol in double distilled water for 30 minutes at each step until reaching 2x30 minute incubations in pure ethyl alcohol. Eyes were infiltrated with 2 parts ethyl alcohol and 1 part epon resin for 30 minutes, then infiltrated with 1 part ethyl alcohol and 2 parts epon resin for 1 hour. Next, the eyes were infiltrated in epon resin for one hour. The epon was changed and the eyes infiltrated overnight. Eyes were then embedded into molds with epon resin and stored at 70 degrees Celsius overnight. Blocks were trimmed and 90 nm sections will be cut with an ultra-microtome (Leica) and collected on copper slot grids coated with Formvar (0.5%).

Gene expression evaluation using microarrays

The effect of elevated circulating EDPs on gene expression in the mouse eye was determined using microarrays. Frozen eyes were cut in half and immediately immersed in the RLT digestion buffer from the Qiagen RNeasy kit. RNA was then isolated with the same kit according to the manufacturer's instructions (Qiagen, Valencia, CA). Microarray analysis was performed by the DNA facility at the University of Iowa, Iowa City, Iowa using Affymetrix gene chip mouse exon 1.0 ST arrays (Affymetrix, Santa Clara, CA). Data was analyzed using Partek software and File Maker Pro.

Bruch's membrane collagen IV morphometrics

Morphometric analysis was used to quantify differences in collagen IV protein presence in Bruch's membrane between EDP injected and control mice. Cryosections of sucrose embedded mouse eyes were collected at a thickness of 7 μm. Immunohistochemistry was performed as described previously, using 4.0 μg/mL of goat anti-human collagen IV antibody (Santa Cruz Biotechnology Inc., Santa Cruz, CA) (65). All sections were developed for 3.5 minutes, rinsed in distilled water, dehydrated in alcohol and Clear Rite (Richard Allan, Kalamazoo, MI). Slides were coverslipped with Permount (Fisher Scientific, Pittsburgh, PA) and images were collected using a BX-41 Olympus microscope with a SPOT-RT camera at 100x. Five images were randomly collected along the length of the choroid for each eye. These images were all converted to grayscale inverted so that black pixels had a value of 0 and white pixels had a value of 255 on the pixel intensity scale. The average anti-collagen IV intensity along the entire length of Bruch's membrane was measured using the polygon tracing tool in ImageJ for each image. The average values for all EDP injected mouse images were averaged together, as were the values for the control images. Comparisons were analyzed using a two-way paired Student's t-test.

Results

Electroretinograms of injected and control mice

The a- and b-wave heights were within the normal range for all control and EDP injected mice (Figure 37). The average a-wave value for control mice was 260 μV and the average b-wave amplitude was 345 μV. The average a-wave amplitude for the EDP injected mice was 275 μV and the average b-wave amplitude was 363 μV. There was also no difference in the a-wave latency following stimulus. These results indicate that the rod photoreceptors and 'on' bipolar cells were functioning normally in all of the mice without any discernable differences between the two experimental groups.

ICAM-1 immunohistochemistry

The labeling of ICAM-1 in the mouse retina and choroid had a similar pattern to that found previously in the human retina and choroid (65). This pattern included intense labeling of the choriocapillaries and the external limiting membrane (Figure 38). There was no difference in the intensity of this labeling pattern between the two different experimental groups. The expression of ICAM-1 does not appear to be altered in the presence of elevated serum elastin fragments.

Ultrastructural observations using transmission electron microscopy

All of the tissues in both groups had normal morphologies (Figure 39). The capillary endothelial cells did not show any sign of cell division or migration. It was hypothesized that endothelial cells in the choroid getting ready to, or in the process of, migrating would have observable morphological changes such as cytoskeletal rearrangements or extensions away from the normal vasculature. This was not observed in any of the samples. Some podosome-like extensions were noted in larger vessels, extending into the lumens, but this observation was made in control samples as well as

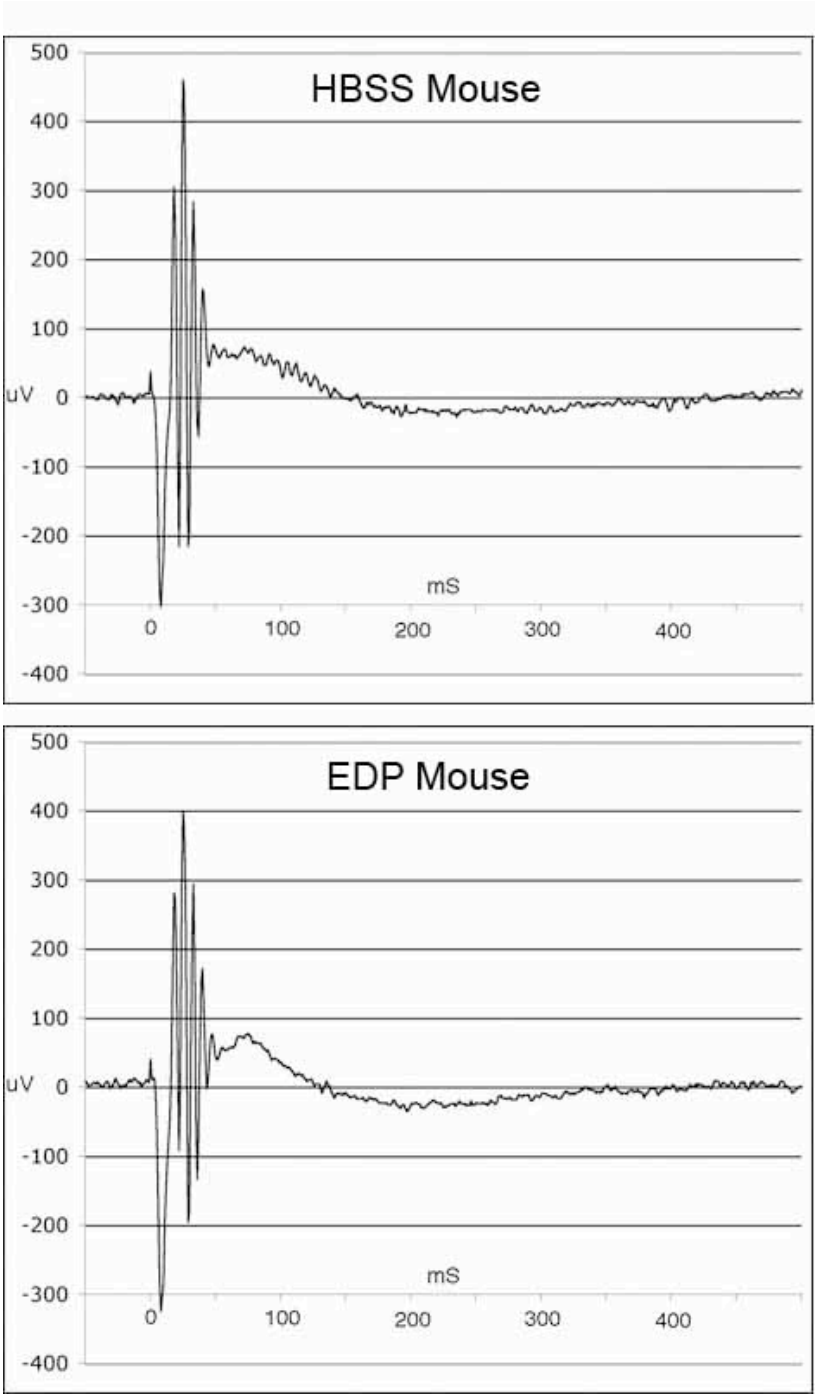

Figure 37. Mouse ERGs. An example of an ERG from one of the four mice in each experimental group is shown. The a-wave is measured from baseline to the bottom of the biggest trough (approximately 300 uV in these graphs) and the b-wave is measured from the bottom of the a-wave to the highest peak (approximately 700 uV for these graphs). All of the wave forms were similar for the mice between the two experimental groups.

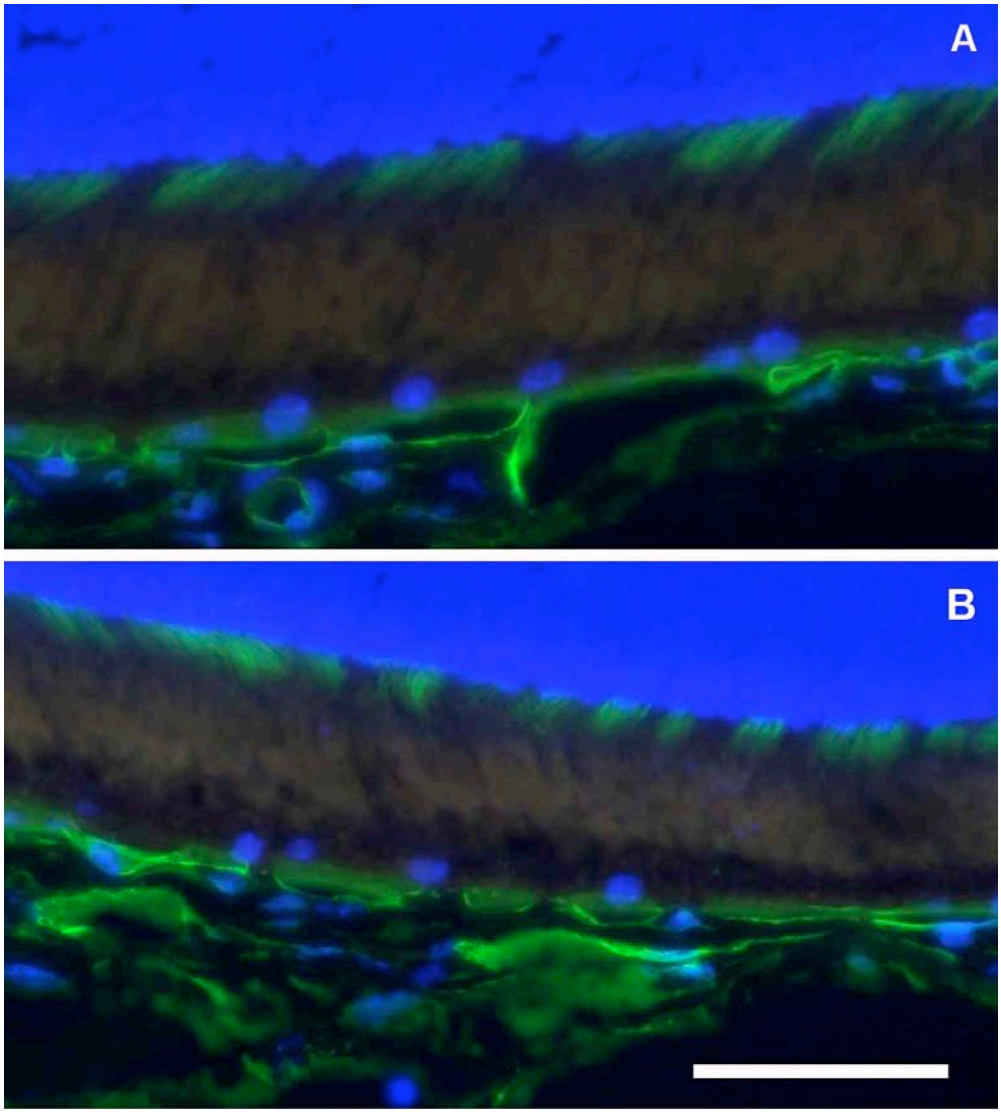

Figure 38. ICAM-1 localization in EDP mouse. The anti-ICAM-1 labeling (green) pattern was similar for both control (A) and EDP injected mice (B). There is intense labeling of the capillaries in the choroid, and moderate labeling of the external limiting membrane (ELM). There was not a significance of the labeling intensities in either of these regions between experimental groups. These images are representative images of each group. Scale bar = 50 μm.

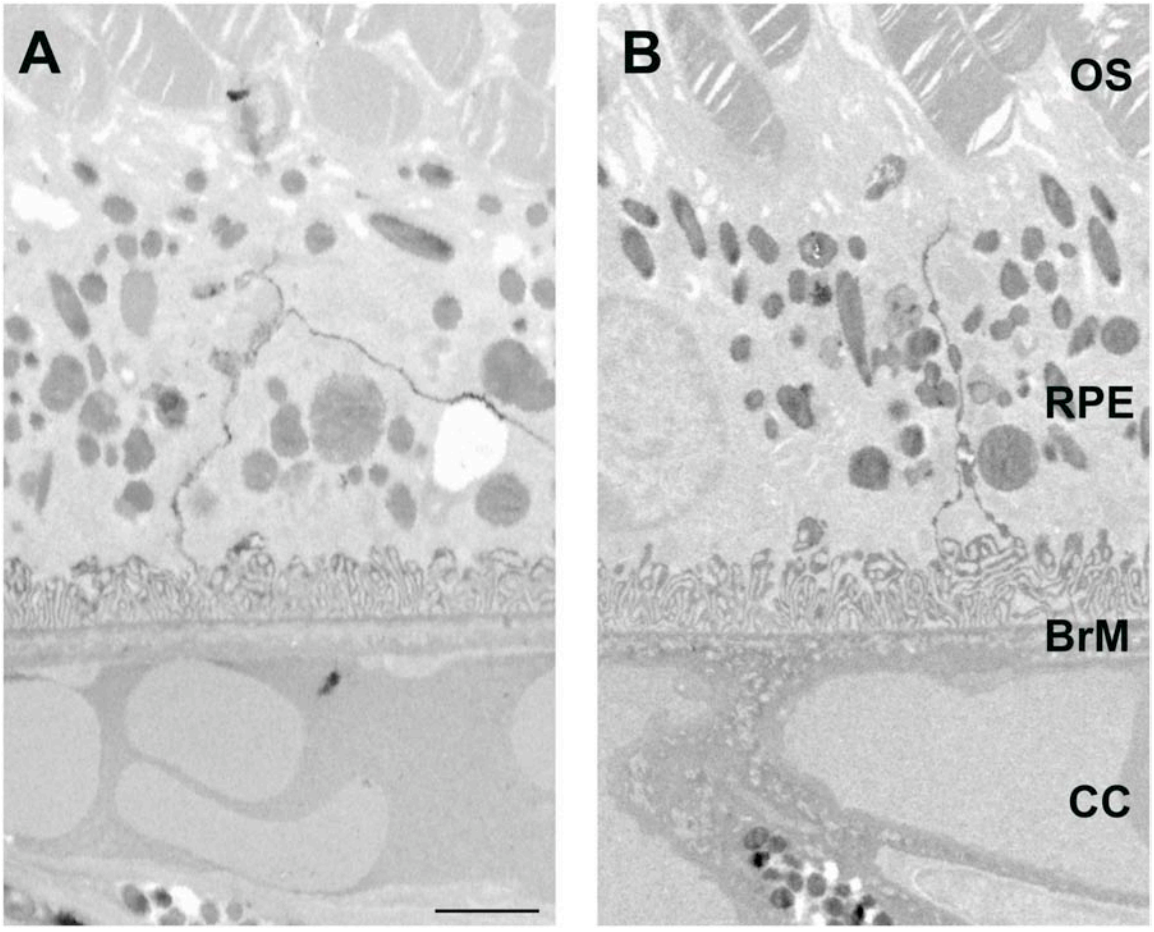

Figure 39. TEM images of EDP injected mice. TEM observations of the retina and choroid tissue allowed for observation of these tissues at an ultrastructural level. Although many regions were observed, the major area of interest was the RPE/Bruch's membrane/choroid complex, as shown. Ultrastructurally, there were no differences noticed between HBSS (A) and EDP injected mice (B). Scale bar = 2 μm.

EDP injected samples. There were some macrophages found between the choriocapillary endothelial cells and Bruch's membrane. Again, this observation was made in both groups of mice. There was no difference in the number of macrophages observed. The penta-laminar structure of Bruch's membrane appeared normal in all of the samples. None of the layers were missing or appeared to be clearly altered. All of the layers of the retina were intact and had no gross morphological changes in thickness or fragmentation in any of the samples.

Changes in gene expression in elastin fragment injected mice using microarray analysis

There were several genes with a greater than 50% change in expression in the EDP injected mice compared to the control mice. These genes and their fold changes (with corresponding p-values) are summarized in Table 4. Most notably, there was a 53% increased expression of *Col4a2* (p-value <0.01), which could be associated with extracellular matrix turnover.

Collagen IV morphometrics in Bruch's membrane

The morphometric analysis of collagen IV labeling intensity in the control mouse eyes compared to the EDP mouse eyes indicated that there is a 4.6% increased labeling intensity of collagen IV in Bruch's membrane of the EDP injected eyes (p-value <0.02).

Discussion

In studies using cell cultures, we have found that soluble elastin fragments can bind to and activate choroidal endothelial cells to become more angiogenic. We have also shown that choroidal endothelial cells can bind to elastin fragments via GLB1 *in vivo*. Since there is a correlation between elevated serum concentrations of elastin fragments and AMD severity in humans, we sought to determine if we could see any

Table 4. EDP injected mouse gene microarray results.

Gene	Fold Change (base 10)	P-value
Ptpru	1.88	0.005
Ces7	2.02	0.008
Plekha4	1.66	0.006
Pacsin3	1.52	0.006
Emid1	1.56	0.010
2210019G1Rik	1.74	0.001
Cr1	1.79	0.010
Ceacam10	1.91	0.009
Rspo1	1.73	0.005
Tomm40	1.53	0.007
Mypn	1.59	0.001
C030030A07Rik	1.62	0.009
LOC100046788	1.97	0.008
Clic5	1.57	0.007
Ankrd24	1.77	0.006
Dnase2b	2.01	0.010
LOC100048029	1.79	0.010
Col4a2	1.54	0.008
Hspb1	1.52	0.003

early signs of choroidal endothelial cell activation, or any AMD characteristics, in a mouse model of elevated serum elastin fragments.

Using immunohistochemistry, ICAM-1 was investigated because of its important role in inflammation and trafficking leukocytes from the circulation to surrounding tissues. It is expressed by endothelial cells in the choroid and has been shown to have a higher level of expression in the retina and choroid within the macula than in the periphery in humans (65). Up-regulation of this protein could increase leukocyte infiltration, thereby increasing local levels of inflammation. In our preliminary studies, we found that the expression of ICAM-1 did not change in the eyes of mice injected with elastin-derived fragments in comparison to littermate controls. Therefore, ICAM-1 mediated leukocyte infiltration is not likely a result of elevated levels of elastin fragments in the circulation.

Ultrastructurally, we did not observe any major changes in the injected eyes in comparison to the control eyes. We had anticipated possible changes in macrophage infiltration, deposits within Bruch's membrane, thickness changes in Bruch's membrane, and cell morphological changes based on the cell culture migration and PCR profiling results found previously (Chapter 5). Since these changes occur over long periods of time (decades) in humans, we may not be able to observe them after only one month of injections, but they may be beginning. It would be beneficial to repeat this experiment over a longer course of time in order to determine if this is true.

To assess molecular changes that may precede structural or functional changes, we performed microarray analysis on injected and control mouse eyes. We have found that eyes of mice injected with elastin fragments did have a greater than 50% increase in expression of 20 genes including *Ceacam10, Ces7, Hspb1, Pacsin3,* and *Col4a2* (p-values < 0.01). Although all of these genes may provide insightful information about elevated elastin in the eye, we have only investigated the role of *Col4a2* in greater detail.

Collagen IV is a major component of the choriocapillaris basement membrane (49, 217), which is one of the five layers within Bruch's membrane. The Collagen IV helices link head-to-head and form disorganized sheets with many kinks, a characteristic that is unique to collagen IV in comparison to the other collagens. This suits collagen IV for basement membranes as it allows transfer of nutrients, waste, and cells. With increasing age, collagen IV deposition causes a dramatic thickening of Bruch's membrane in the macula (49).

We found that the expression of mRNA for precursor alpha 2 for collagen IV was increased by 53%. In Bruch's membrane, we found an increase of 4.5% anti-collagen IV intensity using morphometric analysis. There are reasons that can contribute for this discrepancy in values. First, the microarray analyzed mRNA levels from all tissues in the posterior pole of the mouse eye. This included retina, RPE, Bruch's membrane, choroid and sclera. From the micrographs of anti-collagen IV immunohistochemistry, we saw labeling in all of these tissues. If the protein is present in all of these tissues, the precursors (collagen IV alpha 1-6) for this protein are likely to have a wide distribution as well. Since we only measured Bruch's membrane in the morphometric analysis, we drastically decreased the amount of tissue analyzed in comparison to the microarray analysis. Second, the microarray result was for pre-collagen IV alpha 2 mRNA, whereas we measured whole collagen IV protein labeling with morphometrics. Not all of the precursor alpha 2 mRNAs may have ended up being translated and assembled into whole collagen IV protein.

An increased collagen IV labeling of 4.6% in our EDP injected mice does not seem like a large value at first glance. However, it is unknown how this increased amount of collagen IV affects the microenvironment within the posterior eye. This may be enough to change oxygen partial pressures across Bruch's membrane, create difficulty for nutrients to cross towards the retina, or even trap waste products from the retina and RPE. In AMD, material trapped within Bruch's membrane are correlated with drusen

formation and tissue atrophy. A lack of nutrients and hypoxic conditions can also lead to tissue atrophy. These manifestations take a long period of time to develop, though. As mentioned previously in regards to the ultrastructural analyses, this animal modeling experiment should be repeated for a longer period of time. Had injections in the mice taken place over a longer period of time, perhaps a year rather than a month, we may have seen some of these changes occur, mimicking more closely the pathology occurring in AMD. The interesting finding of collagen IV increased deposition in Bruch's membrane may increase dramatically over a longer period of time. If this occurs, this mouse model will show the important correlation between elevated elastin fragments with collagen IV deposition in Bruch's membrane, which may translate to the connection with increased AMD in humans to elastin fragment mediated collagen IV deposition in the macula.

CHAPTER 7. THESIS CONCLUSIONS

AMD is complex both in cause and presentation. Despite extensive research to unfold the intricacies of AMD pathology, the mechanisms are still poorly understood, and this limits development of more effective treatments. The goal of this body of work was to contribute to this body of knowledge.

The hypotheses on which this work was based were:

1. *Endothelial cell activation causes development of CNVM.*
2. *Primary human choroidal endothelial cells provide an effective platform for modeling events that occur during CNVM formation.*
3. *Elastin fragments, C5a, and angiogenin promote choroidal endothelial cell activation.*

Endothelial cell activation and CNVM. The first hypothesis suggested by previous investigations was supported by experiments conducted during this project. Specifically, activation of endothelial cells increased vascularizing behaviors consistent with CNVM formation.

Through previous studies, several properties of endothelial cells have been identified that could contribute to the development of neovascular AMD. Endothelial cells must proliferate and migrate in order for new vessels to form into a CNVM. So if endothelial cells become angiogenic, they may grow into areas that they normally would not. They may also increase local inflammation by up-regulating adhesion molecules that in turn traffic leukocytes into the surrounding tissues. Finally, they may increase nearby matrix turnover in Bruch's membrane, changing its integrity that then contributes to CNVM formation because blood vessels can break through this membrane and grow into the RPE and retinal spaces.

During this investigation we showed that conditions present in AMD could activate human choroidal endothelial cells to migrate at a greater rate, with increased ability to close inflicted wounds in the presence of a stimulus. Cells also up-regulated or down-regulated the expression of genes associated with inflammation, matrix turnover, and migration. All of these changes indicate the ability of choroidal endothelial cells to become capable of angiogenesis and to contribute to inflammation in AMD, and therefore potentially actively contribute to CNVM formation.

Primary human choroidal endothelial cell culture. To study these properties of endothelial cells, it was first necessary to develop a reliable choroidal endothelial cell culture platform. Designing a reliable isolation and culture technique, along with stringent purity assays, has provided the ability to use human choroidal endothelial cells to study neovascular AMD. The positive results of the purity assays support the second hypothesis; primary cultures of human choroidal endothelial cells provide an effective platform for the study of CNVM formation. These cells were considered more appropriate for this study than the commercially available monkey cell line, Rf/6a because they are from human donors and they are from the choroid only.

Despite the improvement offered by this cell line, they were limited in supply so were not used for every experiment. Primary cultures differentiate from their normal physiology in early passages because they are not immortalized like the commercially available cell lines. Therefore, these cells have to be purified and used within the first few passages to retain their character. This makes it difficult to amplify the cultures for large scale use. Therefore, the Rf/6a cell line was used for all of the preliminary experiments, and primary human cells only used in proven experimental protocols.

Interestingly, results were similar between Rf/6a and human cells. This indicates that the Rf/6a cells may be a relatively good culture platform for choroidal endothelial cell research, particularly when studies are repeated in the human cell line.

Activators of endothelial cells. There are several proteins capable of altering the activities of endothelial cells. This body of work focused on three of these; complement component C5 anaphylatoxin (C5a), soluble elastin fragments (EDPs), and angiogenin.

Complement component C5a was chosen because recent findings have shown important correlations between complement system protein gene mutations and the risk for developing AMD. Complement proteins have also been shown to be present in drusen, a characteristic of AMD (30), demonstrating the presence of these proteins during the pathology of the disease. Since C5a is a by-product of the enzymatic cleavage of protein C5, it was not a goal to find any genetic correlation between mutations in its gene (which does not exist other than as a part of the gene for C5), but rather to determine the effects of elevated levels of this protein.

Angiogenin was chosen based on the fact that it increases angiogenesis in many other disease mechanisms, however, no one has determined its expression or impact with respect to the human eye. This was a novel protein to investigate with the base hypothesis that this protein may affect pathologic angiogenesis in AMD.

Finally, EDPs were chosen because in 2005, it was found that patients with AMD had higher serum levels of EDPs than control patients (183), and patients with CNVMs had even higher concentrations than AMD patients without CNVM. Determining if these fragments play a role in the behavior of endothelial cells during AMD progression became a large portion of this set of investigations.

C5a increases inflammation in the human choroid. First, it was shown that the receptor for C5a (C5aR) is expressed on the endothelium of the choroid. This demonstrated that choroidal endothelial cells are capable of being activated by the C5a protein. Using morphometric analysis, it was found that C5a increases the amount of ICAM-1 expressed by choriocapillaries. ICAM-1 mediates leukocyte trafficking from the blood into nearby tissues, and increased levels of leukocytes in a tissue are a sign of inflammation. It is still unknown if increased leukocyte infiltration is beneficial or

harmful in AMD. These cells aid with removing debris, possibly reducing the deposits within Bruch's membrane, but might also cause mechanical stress to the endothelial cells as they filter through their junctions to move into the tissues. They are also capable of invading and disrupting Bruch's membrane in two ways. The mechanical stress of the cell moving through the layers of the membrane can disrupt its structure, but leukocytes also release enzymes capable of breaking down the matrix proteins. If increased leukocyte infiltration is beneficial in AMD, increased ICAM-1 expression as a result of increased C5a protein would be beneficial in slowing down the progression of AMD. However, it is more likely that an increased level of C5a indicates elevated complement cascade activation, and associated inflammation decreases the integrity of Bruch's membrane making it more susceptible to breaks for the passage of new vessels in early CNVM formation. There are two ideas supporting this hypothesis.

First, loss of function of complement factor H (CFH), an inhibitor of the complement cascade, is associated with increased risk for development of AMD (28, 119-122, 145). C5 is later in the complement cascade and acts to activate or induce inflammation.

A second important finding was that endothelial cells exposed to higher levels of C5a recombinant protein increased their expression of integrin alpha 8 (ITGA8). Integrin is capable of binding vitronectin (143), an inhibitor of membrane attack complex formation. Choroidal endothelial cells may increase expression of ITGA8 to elevate vitronectin binding in response to C5a. This may prevent elevated levels of membrane attack complexes from being formed, which could cause local tissue damage.

Angiogenin is present in the human choroid and internalized by choroidal endothelial cells. Angiogenin is a potent stimulus for angiogenesis in other systems, and we found that it is endogenously present in the cytosol of human choroidal endothelial cells. Despite this, elevated levels of this protein do not elicit a change in angiogenic behavior of these cells. Angiogenin is internalized by Rf/6a cells from their surrounding

culture medium, so we presume angiogenin is also internalized by human primary cells. Therefore, if this protein is capable of acting like a 'third messenger' after translocating to the nucleus, it is capable of altering gene expression. We have shown that the resultant gene expression changes are not associated with angiogenesis. Angiogenin may activate endothelial cells in another way that contributes to AMD pathology. For instance, C5a did not elicit a change in angiogenic behaviors by choroidal endothelial cells, but did change their inflammatory surface protein expression. It would be beneficial to study gene expression changes in response to elevated levels of angiogenin in culture using SABiosciences gene arrays or even microarrays. Subsequent protein expression change analyses could then be performed using immunoblotting or morphometrics.

Elastin-derived peptides increase choroidal endothelial cell migration and contribute to changes in Bruch's membrane. When Sivaprasad et al. found that circulating serum levels of elastin derived peptides increased in line with severity of AMD, it was not known if these peptides were even able to affect cells in the retina and/or choroid. Applying elastin fragments to these tissues, then using an anti-elastin antibody to find where they bind, it was discovered that these fragments bind to endothelial cells in the choroid. It was then necessary to determine what this interaction did to these cells. Use of a Boyden chamber assay showed that EDPs increased migration, a key event in angiogenesis. Further, the chemotactic effect of EDPs on the cells was concentration-dependent. We also showed that this response is mediated through the binding of elastin fragments to the peripheral binding protein, an alternatively spliced form of GLB1. This alternatively spliced form of GLB1 is expressed by choroidal endothelial cells, and if blocked, decreases their migration in the Boyden chamber assay. Together these findings identify a mechanism for the correlation of serum concentration of EDPs and AMD severity, and a potential therapeutic target in GLB1.

EDPs also stimulate endothelial cells to increase their expression of genes involved in matrix turnover (matrix metalloproteinase 9 or MMP-9), and in leukocyte

trafficking associated with inflammation (monocyte chemotactic protein 1 or MCP-1, and L selectin LSEL). As noted with the changes in inflammation mediated by C5a protein, this could be beneficial or detrimental during AMD pathogenesis. MMP-9 is an enzyme, which participates in matrix turnover by degrading elastin and collagens, so an increase in MMP-9 is detrimental to the integrity of Bruch's membrane. This may increase CNVM formation by two mechanisms. First, degrading Bruch's membrane decreases its ability to serve as a mechanical barrier in the prevention of vessels from the choroid growing into the sub-retinal space. Second, the digestion of elastin within Bruch's membrane presumably creates a local source of soluble elastin fragments that might increase migration of nearby endothelial cells. If the response is large enough, and Bruch's membrane is weak enough, these cells could migrate into the sub-retinal space and commence CNVM formation.

The effect of EDPs was also tested *in vivo* using a mouse model. Elevated levels of EDPs resulted in an increased amount of collagen IV precursor alpha 2 gene expression and total collagen IV protein within Bruch's membrane. This is consistent with the increased amount of collagen IV found in the macula of aging eyes (48, 49). Increased thickness of Bruch's membrane in the macula could affect the transfer of nutrients, oxygen and waste to and from the retina. This could result in deposition of waste materials, tissue atrophy, and hypoxia-induced endothelial cell activation. All of these events are common to AMD pathogenesis. In the future, it would be interesting to determine the effects of serum elevation of C5a as well.

All three of these proteins have been shown to affect endothelial cell activation in different ways. The resultant endothelial cell changes in parallel with reduced integrity of Bruch's membrane with increasing age create an environment favorable for CNVM formation in AMD. However, it is important to remember that the choroid, RPE, and retina form a very complex system. There are many activators and inhibitors of angiogenesis and inflammation working together in trying to maintain an equilibrium.

C5a, angiogenin, and EDPs may initiate or accentuate an unbalancing in this system, resulting in the various manifestations of AMD pathology, however pathology is likely dependent on simultaneous abnormalities of several other factors.

Currently, it is accepted that VEGF plays a key role in CNVM formation, and if the VEGF protein-receptor interaction is blocked, the membrane can often be controlled or reduced in size. However, this only allows for treatment of existing CNVMs and vision may be lost between initial CNVM formation and a clinic visit. The goal of this work was to further understand the complex pathobiology of CNVM formation to support development of preventative treatments and perhaps develop tests that predict patient risk. The body of work presented in this thesis provides three new mechanisms that recapitulate choroidal endothelial cell mechanisms commonly described in neovascular AMD.

REFERENCES

1. Seddon JM, George S, Rosner B, Rifai N. Progression of age-related macular degeneration: prospective assessment of C-reactive protein, interleukin 6, and other cardiovascular biomarkers. Arch Ophthalmol. 2005;123(6):774-82.

2. Bressler NM, Bressler SB, Fine SL. Age-related macular degeneration. Surv Ophthalmol. 1988;32(6):375-413.

3. Green WR, McDonnell PJ, Yeo JH. Pathologic features of senile macular degeneration. Ophthalmology. 1985;92(5):615-27.

4. Spraul CW, Lang GE, Grossniklaus HE, Lang GK. Histologic and morphometric analysis of the choroid, Bruch's membrane, and retinal pigment epithelium in postmortem eyes with age-related macular degeneration and histologic examination of surgically excised choroidal neovascular membranes. Surv Ophthalmol. 1999;44 Suppl 1:S10-32.

5. Vine AK, Stader J, Branham K, Musch DC, Swaroop A. Biomarkers of cardiovascular disease as risk factors for age-related macular degeneration. Ophthalmology. 2005;112(12):2076-80.

6. Gehrs KM, Heriot WJ, de Juan E, Jr. Transmission electron microscopic study of a subretinal choroidal neovascular membrane due to age-related macular degeneration. Arch Ophthalmol. 1992;110(6):833-7.

7. Curcio CA, Drucker DN. Retinal ganglion cells in Alzheimer's disease and aging. Ann Neurol. 1993;33(3):248-57.

8. Curcio CA, Millican CL, Allen KA, Kalina RE. Aging of the human photoreceptor mosaic: evidence for selective vulnerability of rods in central retina. Invest Ophthalmol Vis Sci. 1993;34(12):3278-96.

9. Young RW, Bok D. Participation of the retinal pigment epithelium in the rod outer segment renewal process. J Cell Biol. 1969;42(2):392-403. PMCID: 2107669.

10. Marshall J, Grindle J, Ansell PL, Borwein B. Convolution in human rods: an ageing process. Br J Ophthalmol. 1979;63(3):181-7. PMCID: 1043437.

11. Keunen JE, van Norren D, van Meel GJ. Density of foveal cone pigments at older age. Invest Ophthalmol Vis Sci. 1987;28(6):985-91.

12. Adler AJ, Severin KM. Proteins of the bovine interphotoreceptor matrix: tissues of origin. Exp Eye Res. 1981;32(6):755-69.

13. Adler AJ, Klucznik KM. Proteins and glycoproteins of the bovine interphotoreceptor matrix: composition and fractionation. Exp Eye Res. 1982;34(3):423-34.

14. Johnson LV, Hageman GS, Blanks JC. Interphotoreceptor matrix domains ensheath vertebrate cone photoreceptor cells. Invest Ophthalmol Vis Sci. 1986;27(2):129-35.

15. Adler AJ, Martin KJ. Retinol-binding proteins in bovine interphotoreceptor matrix. Biochem Biophys Res Commun. 1982;108(4):1601-8.

16. Padgett LC, Lui GM, Werb Z, LaVail MM. Matrix metalloproteinase-2 and tissue inhibitor of metalloproteinase-1 in the retinal pigment epithelium and interphotoreceptor matrix: vectorial secretion and regulation. Exp Eye Res. 1997;64(6):927-38.

17. Dorey CK, Wu G, Ebenstein D, Garsd A, Weiter JJ. Cell loss in the aging retina. Relationship to lipofuscin accumulation and macular degeneration. Invest Ophthalmol Vis Sci. 1989;30(8):1691-9.

18. Burke JM, Skumatz CM. Autofluorescent inclusions in long-term postconfluent cultures of retinal pigment epithelium. Invest Ophthalmol Vis Sci. 1998;39(8):1478-86.

19. Wassell J, Ellis S, Burke J, Boulton M. Fluorescence properties of autofluorescent granules generated by cultured human RPE cells. Invest Ophthalmol Vis Sci. 1998;39(8):1487-92.

20. Hjelmeland LM, Cristofolo VJ, Funk W, Rakoczy E, Katz ML. Senescence of the retinal pigment epithelium. Mol Vis. 1999;5:33.

21. Pauleikhoff D, Harper CA, Marshall J, Bird AC. Aging changes in Bruch's membrane. A histochemical and morphologic study. Ophthalmology. 1990;97(2):171-8.

22. Chong NH, Keonin J, Luthert PJ, Frennesson CI, Weingeist DM, Wolf RL, et al. Decreased thickness and integrity of the macular elastic layer of Bruch's membrane correspond to the distribution of lesions associated with age-related macular degeneration. Am J Pathol. 2005;166(1):241-51.

23. Sivaprasad S, Bailey TA, Chong VN. Bruch's membrane and the vascular intima: is there a common basis for age-related changes and disease? Clin Experiment Ophthalmol. 2005;33(5):518-23.

24. Lutty G, Grunwald J, Majji AB, Uyama M, Yoneya S. Changes in choriocapillaris and retinal pigment epithelium in age-related macular degeneration. Mol Vis. 1999;5:35.

25. Grunwald JE, Metelitsina TI, Dupont JC, Ying GS, Maguire MG. Reduced foveolar choroidal blood flow in eyes with increasing AMD severity. Invest Ophthalmol Vis Sci. 2005;46(3):1033-8.

26. Zarbin MA. Current concepts in the pathogenesis of age-related macular degeneration. Arch Ophthalmol. 2004;122(4):598-614.

27. Grossniklaus HE, Green WR. Histopathologic and ultrastructural findings of surgically excised choroidal neovascularization. Submacular Surgery Trials Research Group. Arch Ophthalmol. 1998;116(6):745-9.

28. Kijlstra A, La Heij E, Hendrikse F. Immunological factors in the pathogenesis and treatment of age-related macular degeneration. Ocul Immunol Inflamm. 2005;13(1):3-11.

29. Mullins RF, Russell SR, Anderson DH, Hageman GS. Drusen associated with aging and age-related macular degeneration contain proteins common to extracellular deposits associated with atherosclerosis, elastosis, amyloidosis, and dense deposit disease. FASEB J. 2000;14(7):835-46.

30. Spraul CW, Grossniklaus HE. Characteristics of Drusen and Bruch's membrane in postmortem eyes with age-related macular degeneration. Arch Ophthalmol. 1997;115(2):267-73.

31. Johnson LV, Ozaki S, Staples MK, Erickson PA, Anderson DH. A potential role for immune complex pathogenesis in drusen formation. Exp Eye Res. 2000;70(4):441-9.

32. Feeney-Burns L, Ellersieck MR. Age-related changes in the ultrastructure of Bruch's membrane. Am J Ophthalmol. 1985;100(5):686-97.

33. Grossniklaus HE, Martinez JA, Brown VB, Lambert HM, Sternberg P, Jr., Capone A, Jr., et al. Immunohistochemical and histochemical properties of surgically excised subretinal neovascular membranes in age-related macular degeneration. Am J Ophthalmol. 1992;114(4):464-72.

34. Bird AC, Bressler NM, Bressler SB, Chisholm IH, Coscas G, Davis MD, et al. An international classification and grading system for age-related maculopathy and age-related macular degeneration. The International ARM Epidemiological Study Group. Surv Ophthalmol. 1995;39(5):367-74.

35. Small ML, Green WR, Alpar JJ, Drewry RE. Senile mecular degeneration. A clinicopathologic correlation of two cases with neovascularization beneath the retinal pigment epithelium. Arch Ophthalmol. 1976;94(4):601-7.

36. Lopez PF, Lambert HM, Grossniklaus HE, Sternberg P, Jr. Well-defined subfoveal choroidal neovascular membranes in age-related macular degeneration. Ophthalmology. 1993;100(3):415-22.

37. Lopez PF, Sippy BD, Lambert HM, Thach AB, Hinton DR. Transdifferentiated retinal pigment epithelial cells are immunoreactive for vascular endothelial growth factor in surgically excised age-related macular degeneration-related choroidal neovascular membranes. Invest Ophthalmol Vis Sci. 1996;37(5):855-68.

38. Bressler SB, Silva JC, Bressler NM, Alexander J, Green WR. Clinicopathologic correlation of occult choroidal neovascularization in age-related macular degeneration. Arch Ophthalmol. 1992;110(6):827-32.

39. Yeh DC, Bula DV, Miller JW, Gragoudas ES, Arroyo JG. Expression of leukocyte adhesion molecules in human subfoveal choroidal neovascular membranes treated with and without photodynamic therapy. Invest Ophthalmol Vis Sci. 2004;45(7):2368-73.

40. Lafaut BA, Bartz-Schmidt KU, Vanden Broecke C, Aisenbrey S, De Laey JJ, Heimann K. Clinicopathological correlation in exudative age related macular degeneration: histological differentiation between classic and occult choroidal neovascularisation. Br J Ophthalmol. 2000;84(3):239-43.

41. Oshima Y, Oshima S, Nambu H, Kachi S, Takahashi K, Umeda N, et al. Different effects of angiopoietin-2 in different vascular beds: new vessels are most sensitive. Faseb J. 2005;19(8):963-5.

42. Sarks SH. New vessel formation beneath the retinal pigment epithelium in senile eyes. Br J Ophthalmol. 1973;57(12):951-65.

43. Green WR. Histopathology of age-related macular degeneration. Mol Vis. 1999;5:27.

44. Stone EM. A very effective treatment for neovascular macular degeneration. N Engl J Med. 2006;355(14):1493-5.

45. van Wijngaarden P, Coster DJ, Williams KA. Inhibitors of ocular neovascularization: promises and potential problems. Jama. 2005;293(12):1509-13.

46. Mullins RF, Grassi MA, Skeie JM. Glycoconjugates of choroidal neovascular membranes in age-related macular degeneration. Mol Vis. 2005;11:509-17.

47. Hewitt AT, Nakazawa K, Newsome DA. Analysis of newly synthesized Bruch's membrane proteoglycans. Invest Ophthalmol Vis Sci. 1989;30(3):478-86.

48. Newsome DA, Huh W, Green WR. Bruch's membrane age-related changes vary by region. Curr Eye Res. 1987;6(10):1211-21.

49. Marshall GE, Konstas AG, Reid GG, Edwards JG, Lee WR. Collagens in the aged human macula. Graefes Arch Clin Exp Ophthalmol. 1994;232(3):133-40.

50. Nakaizumi Y, Hogan MJ, Feeney L. The Ultrastructure of Bruch's Membrane. 3. The Macular Area of the Human Eye. Arch Ophthalmol. 1964;72:395-400.

51. Hogan MJ, Alvarado J. Studies on the human macula. IV. Aging changes in Bruch's membrane. Arch Ophthalmol. 1967;77(3):410-20.

52. Killingsworth MC, Sarks JP, Sarks SH. Macrophages related to Bruch's membrane in age-related macular degeneration. Eye. 1990;4 (Pt 4):613-21.

53. Jones PA, Werb Z. Degradation of connective tissue matrices by macrophages. II. Influence of matrix composition on proteolysis of glycoproteins, elastin, and collagen by macrophages in culture. J Exp Med. 1980;152(6):1527-36. PMCID: 2186027.

54. Ramrattan RS, van der Schaft TL, Mooy CM, de Bruijn WC, Mulder PG, de Jong PT. Morphometric analysis of Bruch's membrane, the choriocapillaris, and the choroid in aging. Invest Ophthalmol Vis Sci. 1994;35(6):2857-64.

55. Sarks JP, Sarks SH, Killingsworth MC. Morphology of early choroidal neovascularisation in age-related macular degeneration: correlation with activity. Eye. 1997;11 (Pt 4):515-22.

56. Holtkamp GM, Van Rossem M, de Vos AF, Willekens B, Peek R, Kijlstra A. Polarized secretion of IL-6 and IL-8 by human retinal pigment epithelial cells. Clin Exp Immunol. 1998;112(1):34-43. PMCID: 1904947.

57. Deshmane SL, Kremlev S, Amini S, Sawaya BE. Monocyte chemoattractant protein-1 (MCP-1): an overview. J Interferon Cytokine Res. 2009;29(6):313-26. PMCID: 2755091.

58. Kirton CM, Laukkanen ML, Nieminen A, Merinen M, Stolen CM, Armour K, et al. Function-blocking antibodies to human vascular adhesion protein-1: a potential anti-inflammatory therapy. Eur J Immunol. 2005;35(11):3119-30.

59. Salmi M, Jalkanen S. VAP-1: an adhesin and an enzyme. Trends Immunol. 2001;22(4):211-6.

60. Tohka S, Laukkanen M, Jalkanen S, Salmi M. Vascular adhesion protein 1 (VAP-1) functions as a molecular brake during granulocyte rolling and mediates recruitment in vivo. Faseb J. 2001;15(2):373-82.

61. Koskinen K, Vainio PJ, Smith DJ, Pihlavisto M, Yla-Herttuala S, Jalkanen S, et al. Granulocyte transmigration through the endothelium is regulated by the oxidase activity of vascular adhesion protein-1 (VAP-1). Blood. 2004;103(9):3388-95.

62. Merinen M, Irjala H, Salmi M, Jaakkola I, Hanninen A, Jalkanen S. Vascular adhesion protein-1 is involved in both acute and chronic inflammation in the mouse. Am J Pathol. 2005;166(3):793-800.

63. Salmi M, Tohka S, Jalkanen S. Human vascular adhesion protein-1 (VAP-1) plays a critical role in lymphocyte-endothelial cell adhesion cascade under shear. Circ Res. 2000;86(12):1245-51.

64. Isacke CM, Horton MA. The Adhesion Molecule Facts Book. 2 ed. San Diego: Academic Press; 2000.

65. Mullins RF, Skeie JM, Malone EA, Kuehn MH. Macular and peripheral distribution of ICAM-1 in the human choriocapillaris and retina. Mol Vis. 2006;12:224-35.

66. Penfold PL, Wen L, Madigan MC, Gillies MC, King NJ, Provis JM. Triamcinolone acetonide modulates permeability and intercellular adhesion molecule-1 (ICAM-1) expression of the ECV304 cell line: implications for macular degeneration. Clin Exp Immunol. 2000;121(3):458-65.

67. Sakurai E, Taguchi H, Anand A, Ambati BK, Gragoudas ES, Miller JW, et al. Targeted disruption of the CD18 or ICAM-1 gene inhibits choroidal neovascularization. Invest Ophthalmol Vis Sci. 2003;44(6):2743-9.

68. Hindmarsh EJ, Marks RM. Complement activation occurs on subendothelial extracellular matrix in vitro and is initiated by retraction or removal of overlying endothelial cells. J Immunol. 1998;160(12):6128-36.

69. Schlingemann RO. Role of growth factors and the wound healing response in age-related macular degeneration. Graefes Arch Clin Exp Ophthalmol. 2004;242(1):91-101.

70. Folkman J, Merler E, Abernathy C, Williams G. Isolation of a tumor factor responsible for angiogenesis. J Exp Med. 1971;133(2):275-88.

71. Huang AL, Vita JA. Effects of systemic inflammation on endothelium-dependent vasodilation. Trends Cardiovasc Med. 2006;16(1):15-20.

72. Witmer AN, Vrensen GF, Van Noorden CJ, Schlingemann RO. Vascular endothelial growth factors and angiogenesis in eye disease. Prog Retin Eye Res. 2003;22(1):1-29.

73. Keeley EC, Mehrad B, Strieter RM. Chemokines as mediators of neovascularization. Arterioscler Thromb Vasc Biol. 2008;28(11):1928-36. PMCID: 2735456.

74. Ferrara N, Gerber HP. The role of vascular endothelial growth factor in angiogenesis. Acta Haematol. 2001;106(4):148-56.

75. Oh H, Takagi H, Takagi C, Suzuma K, Otani A, Ishida K, et al. The potential angiogenic role of macrophages in the formation of choroidal neovascular membranes. Invest Ophthalmol Vis Sci. 1999;40(9):1891-8.

76. Tolentino MJ. Current molecular understanding and future treatment strategies for pathologic ocular neovascularization. Curr Mol Med. 2009;9(8):973-81.

77. Ishida S, Usui T, Yamashiro K, Kaji Y, Amano S, Ogura Y, et al. VEGF164-mediated inflammation is required for pathological, but not physiological, ischemia-induced retinal neovascularization. J Exp Med. 2003;198(3):483-9.

78. Zarbock R, Hendig D, Szliska C, Kleesiek K, Gotting C. Vascular endothelial growth factor gene polymorphisms as prognostic markers for ocular manifestations in pseudoxanthoma elasticum. Hum Mol Genet. 2009;18(17):3344-51.

79. Qazi Y, Maddula S, Ambati BK. Mediators of ocular angiogenesis. J Genet. 2009;88(4):495-515.

80. Cogan DG, Toussaint D, Kuwabara T. Retinal vascular patterns. IV. Diabetic retinopathy. Arch Ophthalmol. 1961;66:366-78.

81. Adamis AP, Miller JW, Bernal MT, D'Amico DJ, Folkman J, Yeo TK, et al. Increased vascular endothelial growth factor levels in the vitreous of eyes with proliferative diabetic retinopathy. Am J Ophthalmol. 1994;118(4):445-50.

82. Ejaz S, Chekarova I, Ejaz A, Sohail A, Lim CW. Importance of pericytes and mechanisms of pericyte loss during diabetes retinopathy. Diabetes Obes Metab. 2008;10(1):53-63.

83. Motiejunaite R, Kazlauskas A. Pericytes and ocular diseases. Exp Eye Res. 2008;86(2):171-7.

84. Morikawa S, Baluk P, Kaidoh T, Haskell A, Jain RK, McDonald DM. Abnormalities in pericytes on blood vessels and endothelial sprouts in tumors. Am J Pathol. 2002;160(3):985-1000. PMCID: 1867175.

85. Enge M, Bjarnegard M, Gerhardt H, Gustafsson E, Kalen M, Asker N, et al. Endothelium-specific platelet-derived growth factor-B ablation mimics diabetic retinopathy. EMBO J. 2002;21(16):4307-16. PMCID: 126162.

86. Bergen AA, Plomp AS, Hu X, de Jong PT, Gorgels TG. ABCC6 and pseudoxanthoma elasticum. Pflugers Arch. 2007;453(5):685-91.

87. Bergen AA, Plomp AS, Schuurman EJ, Terry S, Breuning M, Dauwerse H, et al. Mutations in ABCC6 cause pseudoxanthoma elasticum. Nat Genet. 2000;25(2):228-31.

88. Goodman RM, Smith EW, Paton D, Bergman RA, Siegel CL, Ottesen OE, et al. Pseudoxanthoma Elasticum: A Clinical and Histopathological Study. Medicine (Baltimore). 1963;42:297-334.

89. Neldner KH. Pseudoxanthoma elasticum. Int J Dermatol. 1988;27(2):98-100.

90. Lafaut BA, Priem H, De Laey JJ. Indocyanine green angiography in angioid streaks. Bull Soc Belge Ophtalmol. 1997;265:21-4.

91. Finger RP, Charbel Issa P, Ladewig M, Holz FG, Scholl HP. Intravitreal bevacizumab for choroidal neovascularisation associated with pseudoxanthoma elasticum. Br J Ophthalmol. 2008;92(4):483-7.

92. Bhatnagar P, Freund KB, Spaide RF, Klancnik JM, Jr., Cooney MJ, Ho I, et al. Intravitreal bevacizumab for the management of choroidal neovascularization in pseudoxanthoma elasticum. Retina. 2007;27(7):897-902.

93. Ashton N, Ward B, Serpell G. Effect of oxygen on developing retinal vessels with particular reference to the problem of retrolental fibroplasia. Br J Ophthalmol. 1954;38(7):397-432. PMCID: 1324374.

94. Chen J, Smith LE. Retinopathy of prematurity. Angiogenesis. 2007;10(2):133-40.

95. Smith LE. Through the eyes of a child: understanding retinopathy through ROP the Friedenwald lecture. Invest Ophthalmol Vis Sci. 2008;49(12):5177-82.

96. Jonas JB, Kreissig I, Degenring R. Intraocular pressure after intravitreal injection of triamcinolone acetonide. Br J Ophthalmol. 2003;87(1):24-7. PMCID: 1771462.

97. Ng EW, Adamis AP. Targeting angiogenesis, the underlying disorder in neovascular age-related macular degeneration. Can J Ophthalmol. 2005;40(3):352-68.

98. Rosenfeld PJ, Schwartz SD, Blumenkranz MS, Miller JW, Haller JA, Reimann JD, et al. Maximum tolerated dose of a humanized anti-vascular endothelial growth factor antibody fragment for treating neovascular age-related macular degeneration. Ophthalmology. 2005;112(6):1048-53.

99. Heier JS, Antoszyk AN, Pavan PR, Leff SR, Rosenfeld PJ, Ciulla TA, et al. Ranibizumab for treatment of neovascular age-related macular degeneration: a phase I/II multicenter, controlled, multidose study. Ophthalmology. 2006;113(4):633 e1-4.

100. Avery RL, Pieramici DJ, Rabena MD, Castellarin AA, Nasir MA, Giust MJ. Intravitreal bevacizumab (Avastin) for neovascular age-related macular degeneration. Ophthalmology. 2006;113(3):363-72 e5.

101. Tao Y, Libondi T, Jonas JB. Long-Term Follow-Up After Multiple Intravitreal Bevacizumab Injections for Exudative Age-Related Macular Degeneration. J Ocul Pharmacol Ther.

102. Kernt M, Staehler M, Stief C, Kampik A, Neubauer AS. Resolution of macular oedema in occult choroidal neovascularization under oral Sorafenib treatment. Acta Ophthalmol. 2008;86(4):456-8.

103. Gitlin JD, D'Amore PA. Culture of retinal capillary cells using selective growth media. Microvasc Res. 1983;26(1):74-80.

104. Hoffmann S, Spee C, Murata T, Cui JZ, Ryan SJ, Hinton DR. Rapid isolation of choriocapillary endothelial cells by Lycopersicon esculentum-coated Dynabeads. Graefes Arch Clin Exp Ophthalmol. 1998;236(10):779-84.

105. Manconi F, Markham R, Fraser IS. Culturing endothelial cells of microvascular origin. Methods Cell Sci. 2000;22(2-3):89-99.

106. He S, Jin ML, Worpel V, Hinton DR. A role for connective tissue growth factor in the pathogenesis of choroidal neovascularization. Arch Ophthalmol. 2003;121(9):1283-8.

107. Wang X, Athayde N, Trudinger B. Placental vascular disease and toll-like receptor 4 gene expression. Am J Obstet Gynecol. 2005;192:961-6.

108. Liu Y, Wei Z, Li L, Li H, Chen H, Li X. Construction and analysis of SSH cDNA library of human vascular endothelial cells related to gastrocarcinoma. World J Gastroenterol. 2003;9:2419-23.

109. Voyta JC, Via DP, Butterfield CE, Zetter BR. Identification and isolation of endothelial cells based on their increased uptake of acetylated-low density lipoprotein. J Cell Biol. 1984;99(6):2034-40. PMCID: 2113570.

110. DeCarlo AA, Cohen JA, Aguado A, Glenn B. Isolation and characterization of human gingival microvascular endothelial cells. J Periodontal Res. 2008;43(2):246-54.

111. Ryan US. Isolation and culture of pulmonary endothelial cells. Environ Health Perspect. 1984;56:103-14. PMCID: 1568192.

112. Congdon N, O'Colmain B, Klaver CC, Klein R, Munoz B, Friedman DS, et al. Causes and prevalence of visual impairment among adults in the United States. Arch Ophthalmol. 2004;122(4):477-85.

113. Sivaprasad S, Chong NV. The complement system and age-related macular degeneration. Eye. 2006;20(8):867-72.

114. Vogt SD, Barnum SR, Curcio CA, Read RW. Distribution of complement anaphylatoxin receptors and membrane-bound regulators in normal human retina. Exp Eye Res. 2006;83(4):834-40.

115. Schraufstatter IU, Trieu K, Sikora L, Sriramarao P, DiScipio R. Complement c3a and c5a induce different signal transduction cascades in endothelial cells. J Immunol. 2002;169(4):2102-10.

116. Walport MJ. Complement. First of two parts. N Engl J Med. 2001;344(14):1058-66.

117. Walport MJ. Complement. Second of two parts. N Engl J Med. 2001;344(15):1140-4.

118. Otani A, Takagi H, Oh H, Koyama S, Matsumura M, Honda Y. Expressions of angiopoietins and Tie2 in human choroidal neovascular membranes. Invest Ophthalmol Vis Sci. 1999;40(9):1912-20.

119. Mullins R HG, editor. Histochemical comparison of ocular "drusen" in monkey and human. In: LaVail M, Hollyfield J, Anderson R, editors. Degenerative Retinal Diseases. : New York: Plenum Press. p 1-10.; 1997. .

120. Bora PS, Sohn JH, Cruz JM, Jha P, Nishihori H, Wang Y, et al. Role of complement and complement membrane attack complex in laser-induced choroidal neovascularization. J Immunol. 2005;174(1):491-7.

121. Nozaki M, Raisler BJ, Sakurai E, Sarma JV, Barnum SR, Lambris JD, et al. Drusen complement components C3a and C5a promote choroidal neovascularization. Proc Natl Acad Sci U S A. 2006;103(7):2328-33. PMCID: 1413680.

122. Klein RJ, Zeiss C, Chew EY, Tsai JY, Sackler RS, Haynes C, et al. Complement factor H polymorphism in age-related macular degeneration. Science. 2005;308(5720):385-9. PMCID: 1512523.

123. Edwards AO, Ritter R, 3rd, Abel KJ, Manning A, Panhuysen C, Farrer LA. Complement factor H polymorphism and age-related macular degeneration. Science. 2005;308(5720):421-4.

124. Haines JL, Hauser MA, Schmidt S, Scott WK, Olson LM, Gallins P, et al. Complement factor H variant increases the risk of age-related macular degeneration. Science. 2005;308(5720):419-21.

125. Hageman GS, Anderson DH, Johnson LV, Hancox LS, Taiber AJ, Hardisty LI, et al. A common haplotype in the complement regulatory gene factor H (HF1/CFH) predisposes individuals to age-related macular degeneration. Proc Natl Acad Sci U S A. 2005;102(20):7227-32. PMCID: 1088171.

126. Gold B, Merriam JE, Zernant J, Hancox LS, Taiber AJ, Gehrs K, et al. Variation in factor B (BF) and complement component 2 (C2) genes is associated with age-related macular degeneration. Nat Genet. 2006;38(4):458-62.

127. Yates JR, Sepp T, Matharu BK, Khan JC, Thurlby DA, Shahid H, et al. Complement C3 variant and the risk of age-related macular degeneration. N Engl J Med. 2007;357(6):553-61.

128. Ennis S, Jomary C, Mullins R, Cree A, Chen X, Macleod A, et al. Association between the SERPING1 gene and age-related macular degeneration: a two-stage case-control study. Lancet. 2008;372(9652):1828-34.

129. Hogan MJ. Role of the retinal pigment epithelium in macular disease. Trans Am Acad Ophthalmol Otolaryngol. 1972;76(1):64-80.

130. Seth A, Cui J, To E, Kwee M, Matsubara J. Complement-associated deposits in the human retina. Invest Ophthalmol Vis Sci. 2008;49(2):743-50.

131. Barthel LK, Raymond PA. Improved method for obtaining 3-microns cryosections for immunocytochemistry. J Histochem Cytochem. 1990;38(9):1383-8.

132. Laemmli UK. Cleavage of structural proteins during the assembly of the head of bacteriophage T4. Nature. 1970;227(5259):680-5.

133. Skeie JM, Mullins RF. Elastin-mediated choroidal endothelial cell migration: possible role in age-related macular degeneration. Invest Ophthalmol Vis Sci. 2008;49(12):5574-80. PMCID: 2609900.

134. Chen HC. Boyden chamber assay. Methods Mol Biol. 2005;294:15-22.

135. Vatne HO, Nicolaissen B, Jr. The human choriocapillaris in organ culture. Acta Ophthalmol (Copenh). 1988;66(6):623-9.

136. Hobden JA. Intercellular adhesion molecule-2 (ICAM-2) and Pseudomonas aeruginosa ocular infection. DNA Cell Biol. 2003;22(10):649-55.

137. Webster AR, Heon E, Lotery AJ, Vandenburgh K, Casavant TL, Oh KT, et al. An analysis of allelic variation in the ABCA4 gene. Invest Ophthalmol Vis Sci. 2001;42(6):1179-89.

138. Rabiet MJ, Huet E, Boulay F. Complement component 5a receptor oligomerization and homologous receptor down-regulation. J Biol Chem. 2008;283(45):31038-46. PMCID: 2662174.

139. Webb DS, Mostowski HS, Gerrard TL. Cytokine-induced enhancement of ICAM-1 expression results in increased vulnerability of tumor cells to monocyte-mediated lysis. J Immunol. 1991;146(10):3682-6.

140. Staunton DE, Dustin ML, Erickson HP, Springer TA. The arrangement of the immunoglobulin-like domains of ICAM-1 and the binding sites for LFA-1 and rhinovirus. Cell. 1990;61(2):243-54.

141. Diamond MS, Staunton DE, Marlin SD, Springer TA. Binding of the integrin Mac-1 (CD11b/CD18) to the third immunoglobulin-like domain of ICAM-1 (CD54) and its regulation by glycosylation. Cell. 1991;65(6):961-71.

142. Radi ZA, Kehrli ME, Jr., Ackermann MR. Cell adhesion molecules, leukocyte trafficking, and strategies to reduce leukocyte infiltration. J Vet Intern Med. 2001;15(6):516-29.

143. Skeie JM, Mullins RF. Macrophages in neovascular age-related macular degeneration: friends or foes? Eye. 2009;23(4):747-55.

144. Varani J, Fligiel SE, Till GO, Kunkel RG, Ryan US, Ward PA. Pulmonary endothelial cell killing by human neutrophils. Possible involvement of hydroxyl radical. Lab Invest. 1985;53(6):656-63.

145. Peri G, Chiaffarino F, Bernasconi S, Padura IM, Mantovani A. Cytotoxicity of activated monocytes on endothelial cells. J Immunol. 1990;144(4):1444-8.

146. Schnapp LM, Hatch N, Ramos DM, Klimanskaya IV, Sheppard D, Pytela R. The human integrin alpha 8 beta 1 functions as a receptor for tenascin, fibronectin, and vitronectin. J Biol Chem. 1995;270(39):23196-202.

147. Milis L, Morris CA, Sheehan MC, Charlesworth JA, Pussell BA. Vitronectin-mediated inhibition of complement: evidence for different binding sites for C5b-7 and C9. Clin Exp Immunol. 1993;92(1):114-9. PMCID: 1554864.

148. Zareparsi S, Branham KE, Li M, Shah S, Klein RJ, Ott J, et al. Strong association of the Y402H variant in complement factor H at 1q32 with susceptibility to age-related macular degeneration. Am J Hum Genet. 2005;77(1):149-53. PMCID: 1226187.

149. Johnson PT, Betts KE, Radeke MJ, Hageman GS, Anderson DH, Johnson LV. Individuals homozygous for the age-related macular degeneration risk-conferring variant of complement factor H have elevated levels of CRP in the choroid. Proc Natl Acad Sci U S A. 2006;103(46):17456-61. PMCID: 1859950.

150. Bressler SB. Introduction: Understanding the role of angiogenesis and antiangiogenic agents in age-related macular degeneration. Ophthalmology. 2009;116(10 Suppl):S1-7.

151. Joussen AM, Bornfeld N. The treatment of wet age-related macular degeneration. Dtsch Arztebl Int. 2009;106(18):312-7. PMCID: 2689592.

152. Frank RN, Amin RH, Eliott D, Puklin JE, Abrams GW. Basic fibroblast growth factor and vascular endothelial growth factor are present in epiretinal and choroidal neovascular membranes. Am J Ophthalmol. 1996;122(3):393-403.

153. Amin R, Puklin JE, Frank RN. Growth factor localization in choroidal neovascular membranes of age-related macular degeneration. Invest Ophthalmol Vis Sci. 1994;35(8):3178-88.

154. Schultz GS, Grant MB. Neovascular growth factors. Eye (Lond). 1991;5 (Pt 2):170-80.

155. Csaky K, Do DV. Safety implications of vascular endothelial growth factor blockade for subjects receiving intravitreal anti-vascular endothelial growth factor therapies. Am J Ophthalmol. 2009;148(5):647-56.

156. Shimomura Y, Hirata A, Ishikawa S, Okinami S. Changes in choriocapillaris fenestration of rat eyes after intravitreal bevacizumab injection. Graefes Arch Clin Exp Ophthalmol. 2009;247(8):1089-94.

157. Strydom DJ, Fett JW, Lobb RR, Alderman EM, Bethune JL, Riordan JF, et al. Amino acid sequence of human tumor derived angiogenin. Biochemistry. 1985;24(20):5486-94.

158. Gao X, Xu Z. Mechanisms of action of angiogenin. Acta Biochim Biophys Sin (Shanghai). 2008;40(7):619-24.

159. Fett JW, Strydom DJ, Lobb RR, Alderman EM, Bethune JL, Riordan JF, et al. Isolation and characterization of angiogenin, an angiogenic protein from human carcinoma cells. Biochemistry. 1985;24(20):5480-6.

160. Soncin F. Angiogenin supports endothelial and fibroblast cell adhesion. Proc Natl Acad Sci U S A. 1992;89(6):2232-6. PMCID: 48631.

161. Hu G, Xu C, Riordan JF. Human angiogenin is rapidly translocated to the nucleus of human umbilical vein endothelial cells and binds to DNA. J Cell Biochem. 2000;76(3):452-62.

162. Laduron PM. From receptor internalization to nuclear translocation. New targets for long-term pharmacology. Biochem Pharmacol. 1994;47(1):3-13.

163. Dickson KA, Kang DK, Kwon YS, Kim JC, Leland PA, Kim BM, et al. Ribonuclease inhibitor regulates neovascularization by human angiogenin. Biochemistry. 2009;48(18):3804-6. PMCID: 2677630.

164. Hu GF, Chang SI, Riordan JF, Vallee BL. An angiogenin-binding protein from endothelial cells. Proc Natl Acad Sci U S A. 1991;88(6):2227-31. PMCID: 51203.

165. Hu GF, Strydom DJ, Fett JW, Riordan JF, Vallee BL. Actin is a binding protein for angiogenin. Proc Natl Acad Sci U S A. 1993;90(4):1217-21. PMCID: 45843.

166. Hallahan TW, Shapiro R, Vallee BL. Dual site model for the organogenic activity of angiogenin. Proc Natl Acad Sci U S A. 1991;88(6):2222-6. PMCID: 51202.

167. Hu GF, Riordan JF. Angiogenin enhances actin acceleration of plasminogen activation. Biochem Biophys Res Commun. 1993;197(2):682-7.

168. Dano K, Andreasen PA, Grondahl-Hansen J, Kristensen P, Nielsen LS, Skriver L. Plasminogen activators, tissue degradation, and cancer. Adv Cancer Res. 1985;44:139-266.

169. Olson KA, Fett JW, French TC, Key ME, Vallee BL. Angiogenin antagonists prevent tumor growth in vivo. Proc Natl Acad Sci U S A. 1995;92(2):442-6. PMCID: 42756.

170. Yuan Y, Wang F, Liu XH, Gong DJ, Cheng HZ, Huang SD. Angiogenin is involved in lung adenocarcinoma cell proliferation and angiogenesis. Lung Cancer. 2009;66(1):28-36.

171. Kim SM, Myoung H, Choung PH, Kim MJ, Lee SK, Lee JH. Metastatic leiomyosarcoma in the oral cavity: case report with protein expression profiles. J Craniomaxillofac Surg. 2009;37(8):454-60.

172. Marioni G, Koussis H, Scola A, Maruzzo M, Giacomelli L, Karahontziti P, et al. Expression of MASPIN and angiogenin in nasopharyngeal carcinoma: novel preliminary clinico-pathological evidence. Acta Otolaryngol.

173. Wang J, Yang J, Yuan D, Zhao J, Wang L. Effects of basic fibroblast growth factor on angiogenin expression and cell proliferation in H7402 human hepatoma cells. J Genet Genomics. 2009;36(7):399-407.

174. Hayden MR, Sowers JR, Tyagi SC. The central role of vascular extracellular matrix and basement membrane remodeling in metabolic syndrome and type 2 diabetes: the matrix preloaded. Cardiovasc Diabetol. 2005;4(1):9.

175. Robinet A, Fahem A, Cauchard JH, Huet E, Vincent L, Lorimier S, et al. Elastin-derived peptides enhance angiogenesis by promoting endothelial cell migration and tubulogenesis through upregulation of MT1-MMP. J Cell Sci. 2005;118(Pt 2):343-56.

176. Basalyga DM, Simionescu DT, Xiong W, Baxter BT, Starcher BC, Vyavahare NR. Elastin degradation and calcification in an abdominal aorta injury model: role of matrix metalloproteinases. Circulation. 2004;110(22):3480-7.

177. Mujumdar VS, Aru GM, Tyagi SC. Induction of oxidative stress by homocyst(e)ine impairs endothelial function. J Cell Biochem. 2001;82(3):491-500.

178. Brooke BS, Karnik SK, Li DY. Extracellular matrix in vascular morphogenesis and disease: structure versus signal. Trends Cell Biol. 2003;13(1):51-6.

179. Blumenkranz MS, Russell SR, Robey MG, Kott-Blumenkranz R, Penneys N. Risk factors in age-related maculopathy complicated by choroidal neovascularization. Ophthalmology. 1986;93(5):552-8.

180. Hogan MJ. Bruch's membrane and disease of the macula. Role of elastic tissue and collagen. Trans Ophthalmol Soc U K. 1967;87:113-61.

181. Stone EM, Braun TA, Russell SR, Kuehn MH, Lotery AJ, Moore PA, et al. Missense variations in the fibulin 5 gene and age-related macular degeneration. N Engl J Med. 2004;351(4):346-53.

182. Yanagisawa H, Davis EC, Starcher BC, Ouchi T, Yanagisawa M, Richardson JA, et al. Fibulin-5 is an elastin-binding protein essential for elastic fibre development in vivo. Nature. 2002;415(6868):168-71.

183. Nakamura T, Lozano PR, Ikeda Y, Iwanaga Y, Hinek A, Minamisawa S, et al. Fibulin-5/DANCE is essential for elastogenesis in vivo. Nature. 2002;415(6868):171-5.

184. Mullins RF, Olvera MA, Clark AF, Stone EM. Fibulin-5 distribution in human eyes: relevance to age-related macular degeneration. Exp Eye Res. 2007;84(2):378-80.

185. Yu HG, Liu X, Kiss S, Connolly E, Gragoudas ES, Michaud N, et al. Increased Choroidal Neovascularization Following Laser Induction in Mice Lacking Lysyl oxidase-like 1. Invest Ophthalmol Vis Sci. 2008.

186. Sivaprasad S, Chong NV, Bailey TA. Serum elastin-derived peptides in age-related macular degeneration. Invest Ophthalmol Vis Sci. 2005;46(9):3046-51.

187. Chau KY, Sivaprasad S, Patel N, Donaldson TA, Luthert PJ, Chong NV. Plasma levels of matrix metalloproteinase-2 and -9 (MMP-2 and MMP-9) in age-related macular degeneration. Eye. 2007.

188. Hinek A, Rabinovitch M. 67-kD elastin-binding protein is a protective "companion" of extracellular insoluble elastin and intracellular tropoelastin. J Cell Biol. 1994;126(2):563-74.

189. Hinek A, Rabinovitch M, Keeley F, Okamura-Oho Y, Callahan J. The 67-kD elastin/laminin-binding protein is related to an enzymatically inactive, alternatively spliced form of beta-galactosidase. J Clin Invest. 1993;91(3):1198-205.

190. Privitera S, Prody CA, Callahan JW, Hinek A. The 67-kDa enzymatically inactive alternatively spliced variant of beta-galactosidase is identical to the elastin/laminin-binding protein. J Biol Chem. 1998;273(11):6319-26.

191. Hinek A. Biological roles of the non-integrin elastin/laminin receptor. Biol Chem. 1996;377(7-8):471-80.

192. Senior RM, Griffin GL, Mecham RP, Wrenn DS, Prasad KU, Urry DW. Val-Gly-Val-Ala-Pro-Gly, a repeating peptide in elastin, is chemotactic for fibroblasts and monocytes. J Cell Biol. 1984;99(3):870-4.

193. Duca L, Blanchevoye C, Cantarelli B, Ghoneim C, Dedieu S, Delacoux F, et al. The elastin receptor complex transduces signals through the catalytic activity of its Neu-1 subunit. J Biol Chem. 2007;282(17):12484-91.

194. Duca L, Floquet N, Alix AJ, Haye B, Debelle L. Elastin as a matrikine. Crit Rev Oncol Hematol. 2004;49(3):235-44.

195. Duca L, Debelle L, Debret R, Antonicelli F, Hornebeck W, Haye B. The elastin peptides-mediated induction of pro-collagenase-1 production by human fibroblasts involves activation of MEK/ERK pathway via PKA- and PI(3)K-dependent signaling. FEBS Lett. 2002;524(1-3):193-8.

196. Rodgers UR, Weiss AS. Cellular interactions with elastin. Pathol Biol (Paris). 2005;53(7):390-8.

197. Rodgers UR, Weiss AS. Integrin alpha v beta 3 binds a unique non-RGD site near the C-terminus of human tropoelastin. Biochimie. 2004;86(3):173-8.

198. Nangia-Makker P, Baccarini S, Raz A. Carbohydrate-recognition and angiogenesis. Cancer Metastasis Rev. 2000;19(1-2):51-7.

199. Friedlander M, Theesfeld CL, Sugita M, Fruttiger M, Thomas MA, Chang S, et al. Involvement of integrins alpha v beta 3 and alpha v beta 5 in ocular neovascular diseases. Proc Natl Acad Sci U S A. 1996;93(18):9764-9.

200. McLaughlin AP, De Vries GW. Role of PLCgamma and Ca(2+) in VEGF- and FGF-induced choroidal endothelial cell proliferation. Am J Physiol Cell Physiol. 2001;281(5):C1448-56.

201. Pepper MS, Mandriota SJ, Jeltsch M, Kumar V, Alitalo K. Vascular endothelial growth factor (VEGF)-C synergizes with basic fibroblast growth factor and VEGF in the induction of angiogenesis in vitro and alters endothelial cell extracellular proteolytic activity. J Cell Physiol. 1998;177(3):439-52.

202. Ferrara N, Davis-Smyth T. The biology of vascular endothelial growth factor. Endocr Rev. 1997;18(1):4-25.

203. Ferrara N. Vascular endothelial growth factor and the regulation of angiogenesis. Recent Prog Horm Res. 2000;55:15-35; discussion -6.

204. Schneeberger-Keeley EE, Karnovsky MJ. The ultrastructural basis of alveolar-capillary membrane permeability to peroxidase used as a tracer. J Cell Biol. 1968;37(3):781-93.

205. Hancock CN, Macias A, Lee EK, Yu SY, Mackerell AD, Jr., Shapiro P. Identification of novel extracellular signal-regulated kinase docking domain inhibitors. J Med Chem. 2005;48(14):4586-95.

206. Makowska JS, Grzegorczyk J, Cieslak M, Bienkiewicz B, Kowalski ML. Recruitment of CD34+ progenitor cells into peripheral blood and asthma severity. Ann Allergy Asthma Immunol. 2008;101(4):402-6.

207. Houghton AM, Quintero PA, Perkins DL, Kobayashi DK, Kelley DG, Marconcini LA, et al. Elastin fragments drive disease progression in a murine model of emphysema. J Clin Invest. 2006;116(3):753-9. PMCID: 1361346.

208. Ambati J, Anand A, Fernandez S, Sakurai E, Lynn BC, Kuziel WA, et al. An animal model of age-related macular degeneration in senescent Ccl-2- or Ccr-2-deficient mice. Nat Med. 2003;9(11):1390-7.

209. Malek G, Johnson LV, Mace BE, Saloupis P, Schmechel DE, Rickman DW, et al. Apolipoprotein E allele-dependent pathogenesis: a model for age-related retinal degeneration. Proc Natl Acad Sci U S A. 2005;102(33):11900-5. PMCID: 1187976.

210. Imamura Y, Noda S, Hashizume K, Shinoda K, Yamaguchi M, Uchiyama S, et al. Drusen, choroidal neovascularization, and retinal pigment epithelium dysfunction in SOD1-deficient mice: a model of age-related macular degeneration. Proc Natl Acad Sci U S A. 2006;103(30):11282-7. PMCID: 1544079.

211. Luhmann UF, Robbie S, Munro PM, Barker SE, Duran Y, Luong V, et al. The drusenlike phenotype in aging Ccl2-knockout mice is caused by an accelerated accumulation of swollen autofluorescent subretinal macrophages. Invest Ophthalmol Vis Sci. 2009;50(12):5934-43. PMCID: 2801148.

212. Praddaude F, Cousins SW, Pecher C, Marin-Castano ME. Angiotensin II-induced hypertension regulates AT1 receptor subtypes and extracellular matrix turnover in mouse retinal pigment epithelium. Exp Eye Res. 2009;89(1):109-18. PMCID: 2744298.

213. Yu SY, Ruthmeyer SK, Shepard JW, Jr. Digestion and absorption of radioactive elastins in rats. Proc Soc Exp Biol Med. 1979;161(3):239-43.

214. Yu SY, Yoshida A. The fate of 14C-elastin in the peritoneal cavity of rats. I. Biochemical studies. Lab Invest. 1977;37(2):143-9.

215. Pinto LH, Invergo B, Shimomura K, Takahashi JS, Troy JB. Interpretation of the mouse electroretinogram. Doc Ophthalmol. 2007;115(3):127-36.

216. Saszik SM, Robson JG, Frishman LJ. The scotopic threshold response of the dark-adapted electroretinogram of the mouse. J Physiol. 2002;543(Pt 3):899-916. PMCID: 2290546.

217. Chen L, Miyamura N, Ninomiya Y, Handa JT. Distribution of the collagen IV isoforms in human Bruch's membrane. Br J Ophthalmol. 2003;87(2):212-5. PMCID: 1771521.